



**GEOLOGICAL SURVEY OF CANADA
OPEN FILE 7463**

**Discrimination of Elemental Assemblages in the Alteration
Halo of the Phoenix Deposit, Saskatchewan, Through
Applied GIS**

J. Dann, K. Hattori, E.G. Potter and C. Sorba

2014



Natural Resources
Canada

Ressources naturelles
Canada

Canada



**GEOLOGICAL SURVEY OF CANADA
OPEN FILE 7463**

**Discrimination of Elemental Assemblages in the Alteration
Halo of the Phoenix Deposit, Saskatchewan, Through
Applied GIS**

J. Dann¹, K. Hattori¹, E.G. Potter² and C. Sorba³

- ¹-Department of Earth Sciences, University of Ottawa, Ottawa, ON K1N 6N5
²- Geological Survey of Canada, 601 Booth St, Ottawa, ON K1A 0E9
³- Denison Mines Corp., Suite 200-230 22nd St. East, Saskatoon, SK S7K 0E9

2014

©Her Majesty the Queen in Right of Canada 2014

doi:10.4095/293122

This publication is available for free download through GEOSCAN (<http://geoscan.ess.nrcan.gc.ca/>).

Recommended citation

Dann, J., Hattori, K., Potter, E.G., and Sorba, C., 2014. Discrimination of Elemental Assemblages in the Alteration Halo of the Phoenix Deposit, Saskatchewan, Through Applied GIS; Geological Survey of Canada, Open File 7463. doi:10.4095/293122

Abstract

This study was initiated as part of the TGI-4 uranium ore systems project to evaluate the dispersion of ore-related elements that could be used to increase exploration effectiveness for deeply buried, unconformity-related uranium mineralization. The Phoenix deposit, located in the Athabasca Basin, currently has indicated resources of approximately 52.3 million lbs U_3O_8 . The mineralization consists of four pods termed the A, B, C and D ore zones at ca. 400 meters depth. The pods occur both at the unconformity and within the basement as steeply dipping zones associated with a fault zone termed the WS shear.

The siliciclastic sandstones of the Athabasca Group overlying the Phoenix deposit are characterized by elevated enrichments in the elements Y, W, B, Mg, As, Pb, B, Co and Cu. Preliminary geochemical analyses of sandstone samples from the Manitou Falls Formation indicate a clear migration of Y and W in vertical columns while B, MgO and As data reveal zones of elevated values that extend from the ore zones to upwards of 350m above the deposit and 2.4 km along strike. Away from these chimneys, values of MgO, B, and As are comparable to that of regional outcrop and drillhole data, suggesting localized, well-defined enrichment of these elements in the vicinity of Phoenix. The abundance of other elements elevated in the orebody, such as Ni, Li and V, show little spatial relationship to mineralization in the overlying sandstones. These preliminary results illustrate that certain elements can play a guiding role in the exploration of unconformity-related uranium deposits.

Introduction

Currently, all of Canada's uranium production is from unconformity-related deposits situated in the Athabasca Basin, Saskatchewan. With recent exploration successes at increasing depths in the basin, new efficient means of targeting these deeply buried deposits are required. Under the Targeted Geoscience Initiative Four (TGI-4) program, this study is examining the movement of elements from deep-seated ore deposits to the near surface environment. This subject is of intense interest not only for exploration but also for environmental studies and mine site remediation.

In this study, we discuss the spatial relationship of elevated metals concentrations within sandstones overlying the Phoenix Deposit, located on the Wheeler River Property. As a means of tracking elemental distribution in the sandstones overlying the Phoenix Deposit, interpolations of whole rock litho-geochemistry at 50m intervals have been performed for elements associated with mineralization, recognized pathfinder elements and major elements. A major shear zone (WS shear) is associated with the Phoenix deposit and has been proposed as a potential conduit for pre-, syn- and post-ore fluids (Kerr, 2010; Arseneau and Revering, 2010; this study). Its role in the migration and distribution of elements is discussed herein.

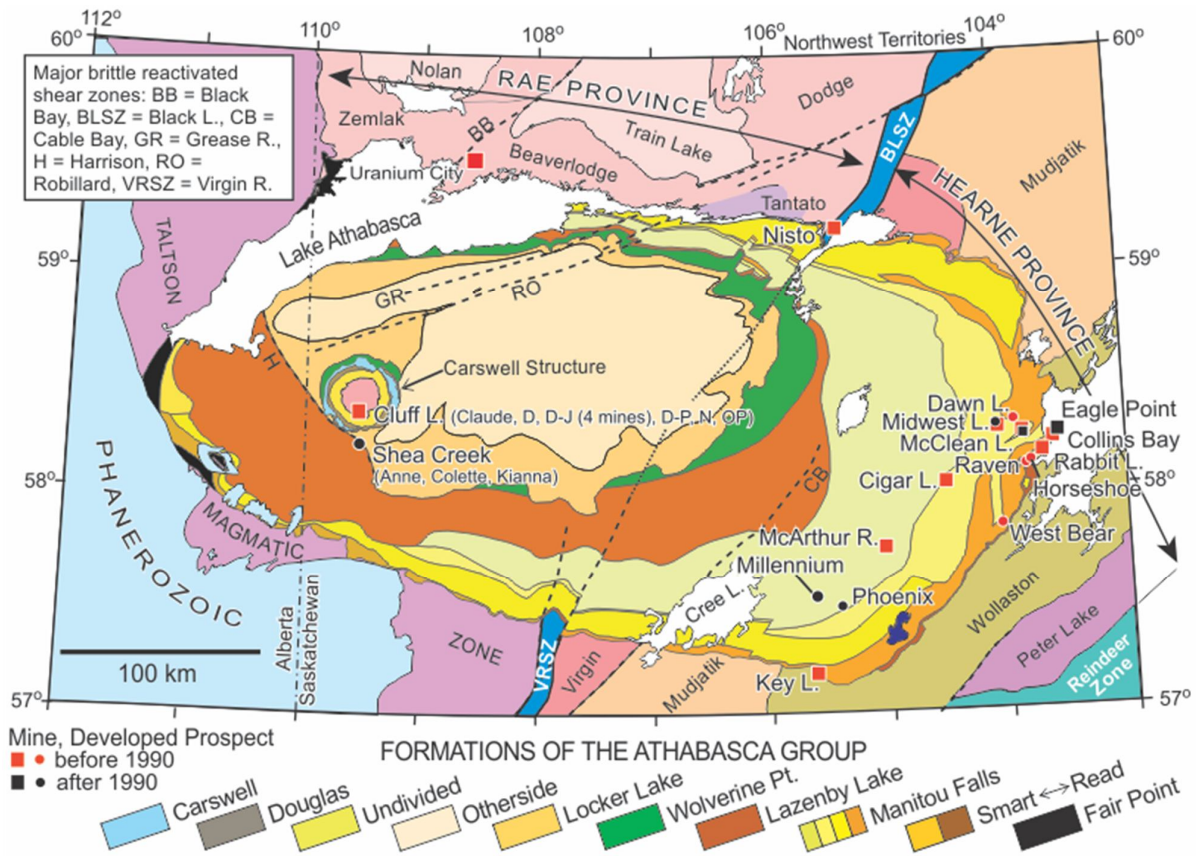


Figure 1: Geologic map of the Athabasca Basin, northern Saskatchewan, Canada. The Phoenix deposit is located in the southeast margin of the Athabasca Basin. Modified from Jefferson et al., (2007).

Regional Geology

The majority of the producing, past-producing and active uranium prospects in the Athabasca Basin overlie the basement transition between the Wollaston and Mudjatik domains of the Hearne Province (Annesley et al., 2005). The transition zone comprises pelitic, quartzose and arkosic paragneissic lithologies that are isoclinally folded and interleaved with Paleoproterozoic orthogneiss and abundant pegmatitic intrusions (Jefferson et al., 2007). Graphitic pelites and paragneiss compose 70 to 85% of the metasedimentary sequence (Annesley et al., 2005).

The Athabasca Basin was formed between 1760-1500 Ma as a series of northeast-southwest sub basins controlled by major Hudsonian age faults in the underlying basement rocks (Ramaekers et al., 2007). These faults have been interpreted to have had played a significant role in localizing uranium-bearing fluids during deposit formation (Jefferson et al., 2007). The dominantly quartzose Athabasca Group is subdivided into ten Formations, which constitute four fluvial, unconformity-bound sequences (Ramaekers et al., 2007; Yeo et al., 2007).

Local Geology

Within the Wheeler River Property, the Athabasca sandstone is composed of a 170 to 560 m thick sequence dominated by the Manitou Falls Formation quartz arenite. At the Phoenix deposit, three members overlie the basal Read Formation (RD; historically termed the MFa): the Bird (MFb), Collins (MFc) and the Dunlop (MFd) members, which can be differentiated based on conglomeratic and interclast material (Ramaekers et al., 2007). The RD is composed of a lower unit of pebble-cobble conglomeratic rocks overlain by an upper unit of well sorted sandstone to pebbly sandstone. The RD varies in thickness, from over 200m west of a basement quartzite ridge, to absent directly above this paleotopographic high (Bosman and Korness, 2007; Kerr, 2010). The MFb is similar to the RD, although it is differentiated by greater than 1.2% conglomeratic material in beds thicker than 2 cm (Ramaekers et al., 2007) and is also absent above the quartzite ridge (Bosman and Korness, 2007; Kerr, 2010). The 30 to 150 m thick MFc is a relatively clean sandstone, with locally scattered pebbles or granules and minor pebble layers interpreted to be pebble lag deposits. The MFd member is characterized by the presence of at least 0.6% clay intraclasts (Jefferson et al., 2007).

The dominant regional diagenetic clay phase in the sandstones of the Athabasca Basin is dickite. The Phoenix deposit also lies within a broad regional illite and chlorite anomaly present in surficial material and outcrops of Athabasca Group sandstone that trends northeast from Key Lake to McArthur River (Earle and Sopuck, 1989; Jefferson et al., 2007). The authors also recognized a tourmaline (dravite) anomaly associated with this trend, but this zone lies west of the Phoenix deposit.

The basement rocks are composed of metasedimentary rocks belonging to the Wollaston Supergroup and Mudjatik domain. These include graphitic and non-graphitic pelitic and semipelitic gneisses, quartzite, and rare calc-silicate rocks together with felsic and quartz feldspathic granitoid gneisses (Arseneau and Revering, 2010). Granitic pegmatites are common, with coarse-grained K-feldspar, quartz and micas. Garnet, cordierite and sillimanite occur in the metapelites, indicating upper amphibolite metamorphic grade (Arseneau and Revering, 2010). The quartzite ridge, a major paleotopographic high at the unconformity and an interpreted impermeable and structural barrier (Arseneau and Revering, 2010) dips between 45° – 75° to the southeast, with an undulating azimuth of around 055°.

Geology of the Phoenix deposit

Discovered in 2008, the Phoenix deposit is operated by Denison Mines Corporation (60%) and co-owned by Cameco Corporation (30%) and JCU Exploration Company Limited (10%). By late 2012, drilling defined four mineralized zones; two which have been subject to extensive drilling (A

and B) and contain 43-101 compliant resource estimates. The remaining two zones (C and D) are still undergoing exploration and resource delineation. The A and B zones contain indicated resources of 52.34 million pounds of U₃O₈ (Arseneau and Revering, 2010; Roscoe, 2012). Uranium mineralization occurs mainly as uraninite, with high levels of Cu (up to 3200 ppm) and Pb up to 2.25 wt %), and minor Ni, Co, As, Zn and Ag in the A and B zones (Arseneau and Revering, 2010).

The Phoenix deposit is situated along the northeast-trending reverse structure of WS Shear which dips to the southeast and is rooted in either the base of the graphitic pelite or along the western edge of the quartzite ridge (Arseneau and Revering, 2010). Mineralization along the WS Shear occurs as steeply dipping, thin (1-3m wide) parallel to sub-parallel bands for up to 20 m below the unconformity. Mineralization in the lowest 15 m of the RD appears to be related to extension of the WS Shear and hanging wall splays, indicating reactivation occurred along these faults after deposition of the RD and MFb (Kerr, 2010).

This study uses a projection of the ore body produced by Denison Mines Corporation in 2011, at a cut-off grade of 0.1% U₃O₈. It is recognized that the actual area of mineralization extends beyond this, although with a lower grade and thickness (grade in wt% U₃O₈*m) of between 0.601 to 0.01.

Athabasca Sandstones above the Phoenix Deposits

Geochemical interpolations were performed along slices at 50m intervals. Where slices pass through more than one lithological unit, stratigraphic boundaries were derived from core logging performed by Denison Mines Corp., staff using the parameters outlined in Ramaekers et al., (2007). The regional data from Card et al., (2011) and Bosman and Card, (2012) followed the same logging parameters.

Table 1: Division of the Athabasca Group in relation to the slices analysed as part of this study.

Depth (msl)	Member/Formation
500	MFd
450	MFc
400	MFc
350	MFc/MFb
300	MFb/MFc
250	MFb
200	MFb/RD

Methods

Geochemical Data

All the geochemical data were produced at the Saskatchewan Research Council Geoanalytical Labs in Saskatoon, Canada for Denison Mines Corporation. Samples were subjected to partial leach method whereby an aliquot of pulp was digested in a hot aqua regia bath for approximately 1 hour, then diluted to 15ml using de-ionized water, followed by Inductively Coupled Plasma Mass Spectrometry (ICP-MS) or Inductively Coupled Plasma - Optical Emission Spectrometry (ICP-OES). Where partial leach data are not available, total digestion values have been used, in which aliquots of pulp were digested in a hot mixture of concentrated acids of HF, HNO₃, and HClO₄. The residue was then dissolved in 15 ml of 5% HNO₃ and made to volume using de-ionized water prior to analysis. For boron, an aliquot of pulp was fused in a mixture of NaO₂/NaCO₃ in a muffle oven. The fused melt was then dissolved in de-ionized Water and analysed by ICP-OES.

This study uses two populations of data: data from DDH WR 190A to WR 269 (number of DDH =23) were derived from ICP-OES whereas DDH WR 270 to WR 384 (number of DDH =111) used ICP-MS. The majority of data used for both interpolations and statistical analysis had values well above detection limits (Table 2), and any values at detection limits were not manipulated and retained for median value calculation. Due to the low variance of tungsten, which had a large number of samples at detection limit, tungsten was excluded from statistical analysis and comparison to regional data. All the geochemical data are summarized in Appendix A.

Table 2: Working Detection limits of elements for both analytical methods applied in this study, compared to the population of each dataset.

Leach Method	Partial Digestion								Total Digestion									
	As	Co	Cu	Mo	Ni	Pb	U	V	Al ₂ O ₃	Fe ₂ O ₃	K ₂ O	MgO	P ₂ O ₅	Li	W	Y	Ce	B
MFb																		
Working Detection Limits from ICP-OES																		
Lowest Value Sample	0.1	0.1	0.2	0.1	0.1	0.2	0.3	0.4	1.4	0.11	0	0.03	0.02	1	0.5	1	21	1
Number of Samples at Lowest Value	13	59	18	163	1	1	153	3	1	1	1	1	2	2	168	2	1	1
% of Population	7.4	34	10	93	0.6	0.6	87	1.7	0.57	0.57	0.6	0.57	1.14	1.1	95.5	1.1	0.6	0.6
Working Detection Limits from ICP-MS																		
Lowest Value Sample	0.2	0	0.1	0	0.2	0.4	0.1	0.1	0.04	0.05	0	0.01	0.02	0.5	0.1	0.3	0.5	20
Number of Samples at Lowest Value	1	1	1	7	1	1	1	1	1	1	1	1	1	2	726	3	1	1
% of Population	0.1	0.1	0.1	0.9	0.1	0.1	0.1	0.1	0.13	0.13	0.1	0.13	0.13	0.3	95.9	0.4	0.1	0.1
MFc																		
Working Detection Limits from ICP-OES																		
Lowest Value Sample	0.1	0.1	0.1	0.1	0.2	0.2	0.3	0.2	0.36	0.03	0	0.03	0.01	1	0.5	1	15	6
Number of Samples at Lowest Value	156	113	3	299	3	1	317	9	1	4	1	1	1	8	313	2	1	1
% of Population	46	33	0.9	87	0.9	0.3	92	2.6	0.29	1.17	0.3	0.29	0.29	2.3	91.3	0.6	0.3	0.3
Working Detection Limits from ICP-MS																		
Lowest Value Sample	0.1	0	0.1	0	0.1	0.2	0.1	0.1	0.48	0.04	0	0.03	0.01	1	0.1	0.1	18	10
Number of Samples at Lowest Value	1	3	1	1	1	1	1	15	1	28	1	1	2	14	1048	3	1	1
% of Population	0.1	0.3	0.1	0.1	0.1	0.1	0.1	1.4	0.09	2.64	0.1	0.09	0.19	0.1	98.9	0.3	0.1	0.1

Table 2: continued.

Leach Method	Partial Digestion								Total Digestion									
	As	Co	Cu	Mo	Ni	Pb	U	V	Al ₂ O ₃	Fe ₂ O ₃ (t)	K ₂ O	MgO	P ₂ O ₅	Li	W	Y	Ce	B
MFd	Working Detection Limits from ICP-OES								Working Detection Limits from ICP-OES									
Lowest Value Sample	0.08	0.05	0.54	0.02	0.4	0.33	0.24	0.2	0.6	0.03	0.02	0.08	0.01	1	0.1	0.4	16	34
Number of Samples at Lowest Value	1	9	1	5	1	1	1	1	1	5	2	1	2	2	67	1	1	1
% of Population	0.29	2.62	0.29	1.46	0.29	0.29	0.29	0.29	0.29	1.46	0.58	0.29	0.58	2.2	19.5	0.29	0.29	0.29
	Working Detection Limits from ICP-MS								Working Detection Limits from ICP-MS									
Lowest Value Sample	0.07	0.04	0.33	0.02	0.2	0.2	0.14	0.1	0.45	0.03	0.02	0.06	0.01	2	0.1	0.27	16	13
Number of Samples at Lowest Value	2	7	1	17	1	1	1	10	2	33	1	1	6	53	134	1	7	1
% of Population	0.58	2.04	0.29	4.96	0.29	0.29	0.29	2.92	0.58	9.62	0.29	0.29	1.75	24	39.1	0.29	2.04	0.29

Note: Total Fe expressed as Fe₂O₃(t);

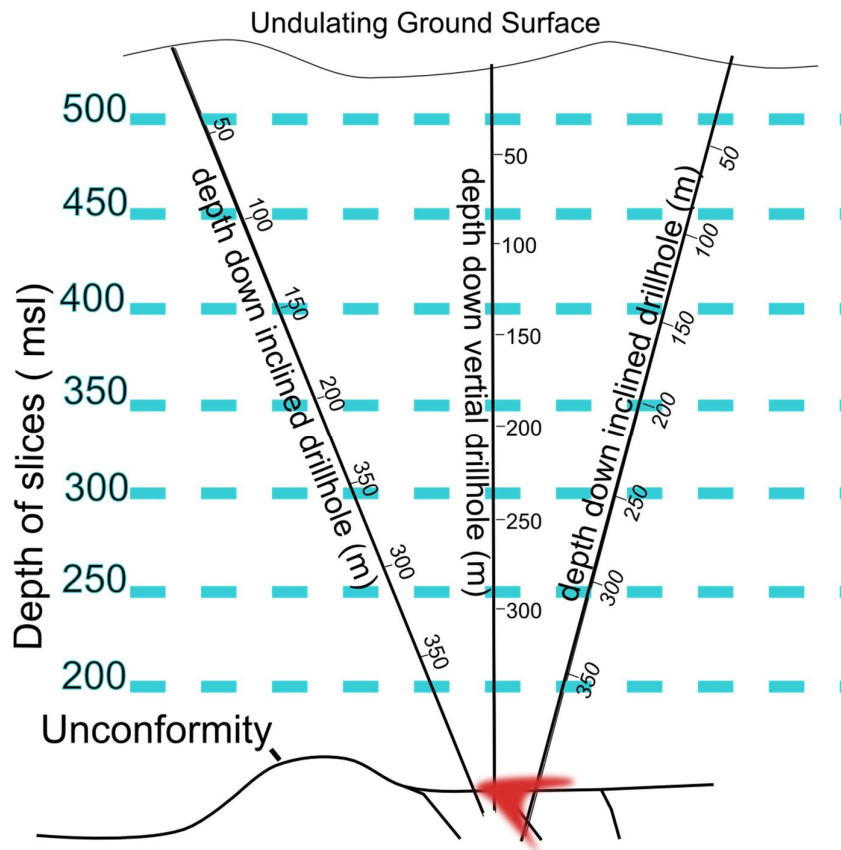


Figure 2: Schematic diagram illustrating organization of diamond drill holes (DDH) and the interpolated slices through the sandstone package. This method allows for inclined DDH on the undulating surface to be laterally compared at the same level as vertical DDH.

Interpolation and Construction of 3D Model

In order to account for inclination of diamond drill holes (DDH) and different elevations of the drill sites, a basic three-dimensional (3D) model was constructed to interpret the data along flat planes through the sandstone. Inclined DDH data were subjected to basic trigonometric functions, allowing the calculation of true depth and placement within a 3D framework, relative to its declination, azimuth, elevation and location (Figure 2).

True depth of each data point is presented relative to meters above mean sea level (msl). The unconformity varies from 94 msl to 195 msl, hence the interpolation of slices of the bulk rock geochemistry above 200 msl were chosen to discuss the compositions of sandstones. The number of data points used were as follows: 200 msl (n= 162), 250 msl (n= 137), 300 msl; (n=90), 350 msl; (n=95), 400 msl; (n=93), 450 msl; (n=90), 500 msl; (n=77). Since drilling was carried out to define an ore body along a linear trend (WS Shear fault), points are primarily focused along this axis.

Maps of the points and limits of interpolation for each slice are provided in Figure 3. Any values quoted in the text are directly from the whole rock litho-geochemistry and not from interpolated

values. The Inverse Distance Weighted (IDW) method was used to interpolate geochemical values. Although more commonly applied to soil data (Kane et al, 1982; Zhang et al, 2008; Grunsky 2010), it allows for visualization of the distribution of elements in a multidimensional space, making it suitable for this study.

Interpolation was performed using ESRI's ArcGIS 10.0 ArcMap software equipped with the Spatial Analysis toolbox. The DDH locations are spread along a 2.4km strike of the WS shear, but only span 200m across the shear structure and with an inconsistent distribution in a 3D space. As a result, the interpolation results are often significantly varied between individual dense points and resulted in the spatial analysis being performed with an IDW algorithm under a power of 2, attempting to mitigate any undue bias of the spatial arrangement of the data. By using IDW, an algorithm calculates the weighted mean of known values inside a moving spatial window that is calculated and assigned to the pixel in the centre, with all interpolated values between minimum and maximum observed values (Bartier and Keller, 1996). This is achieved by running an element-by-element interpolation inside of a defined polygon that surrounds the DDH locations. One barrier was used to maintain consistency through the interpolations. To minimize undue interpolation surrounding the data points, a rectangular barrier was drawn as close as possible to all points. Points which fell outside the barrier and resulted in unwarranted interpolation were excluded. The locations of the DDH and respective barriers are described in Figure 3.

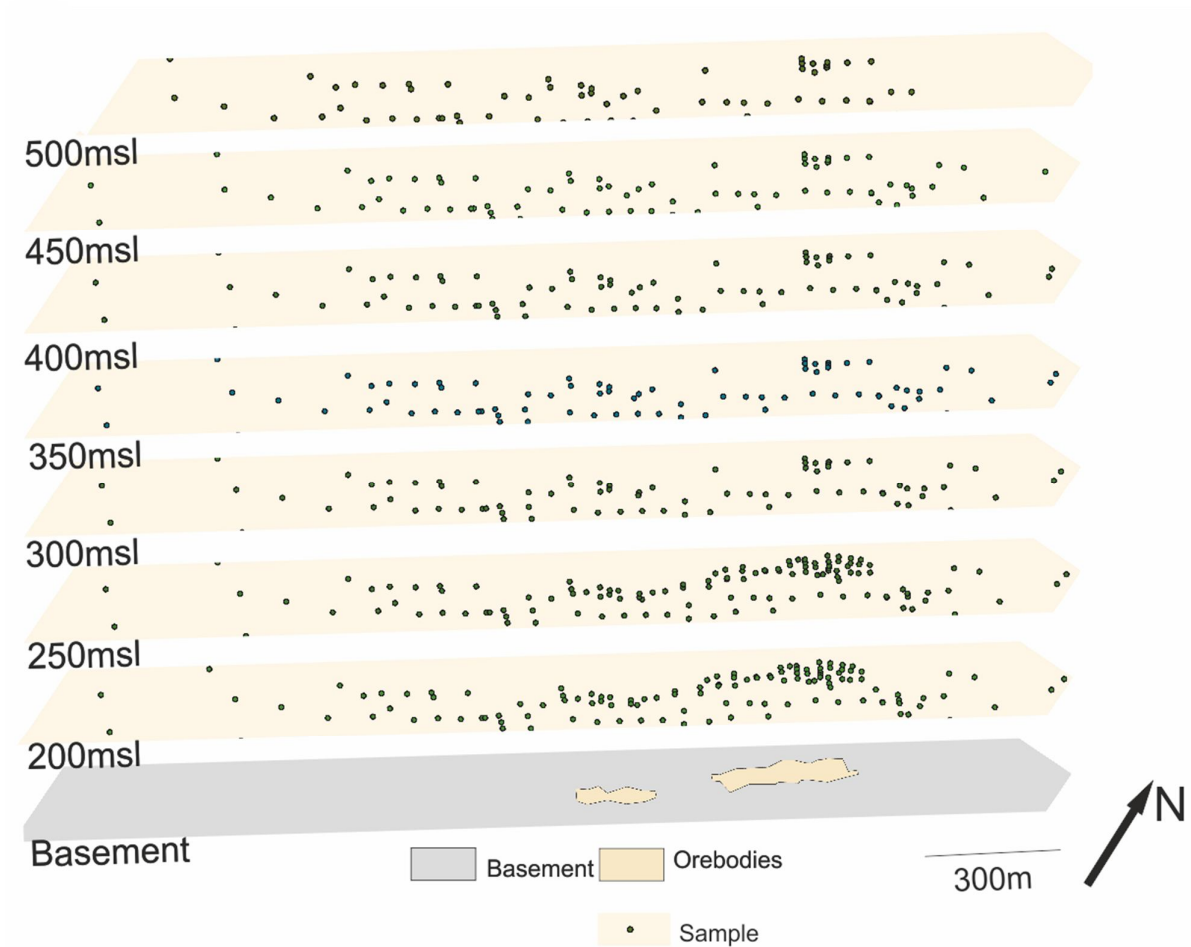


Figure 3: Distribution of points used for interpolation, the boundaries of interpolations and location of the orebodies .

Observations

Spatial Elemental Variation

Interpolations are displayed as pseudo 3D models produced with an isometric viewpoint in Corel Draw 16. This allows for a clear observation of elemental behaviour throughout the sequence. For reference, the locations of the A (northernmost) and B (southern) zone are shown.

Histograms and quantile-quantile (Q-Q) plots are used to compare the data to regional Athabasca Basin outcrop data from Card et al., (2011) and regional DDH data from Bosman and Card (2012). Q-Q plots are a graphical means of comparing a frequency distribution with respect to an expected frequency distribution, which is usually a normal distribution in unaltered systems. These plots are generated by calculating quantile values for the normal frequency distribution (value of the normal frequency distribution over the range of probability, 0.0–1.0) and then plotting these against the ordered observed data. If a frequency distribution is normally distributed, the resulting

plot will be a straight line. If the frequency distribution of the population is skewed or the population is polymodal, the plot will be curved or discontinuous (Grunsky, 2010). The comparative data used in this study also used the Sandstone Exploration Package from Saskatchewan Research Council Geoanalytical Labs.

Insufficient regional data from the Read Formation does not allow comparison with the data from Phoenix and therefore no analysis has been carried out. Read Formation values from Phoenix were simply excluded and have not been used in the statistical analysis of this study. All data obtained during this study are presented in Appendix A.

Uranium

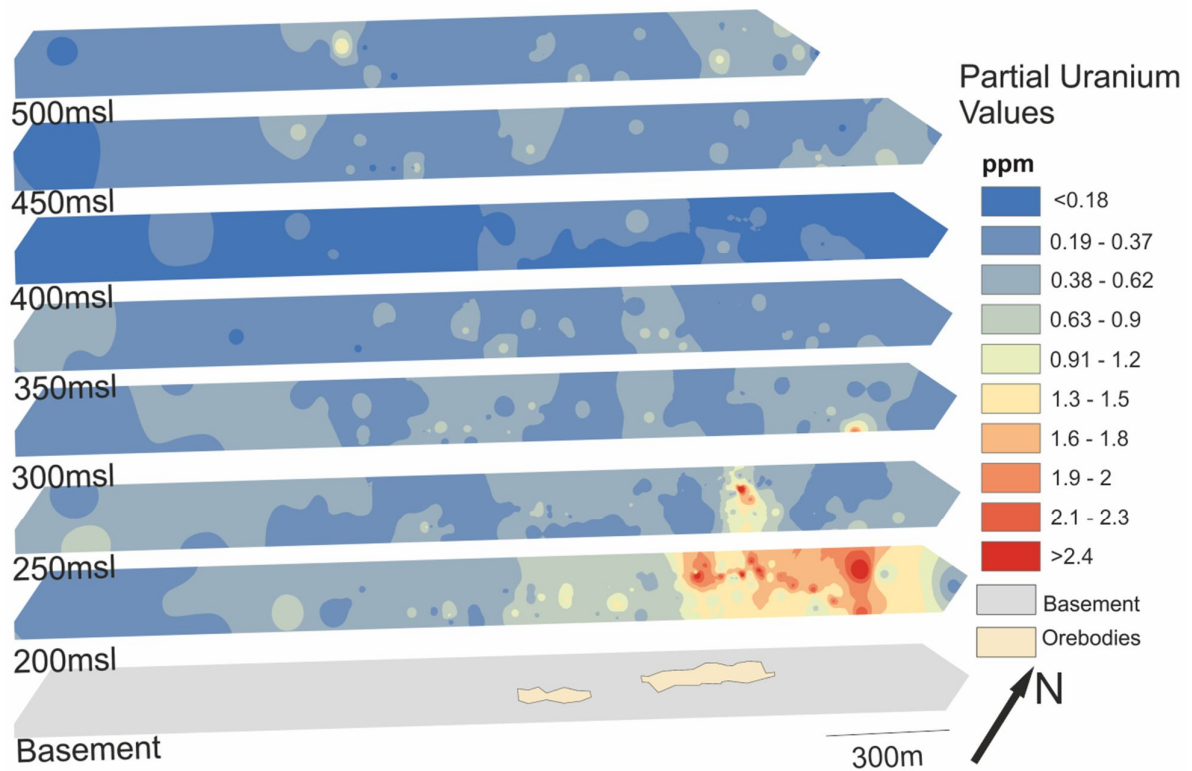
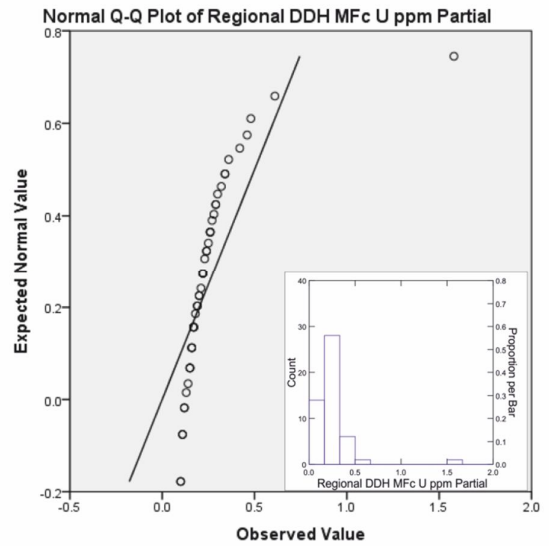
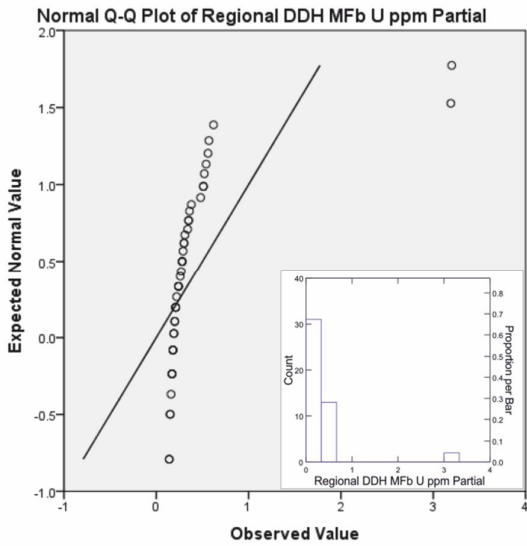
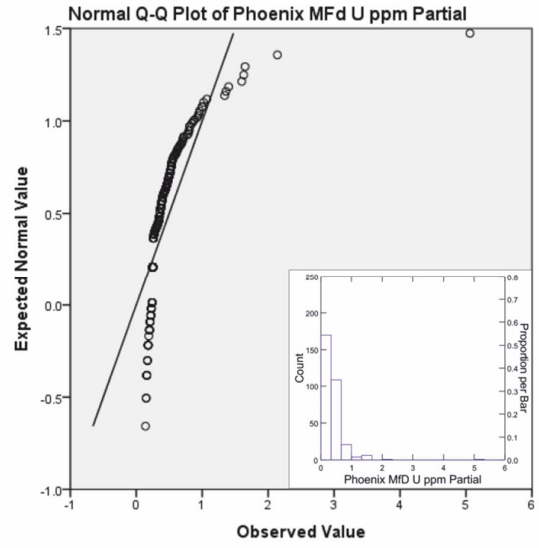
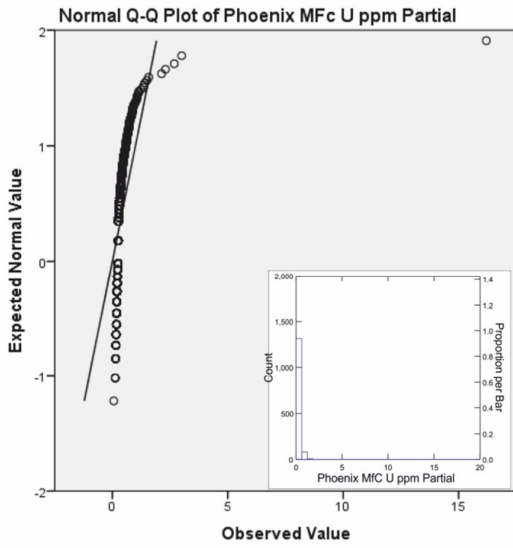
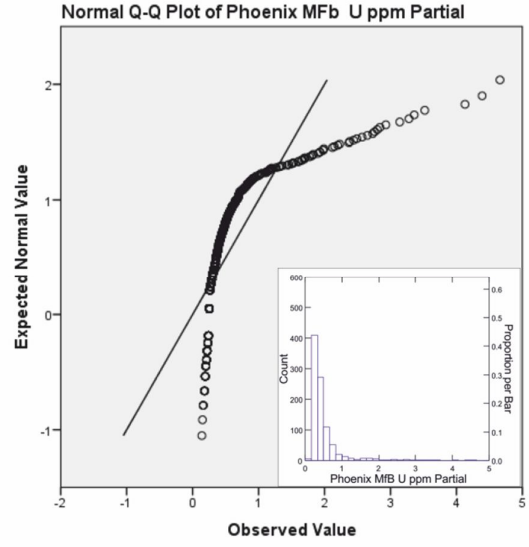
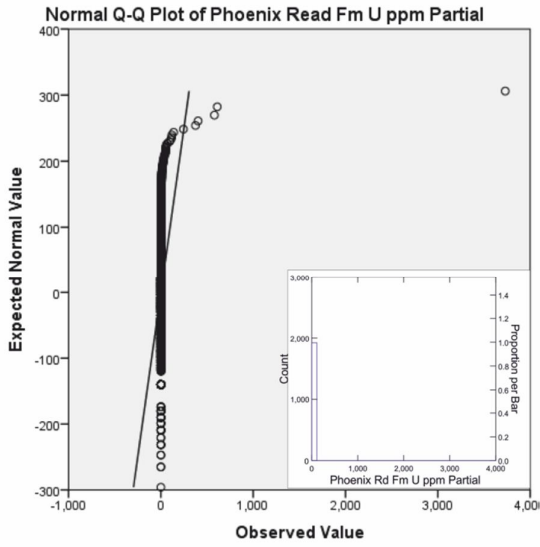


Figure 4: Partial leach uranium values from sandstone overlying the Phoenix deposit. Detection Limit of 0.01ppm U.



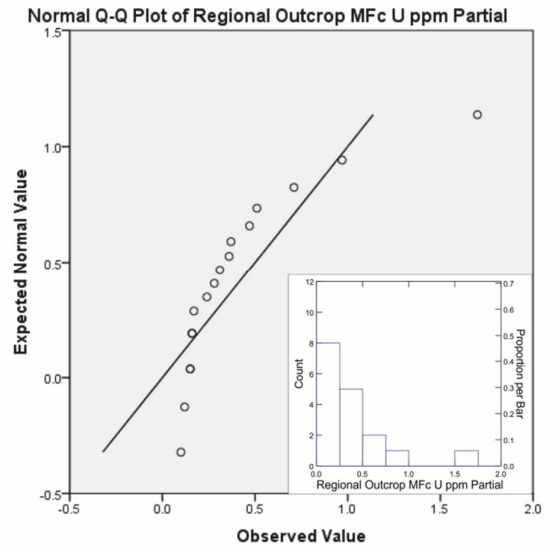
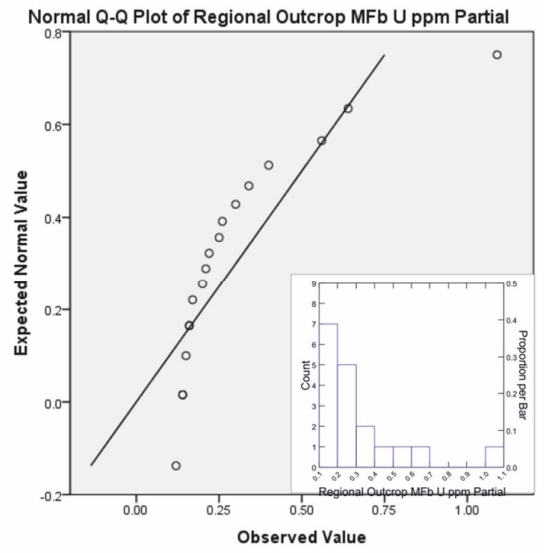
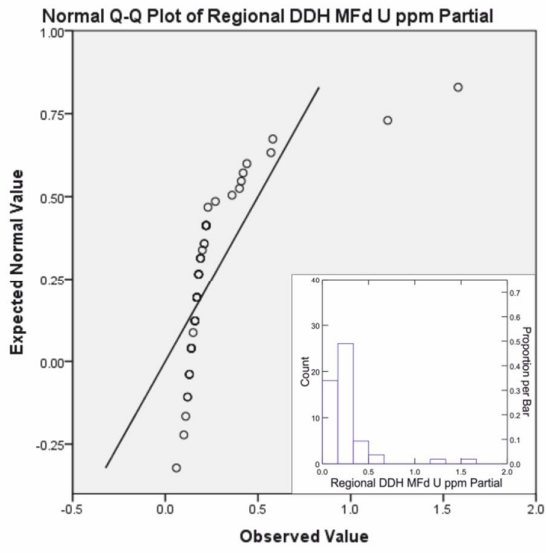


Figure 5: Q-Q and histogram (insets) plots of partial leach uranium values from regional outcrop, regional DDH and sandstones overlying the Phoenix deposit

Arsenic

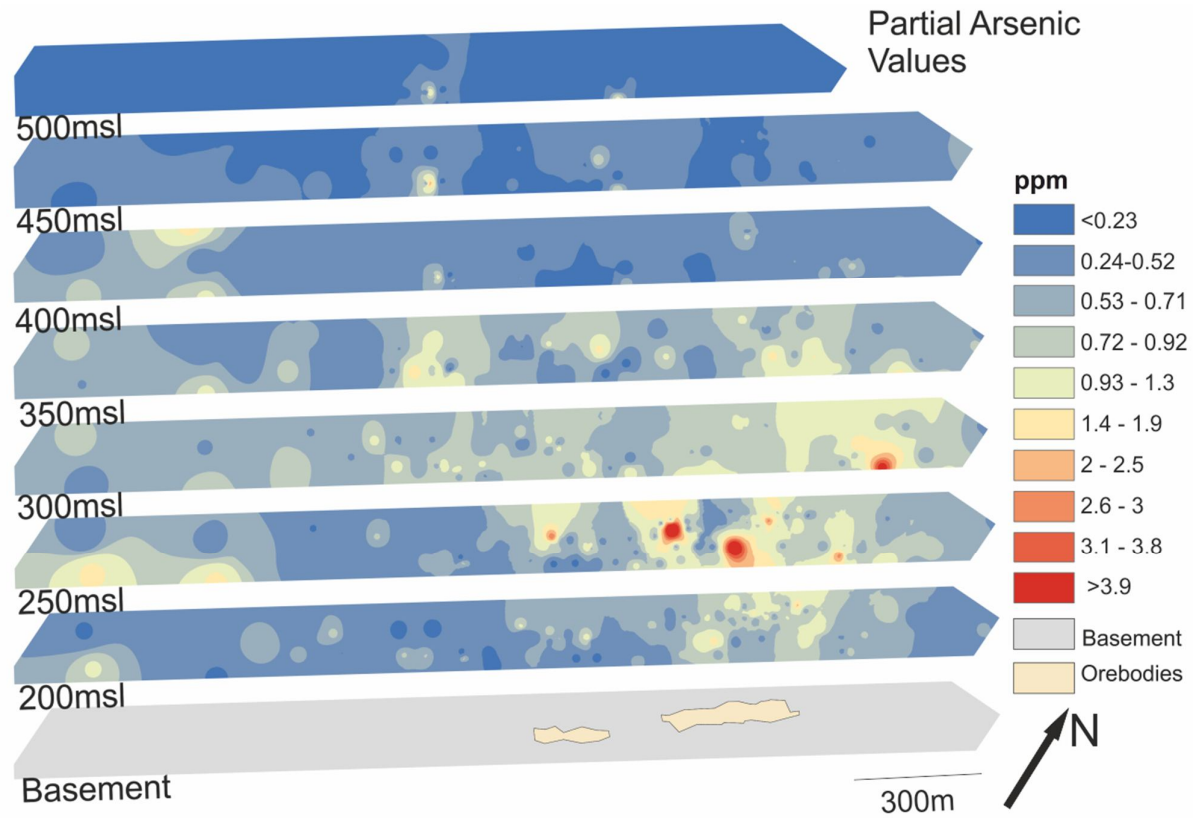
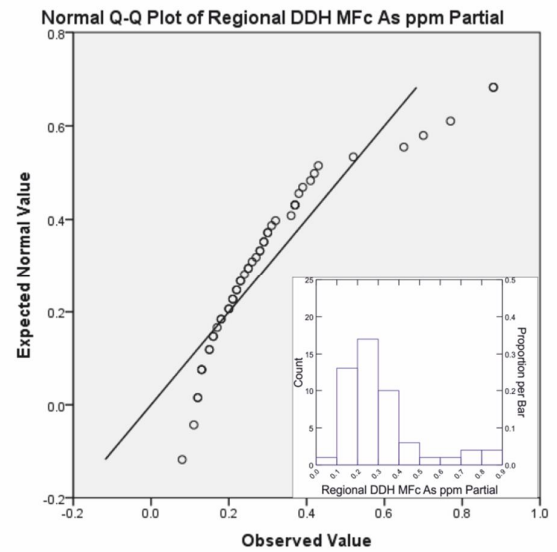
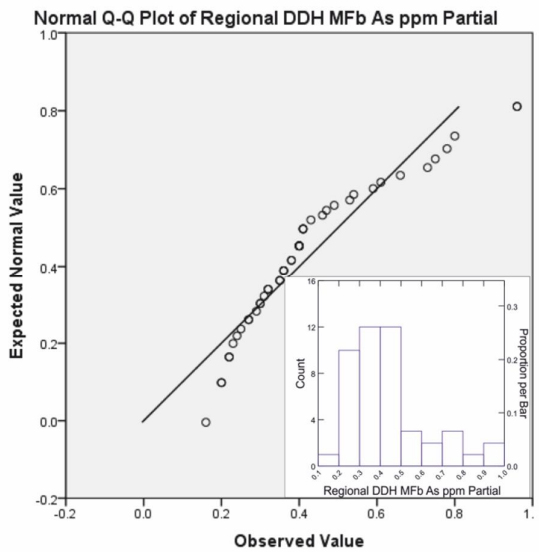
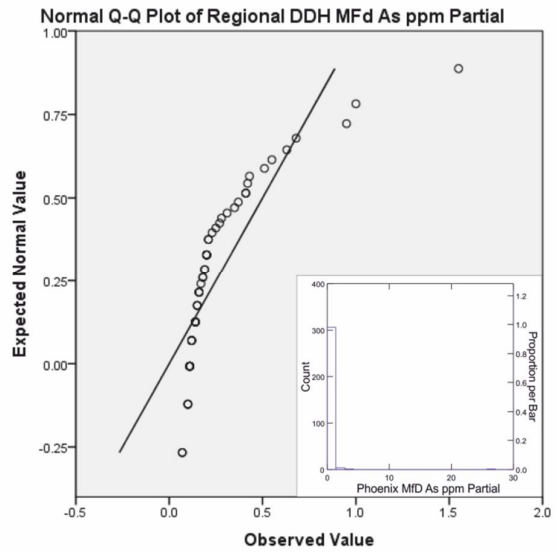
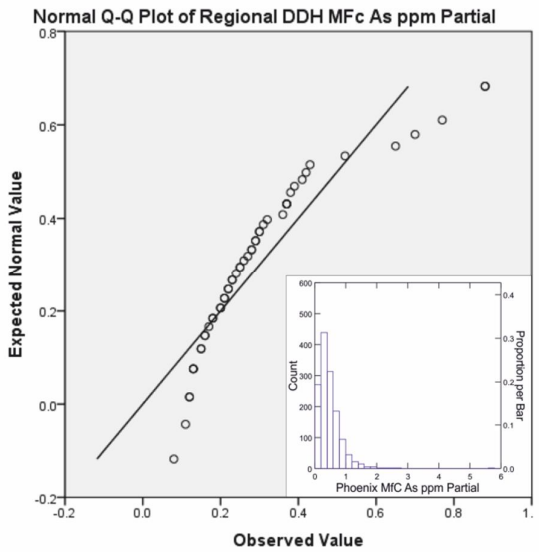
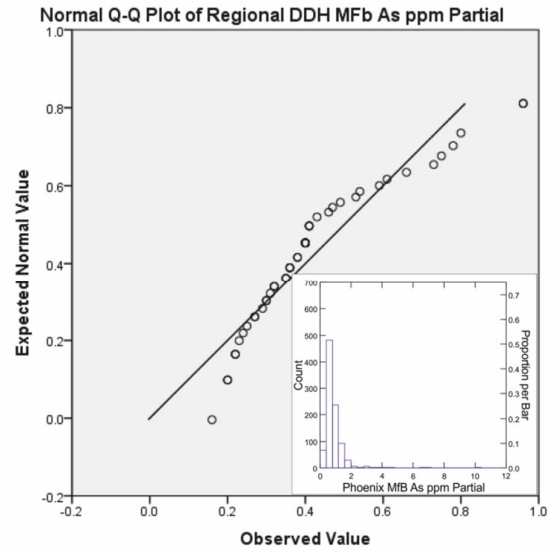
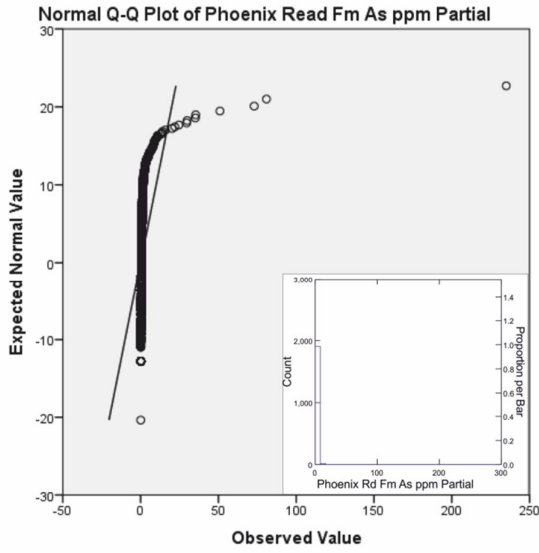


Figure 6: Partial leach As values from sandstone overlying the Phoenix deposit. Detection Limit of 0.01ppm As.



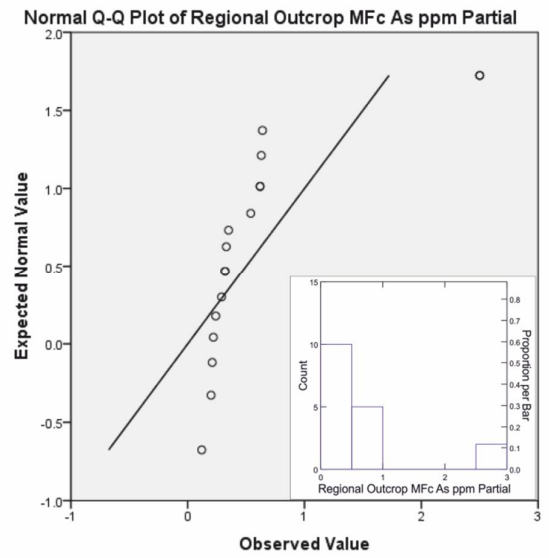
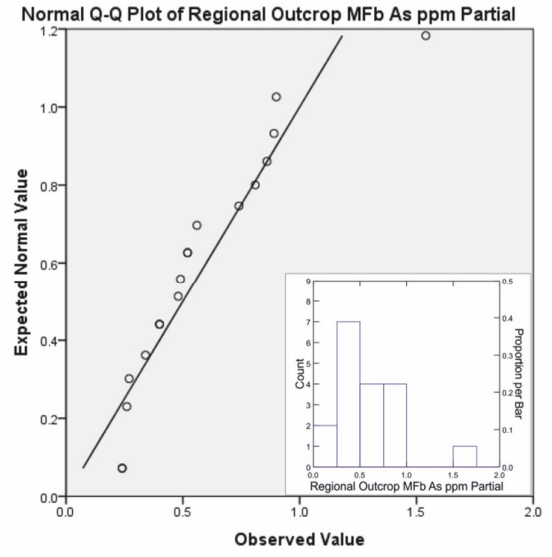
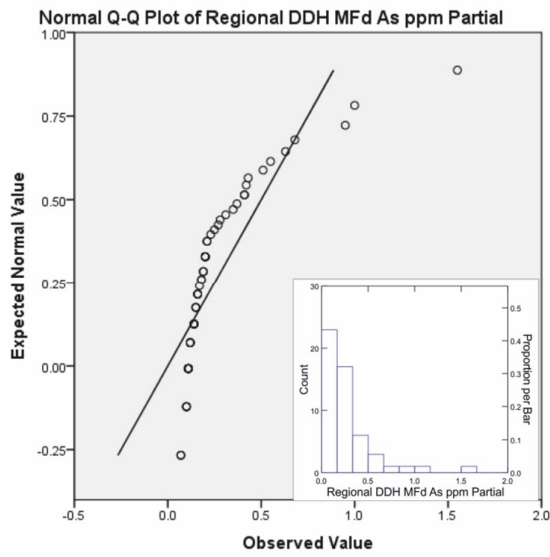


Figure 7: Q-Q and histogram (insets) plots of partial arsenic values from regional outcrop, regional DDH and sandstones overlying the Phoenix

Cobalt

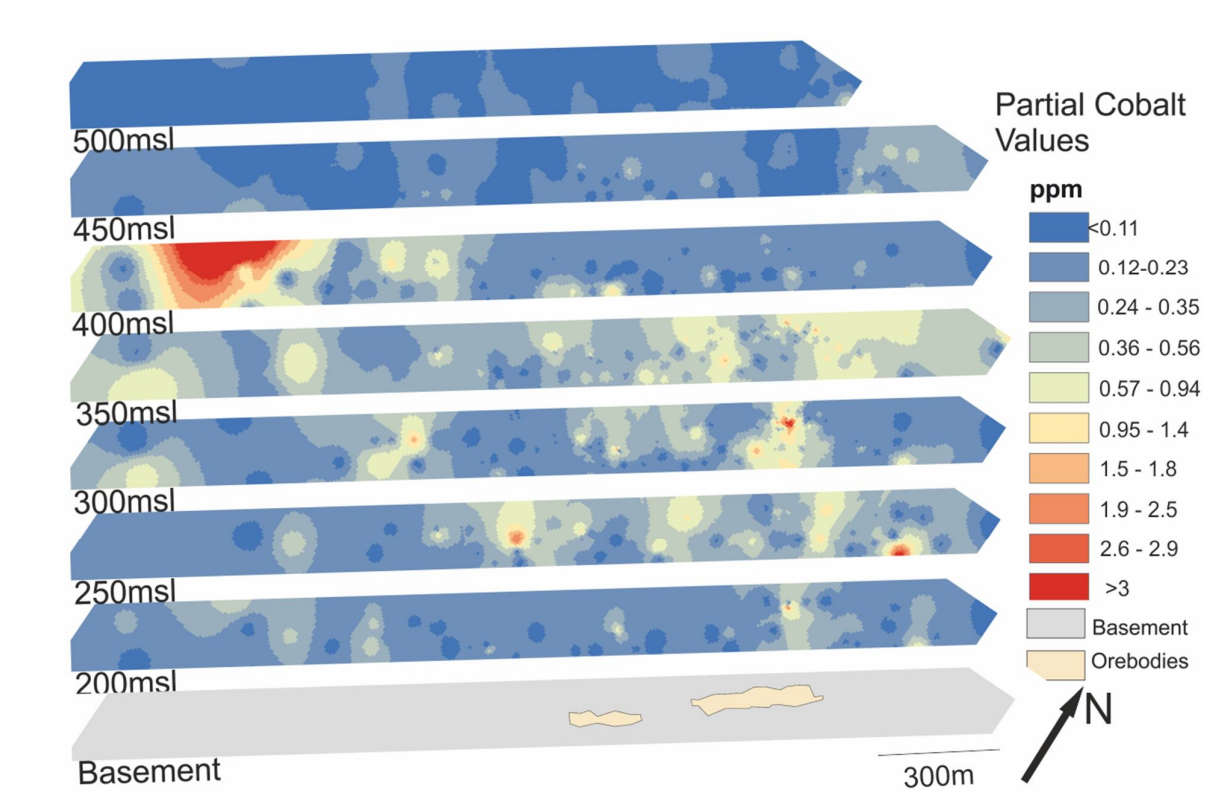
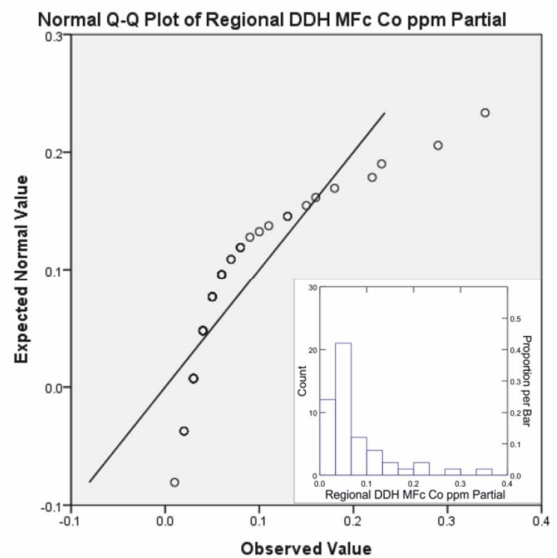
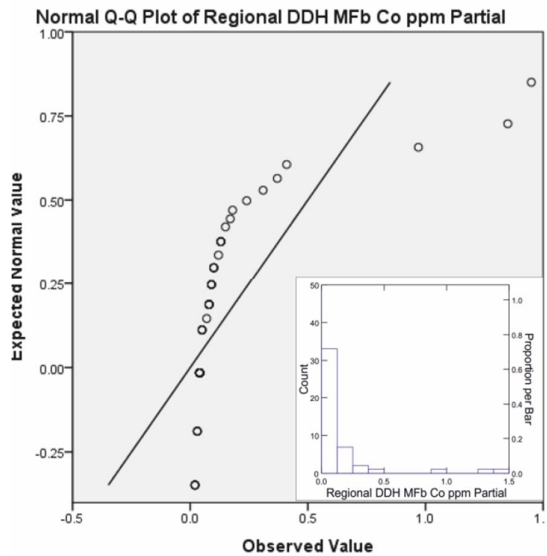
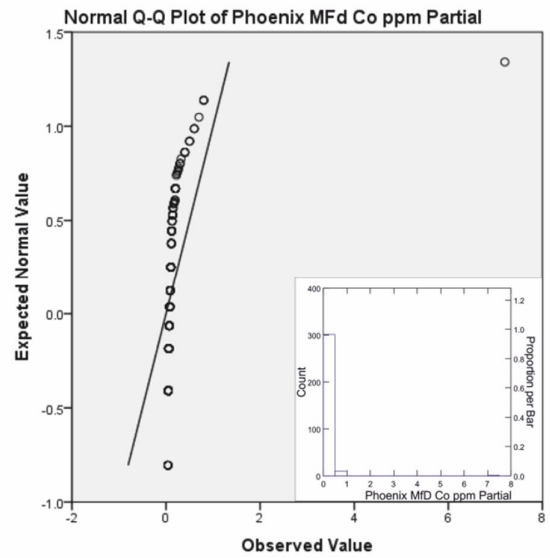
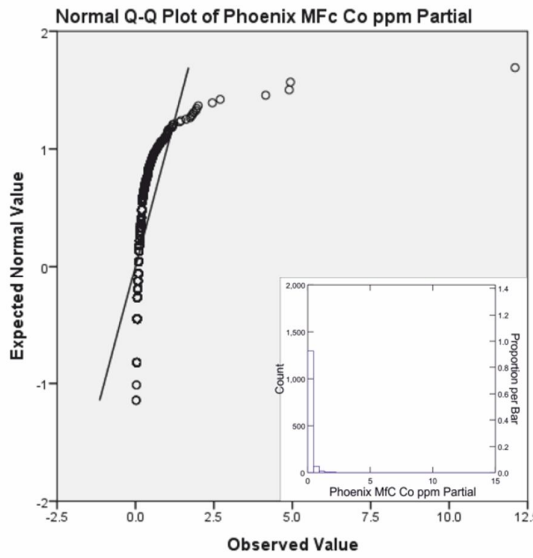
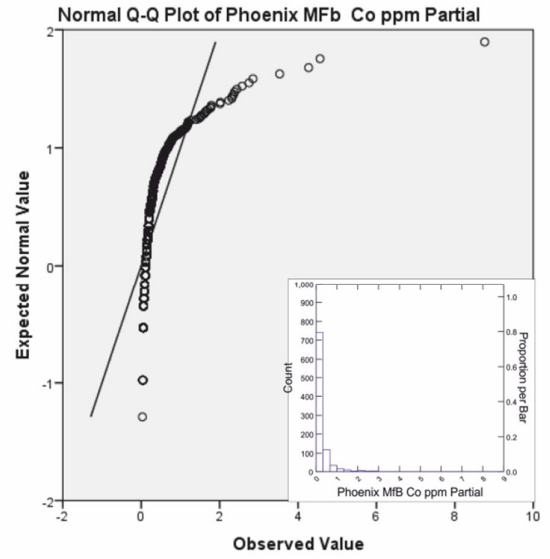
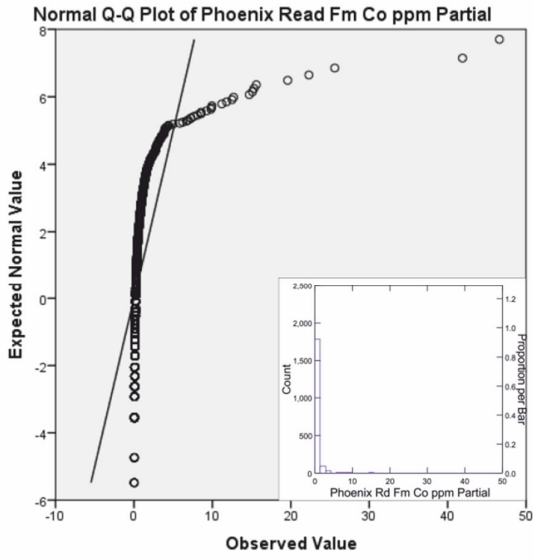


Figure 8: Partial leach cobalt values from sandstone overlying the Phoenix deposit. Detection Limit of 0.01ppm Co.



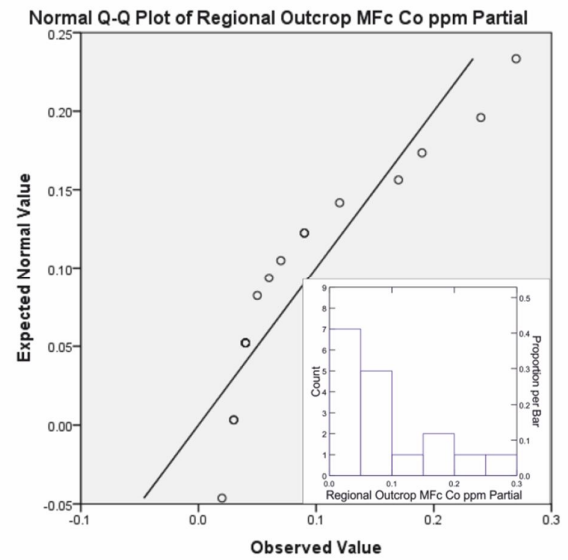
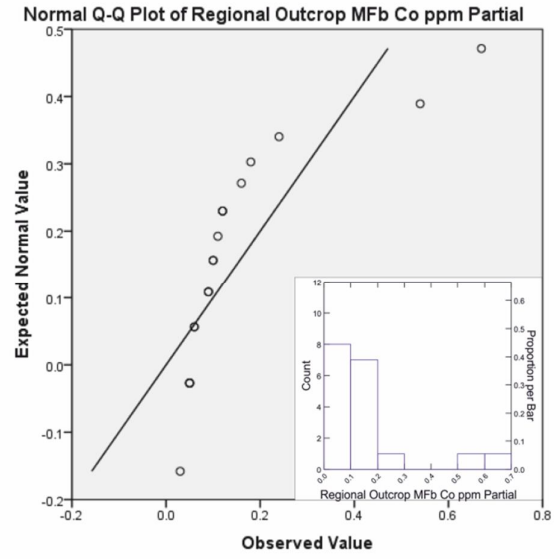
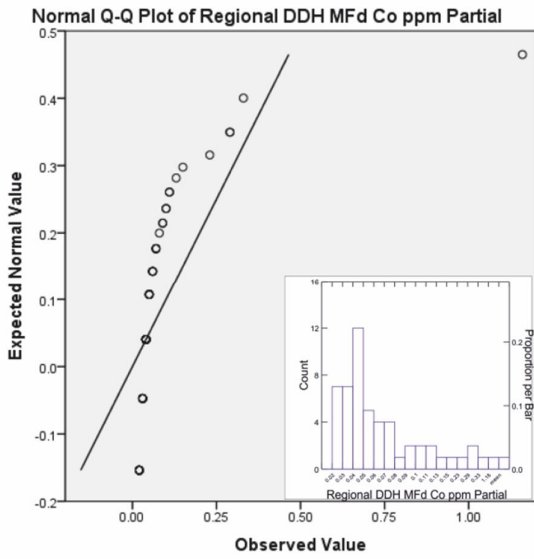


Figure 9: Q-Q and histogram (insets) plots of partial leach cobalt values from regional outcrop, regional DDH and sandstones overlying the Phoenix deposit.

Copper

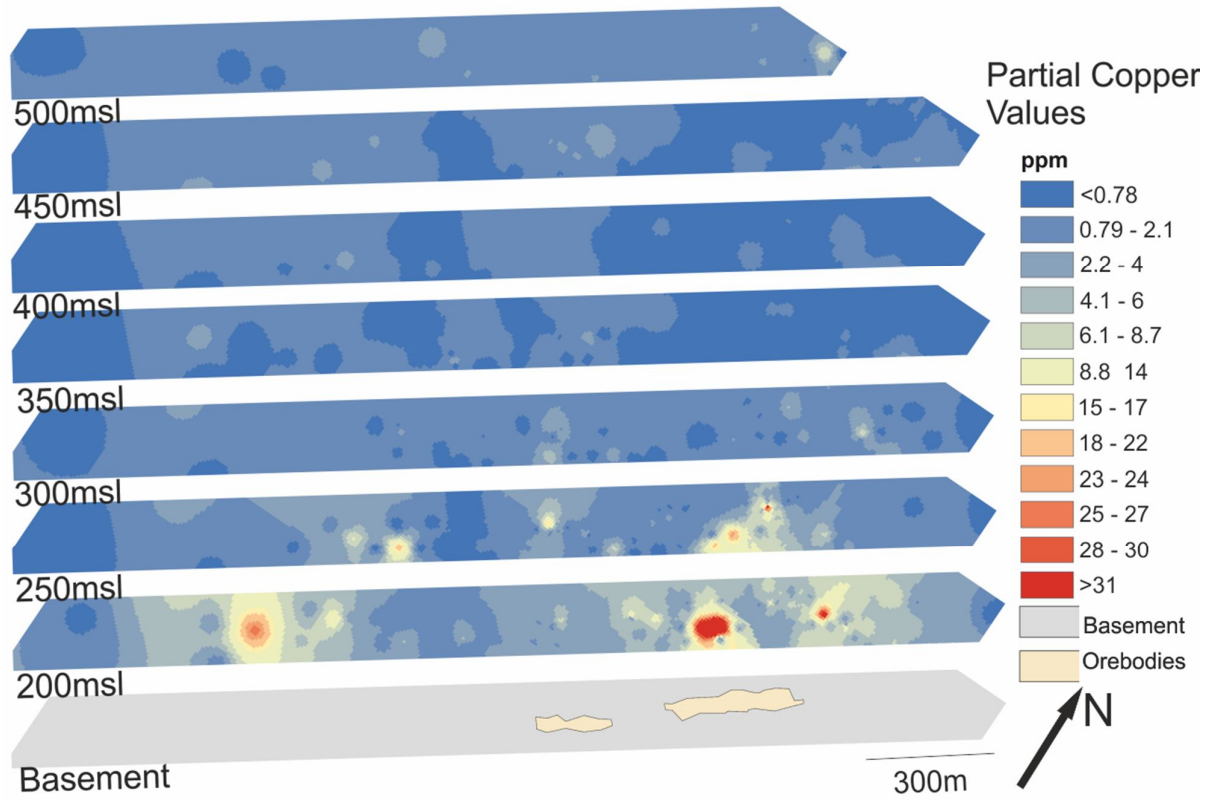
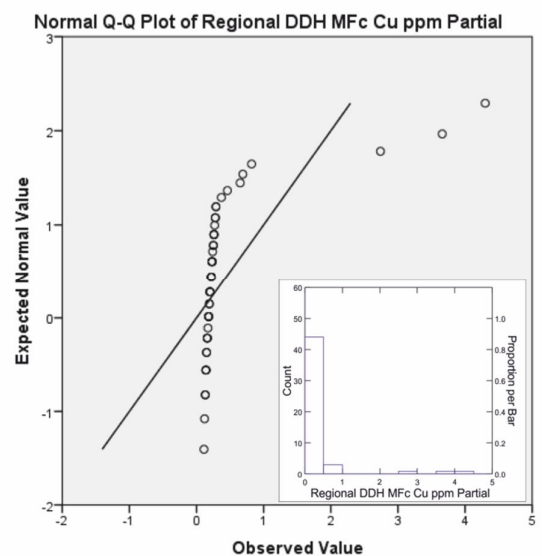
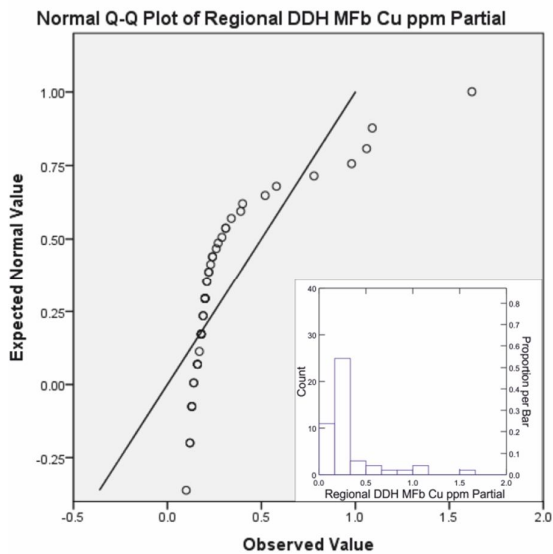
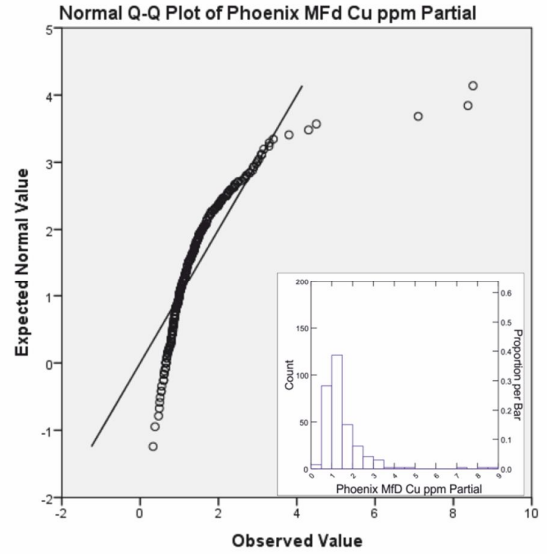
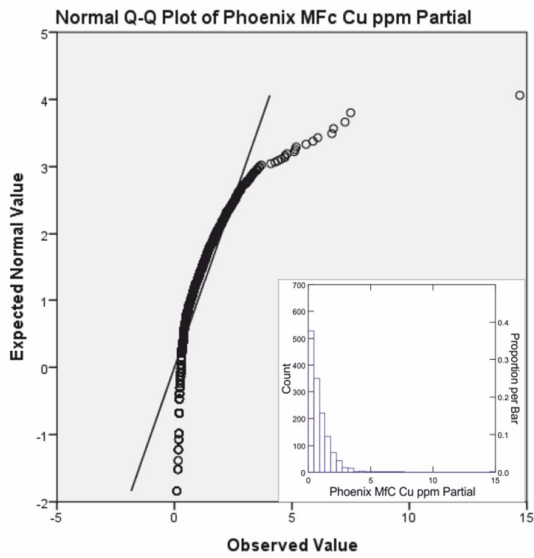
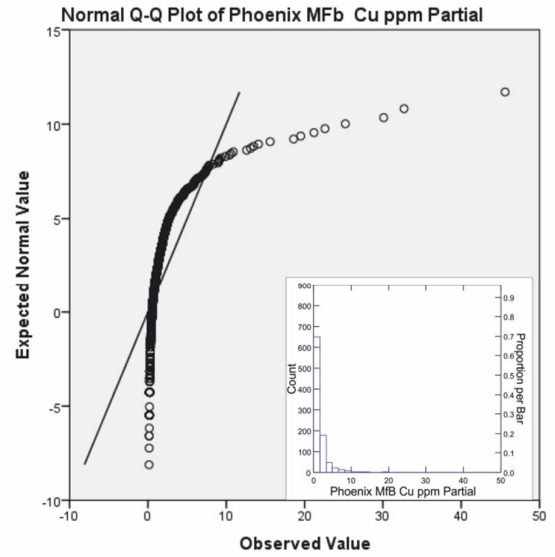
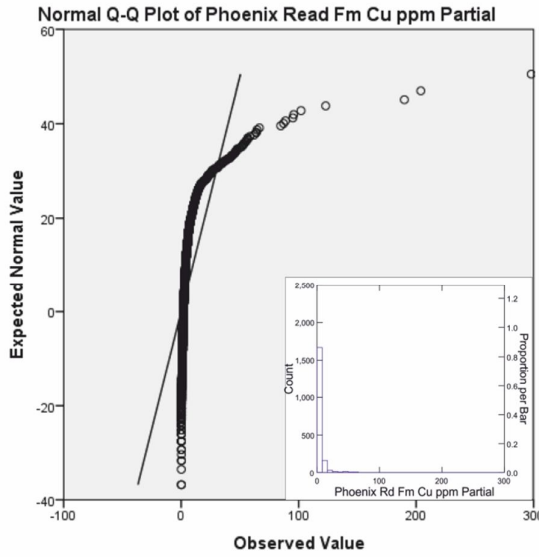


Figure 10: Partial leach copper values from sandstone overlying the Phoenix deposit. Detection Limit of 0.01ppm Cu.



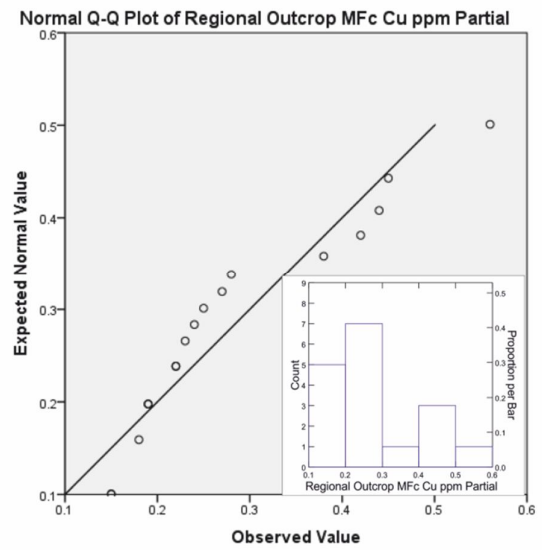
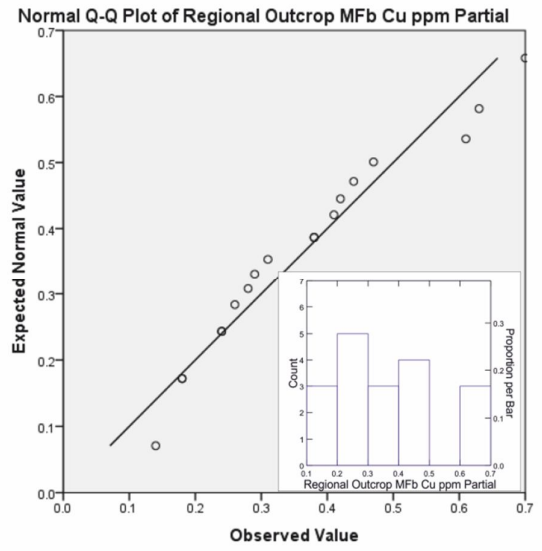
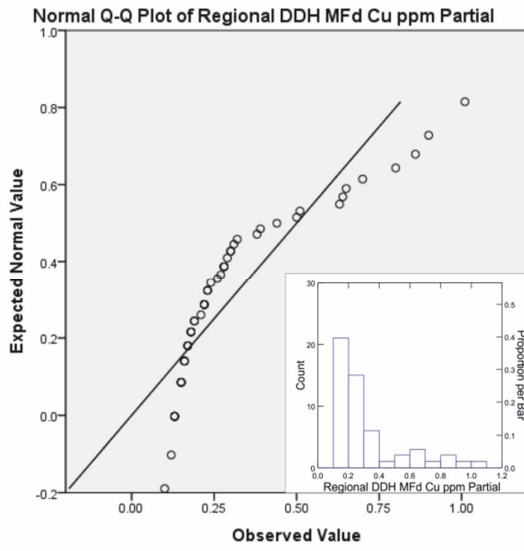


Figure 11: Q-Q and histogram (insets) plots of partial leach copper values from regional outcrop, regional DDH and sandstones overlying the Phoenix deposit.

Molybdenum

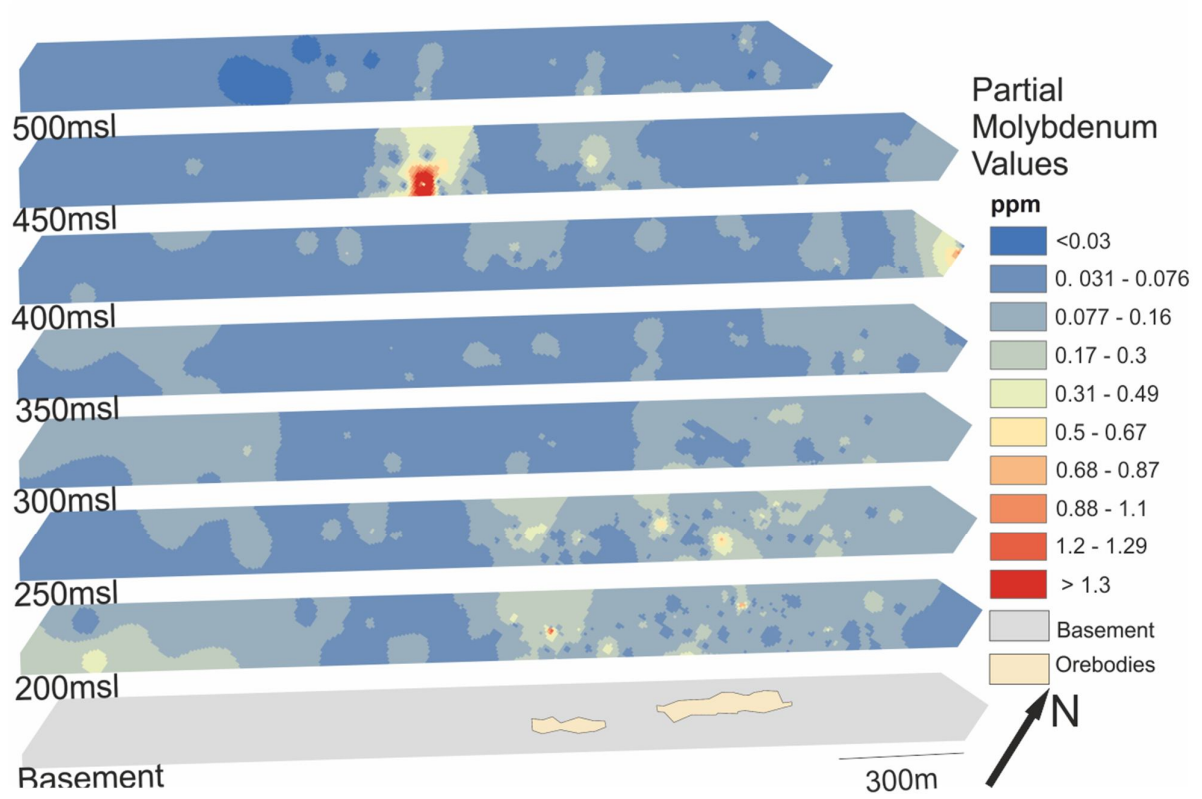
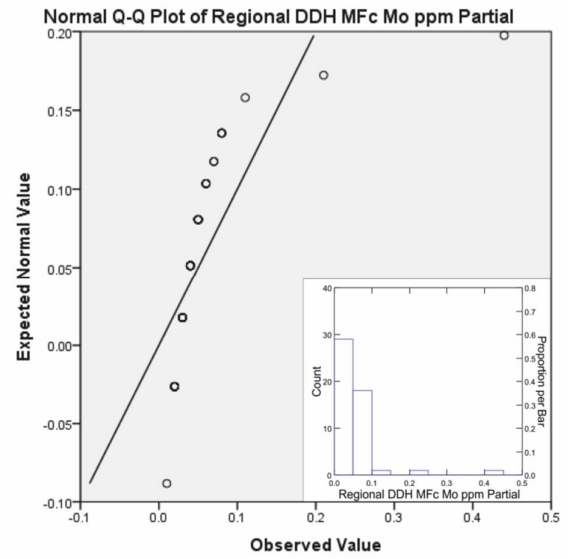
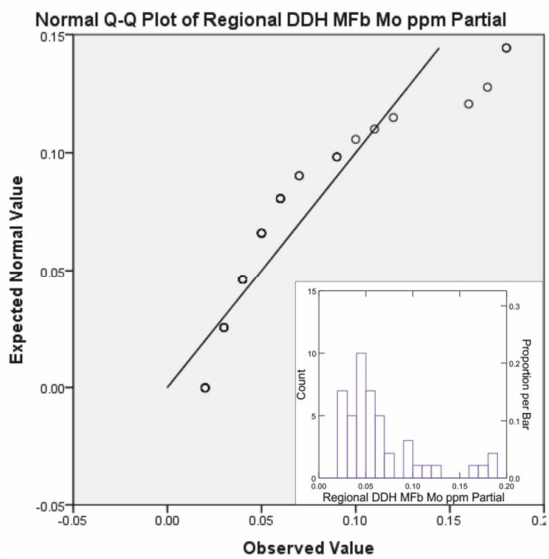
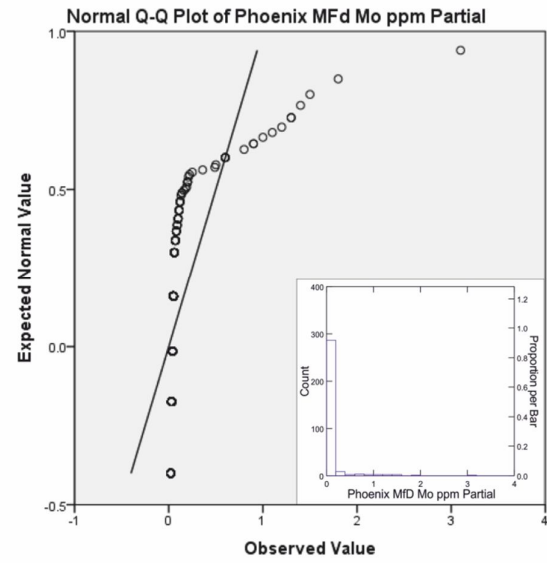
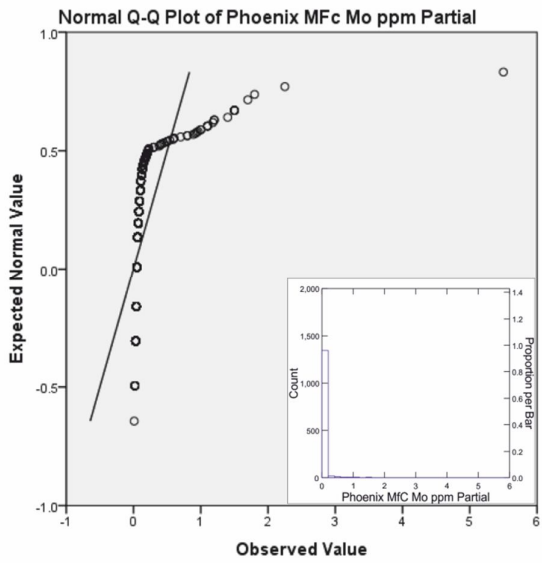
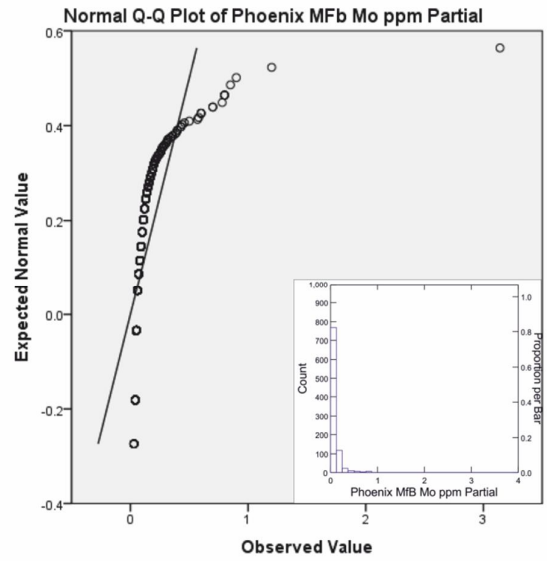
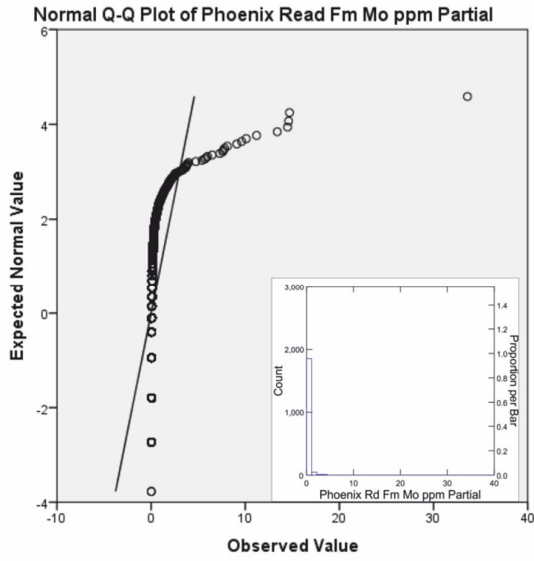


Figure 12: Partial leach molybdenum values from sandstone overlying the Phoenix deposit. Detection Limit of 0.01ppm Mo



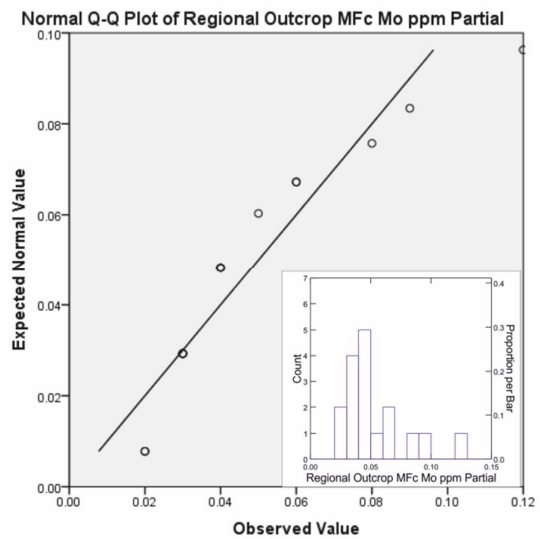
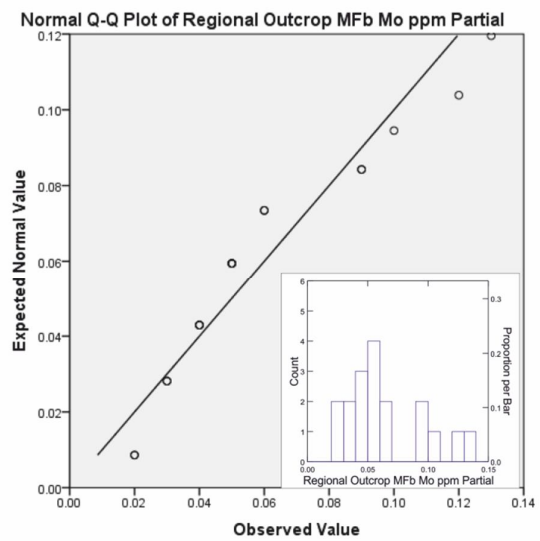
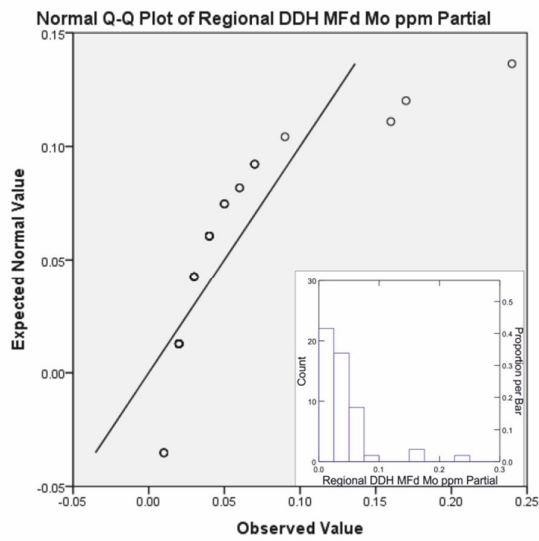


Figure 13: Q-Q and histogram (insets) plots of partial leach molybdenum values from regional outcrop, regional DDH and sandstones overlying the Phoenix deposit.

Nickel

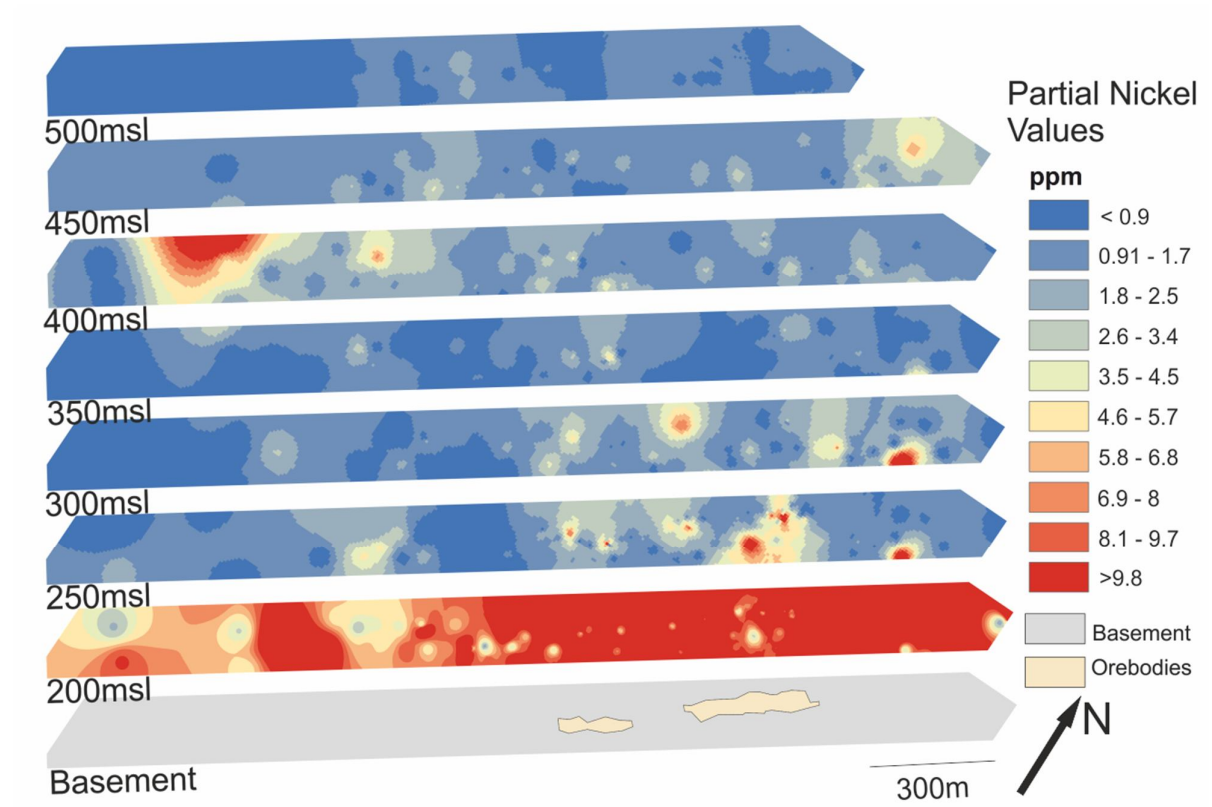
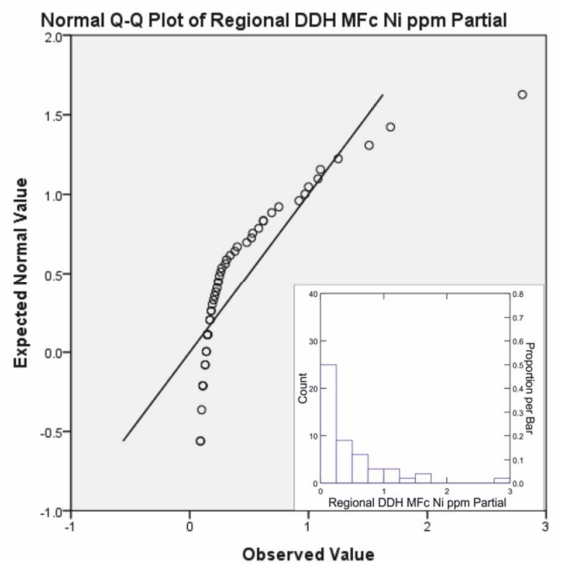
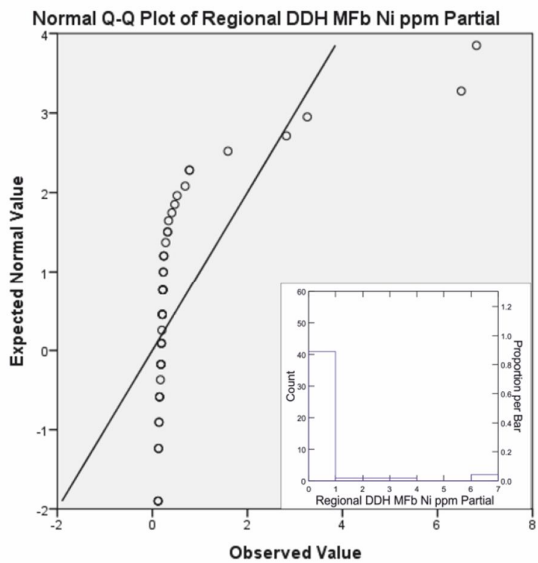
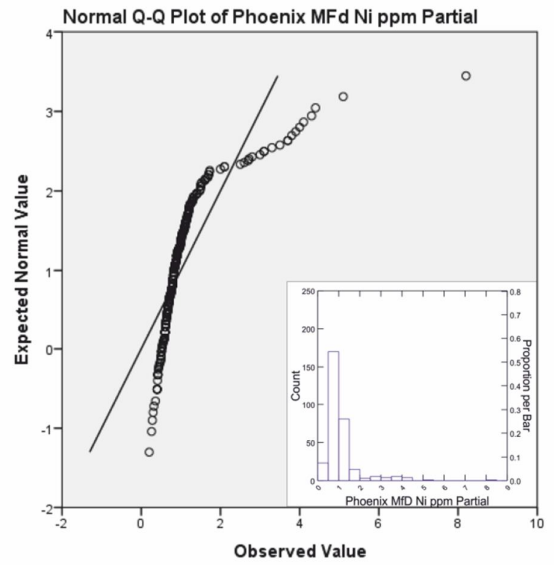
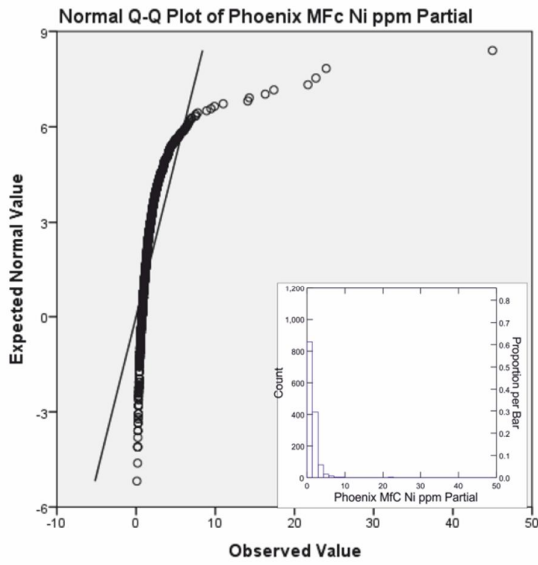
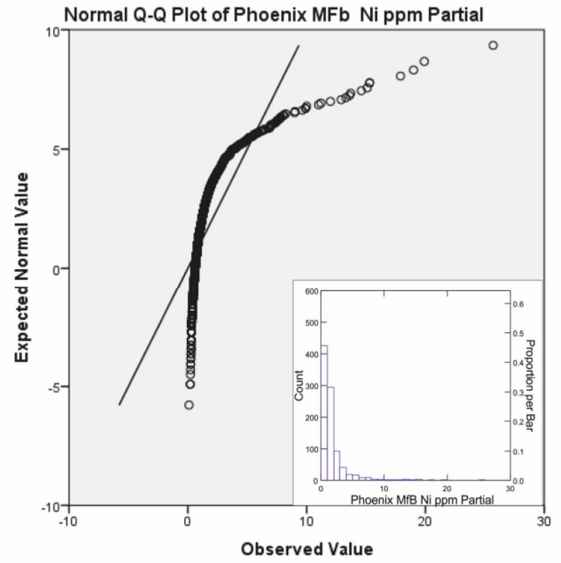
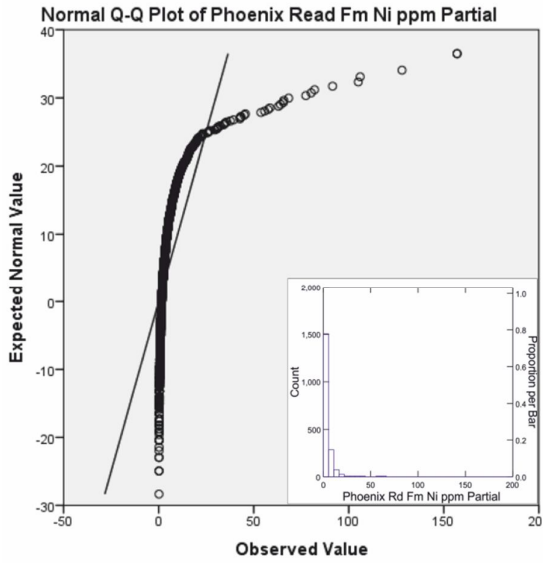


Figure 14: Partial leach nickel values from sandstone overlying the Phoenix deposit. Detection Limit of 0.01ppm Ni.



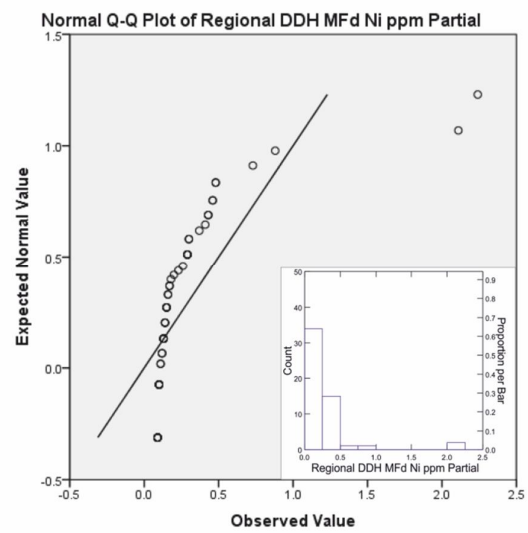
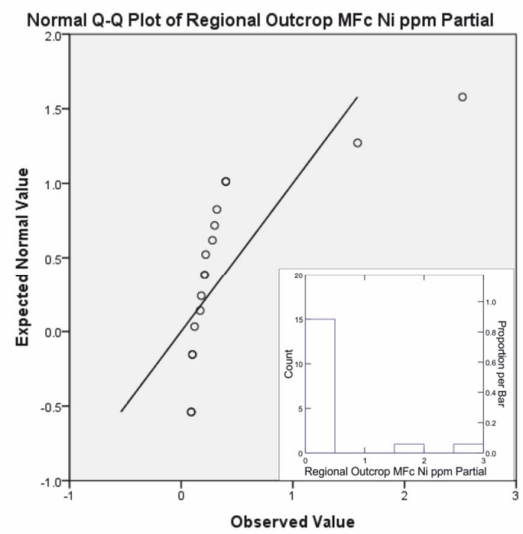
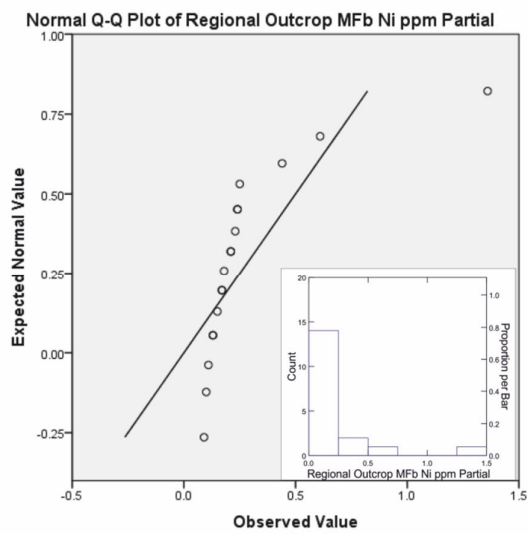


Figure 15: Q-Q and histogram (insets) plots of partial leach nickel values from regional outcrop, regional DDH and sandstones overlying the Phoenix deposit.

Vanadium

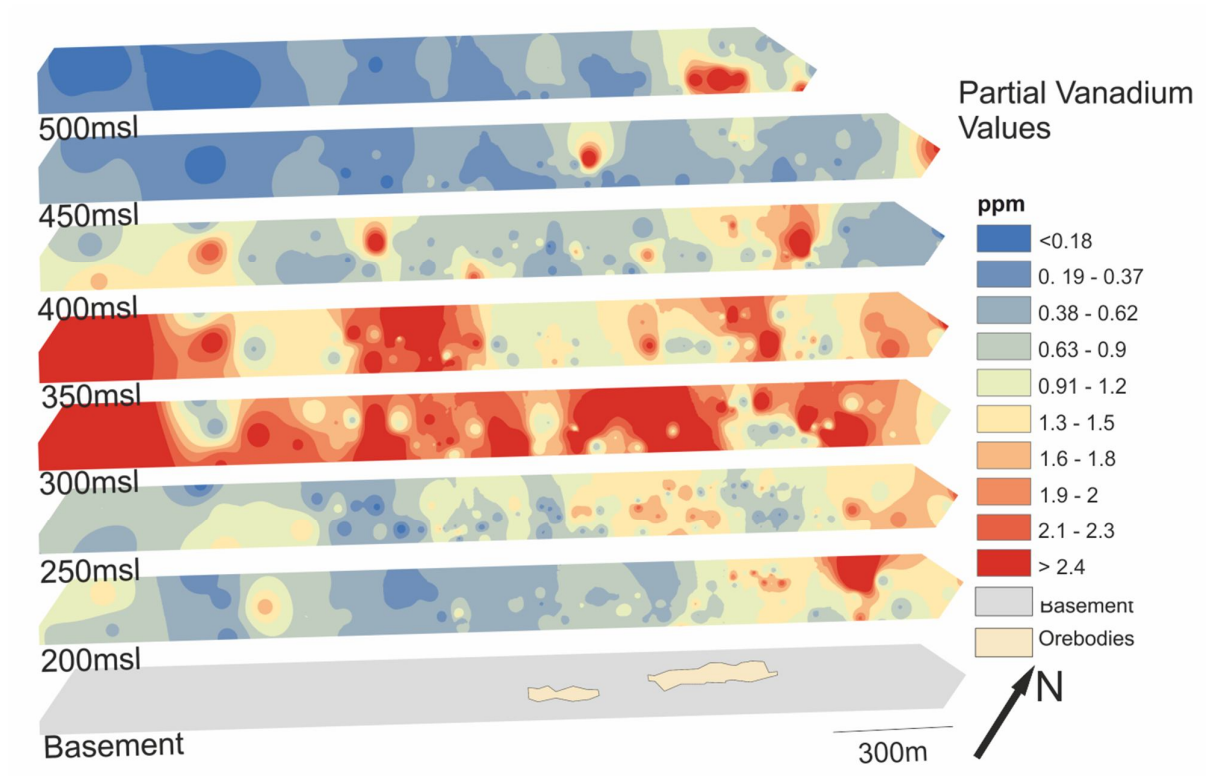
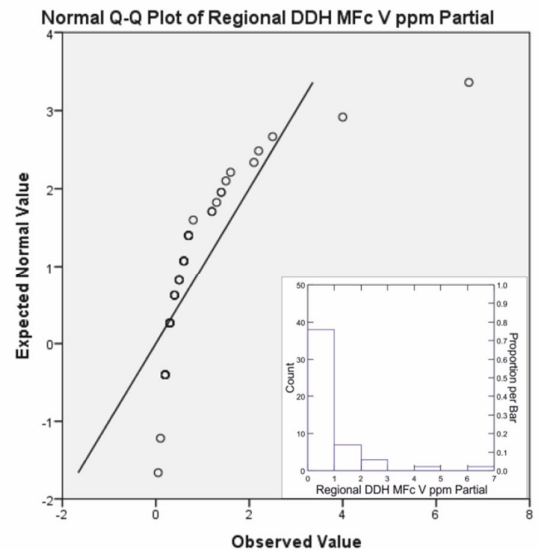
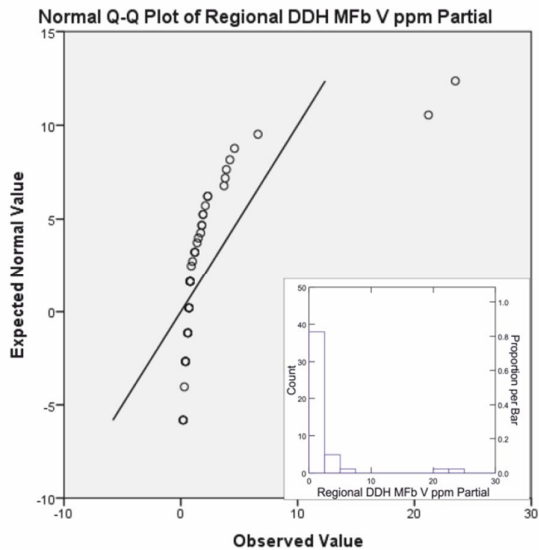
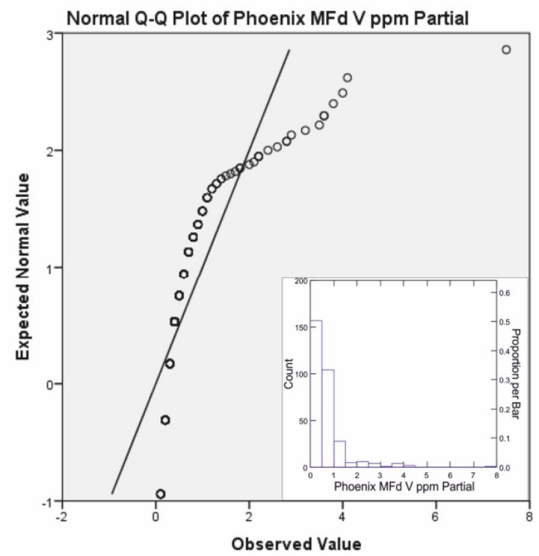
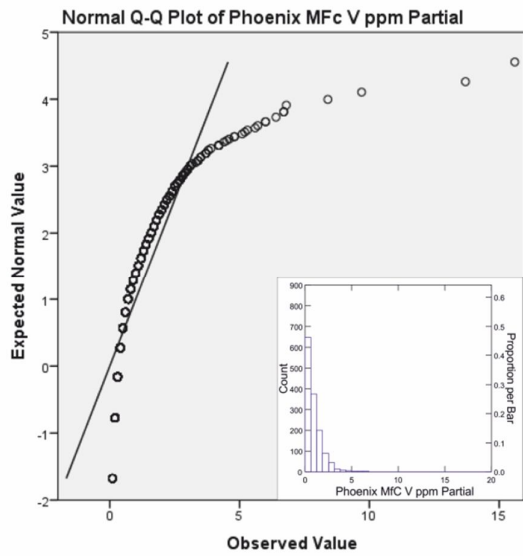
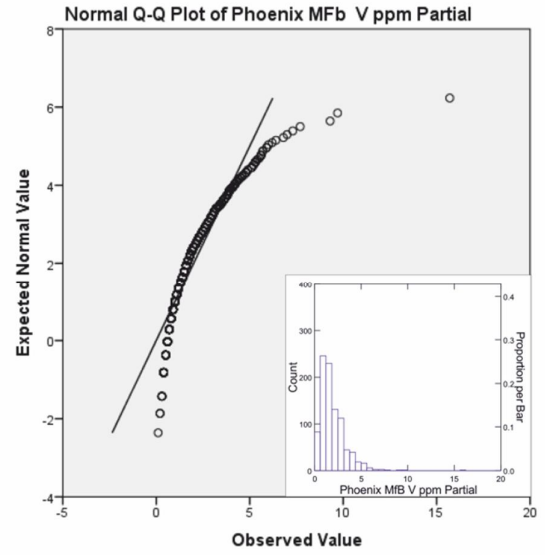
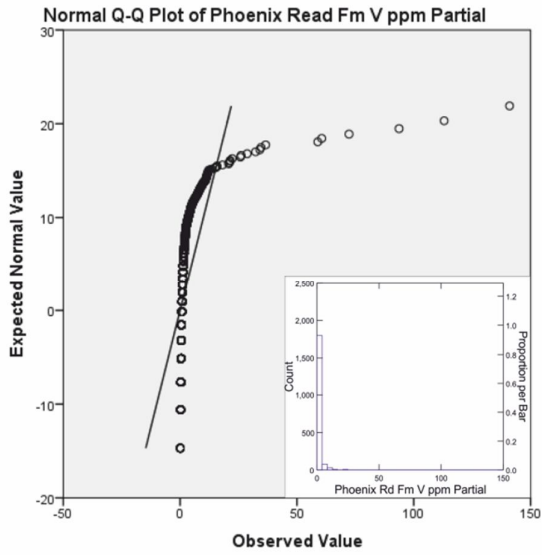


Figure 16: Partial leach vanadium values from sandstone overlying the Phoenix deposit. Detection Limit of 0.01ppm V.



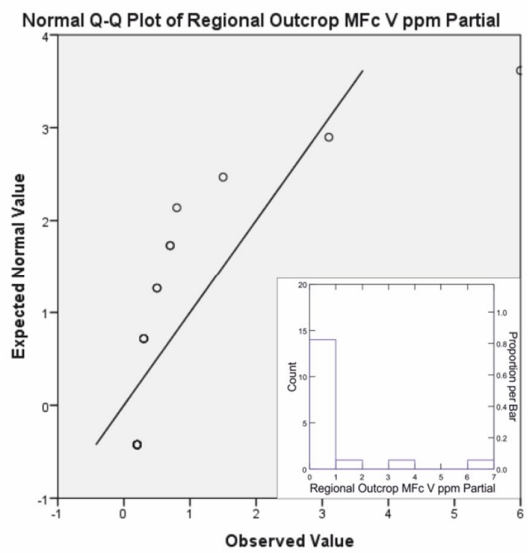
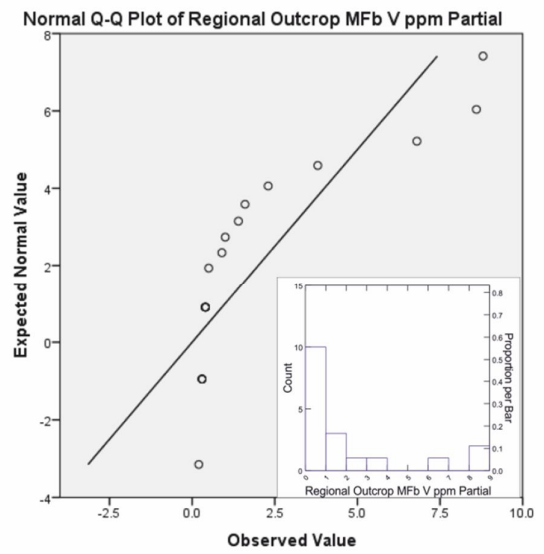
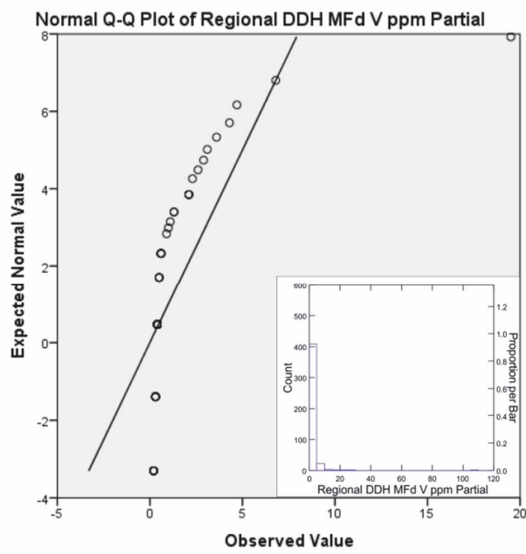


Figure 17: Q-Q and histogram (insets) plots of vanadium values from regional outcrop, regional DDH and sandstones overlying the Phoenix deposit.

Lead

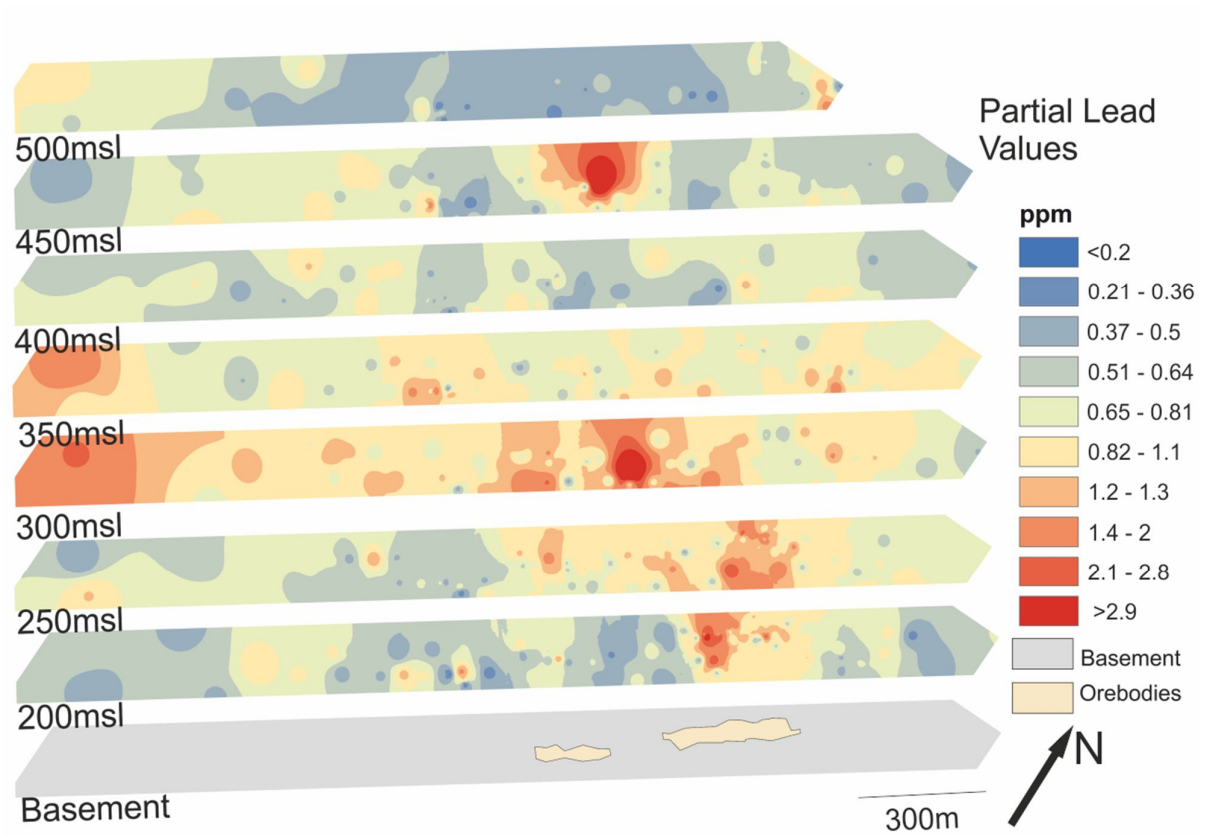
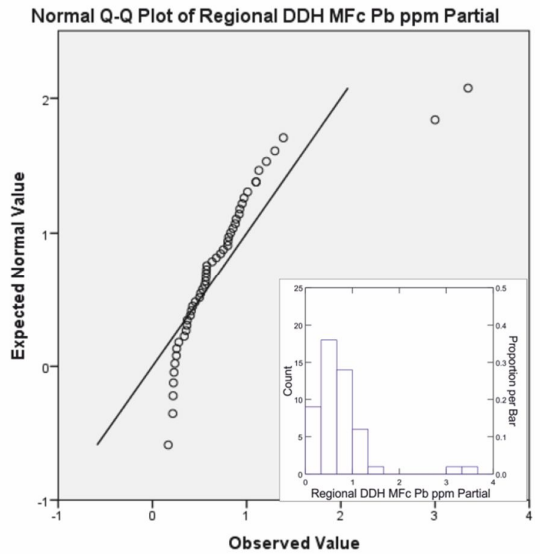
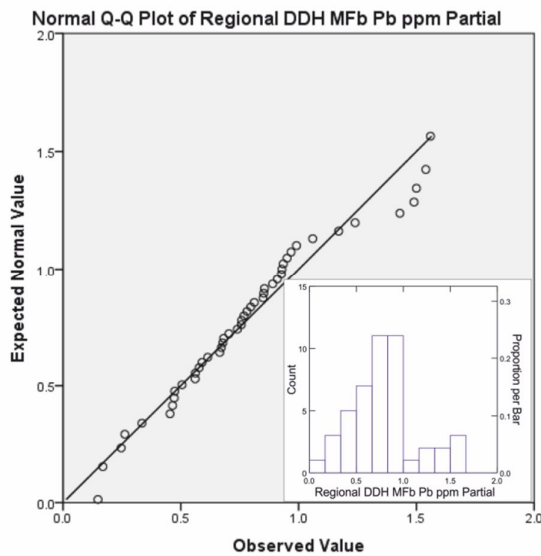
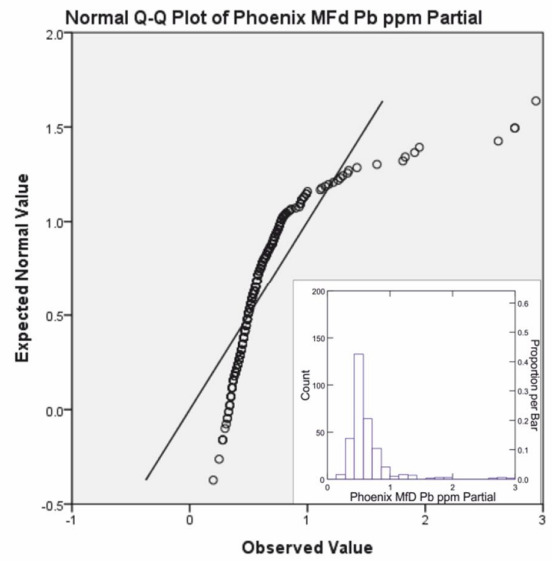
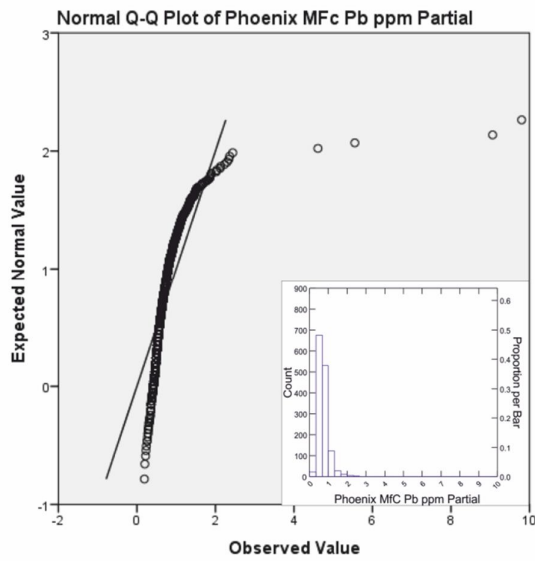
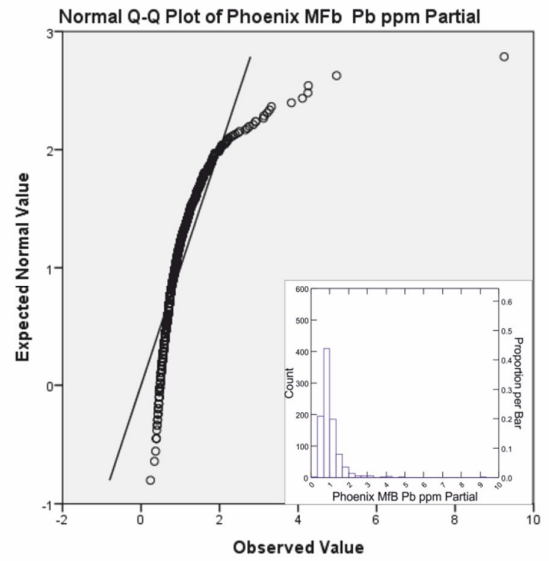
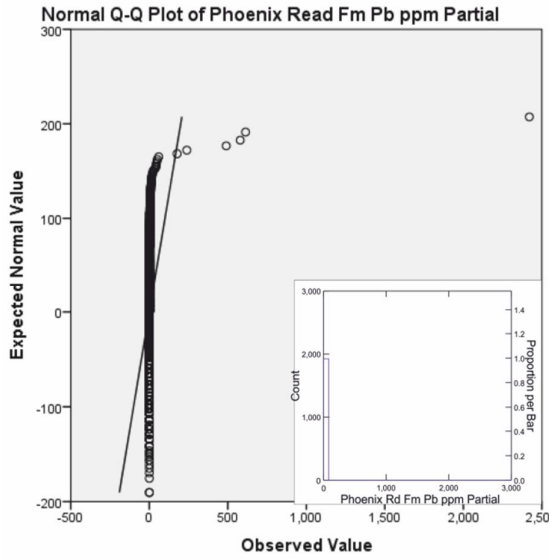


Figure 18: Partial leach lead values from sandstone overlying the Phoenix deposit. Detection Limit of 0.02ppm Pb.



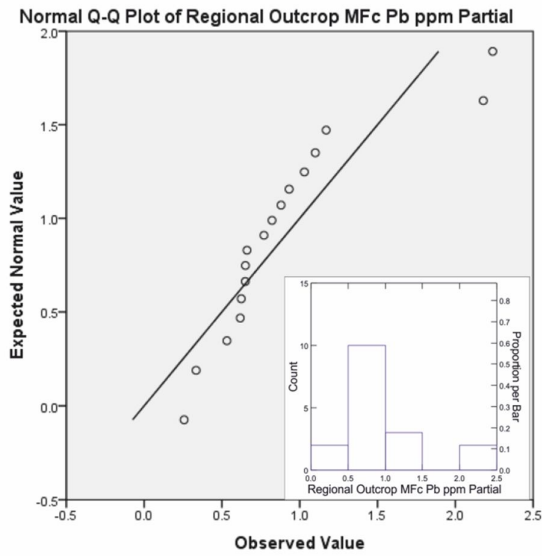
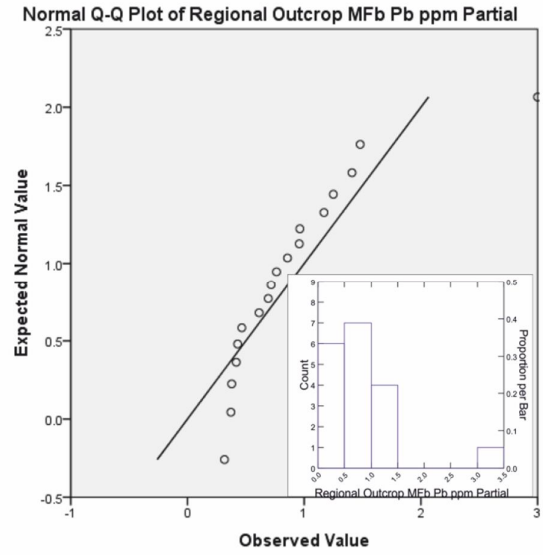
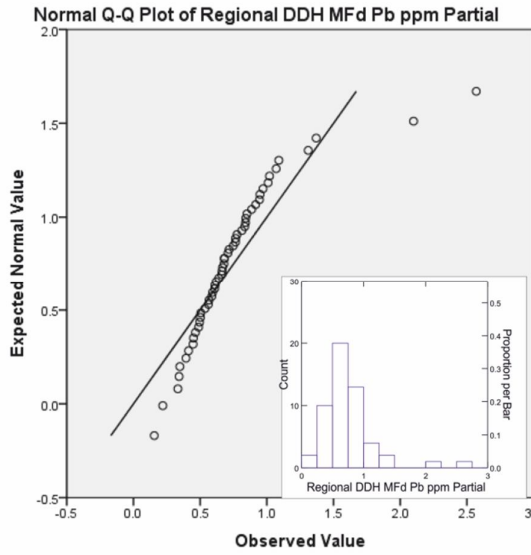


Figure 19: Q-Q and histogram (insets) plots of partial lead values from regional outcrop, regional DDH and sandstones overlying the Phoenix deposit.

Magnesium

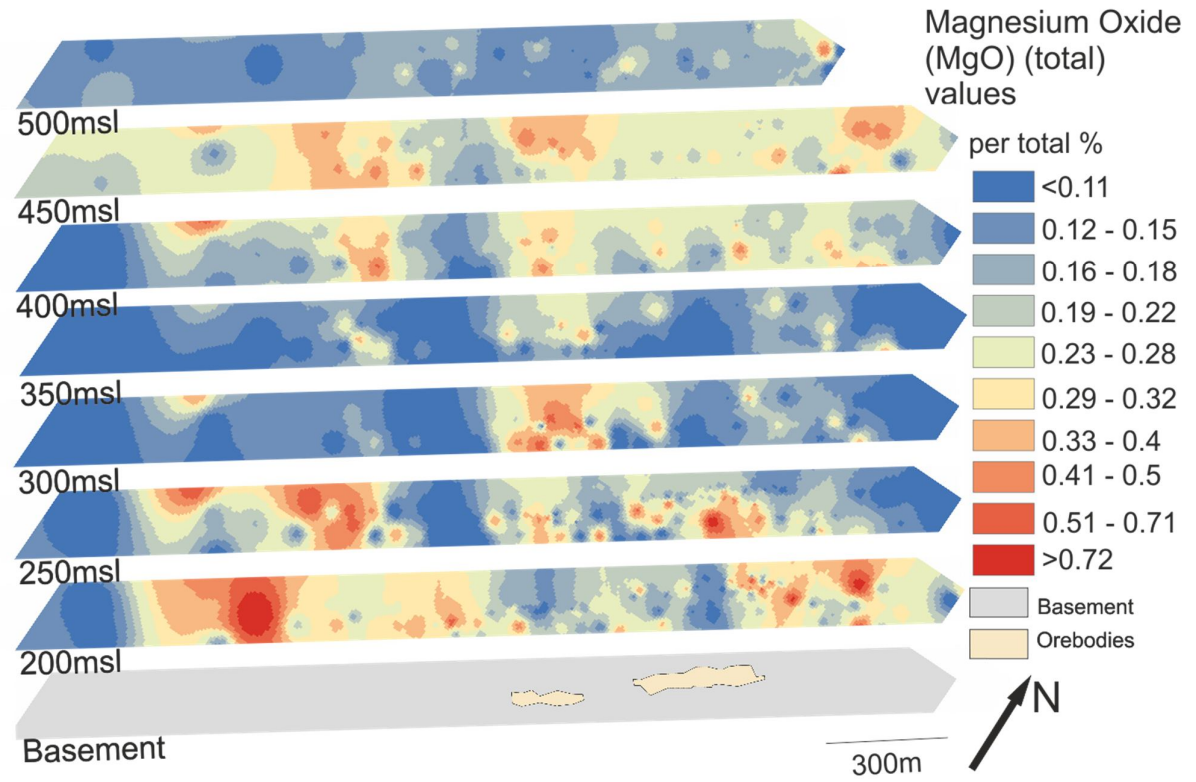
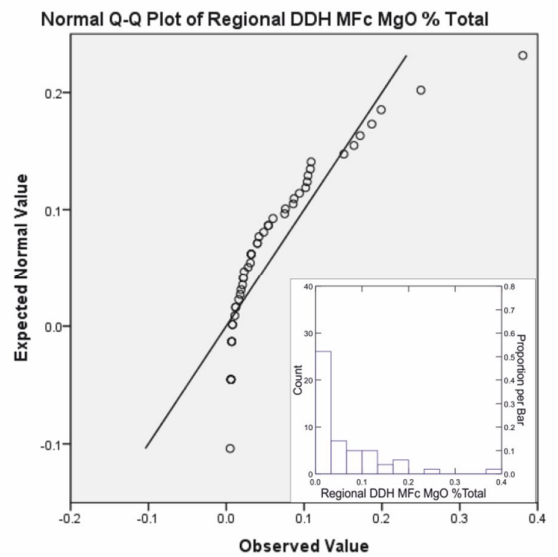
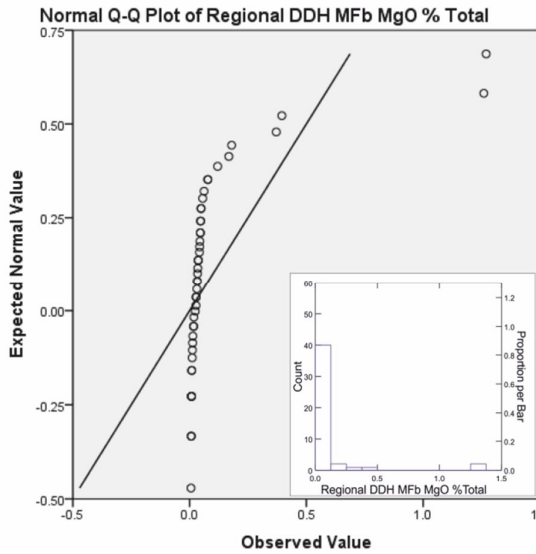
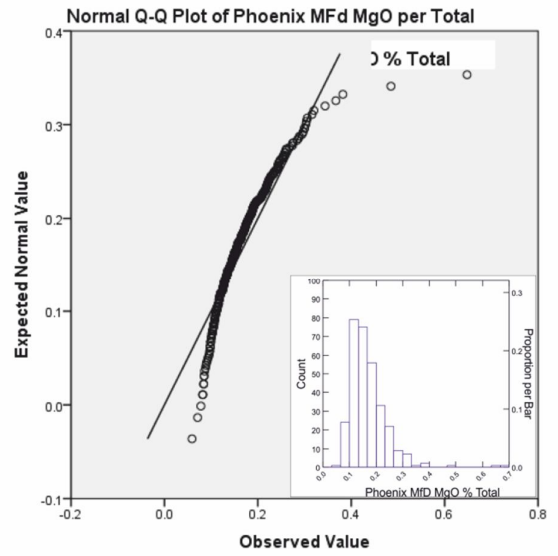
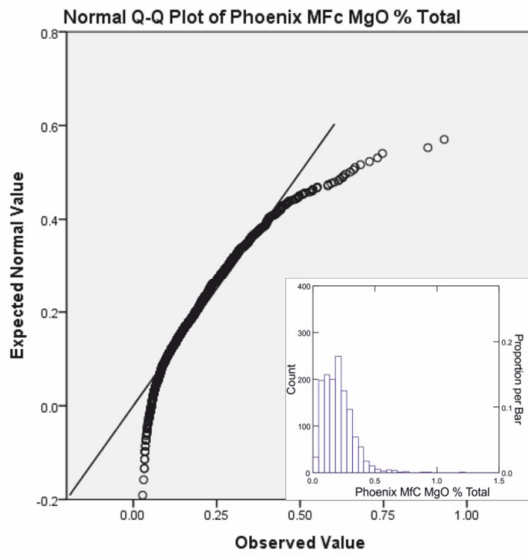
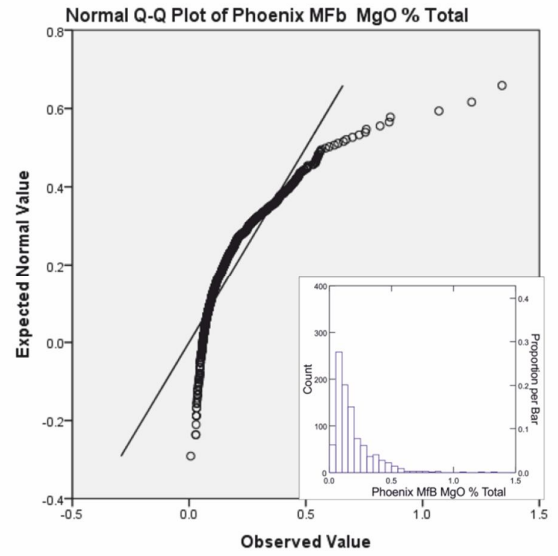
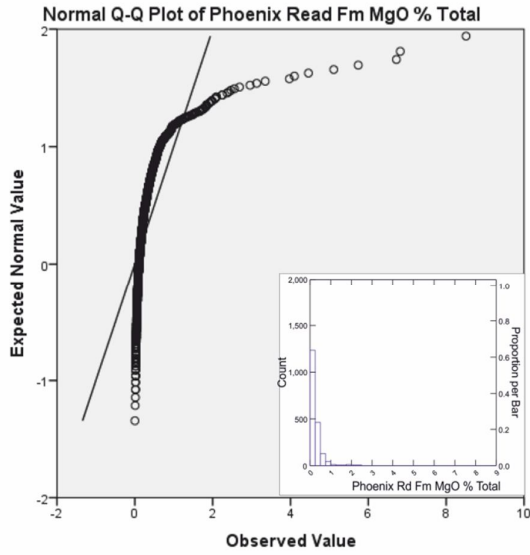


Figure 20: Total digestion magnesium oxide values from sandstone overlying the Phoenix deposit. Detection limit of 0.001% MgO.



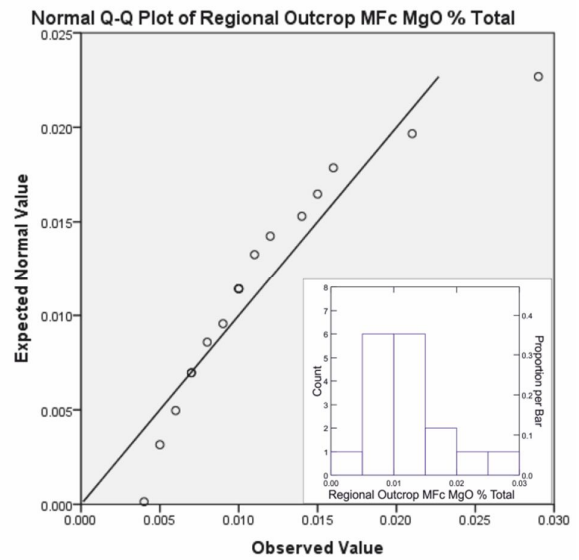
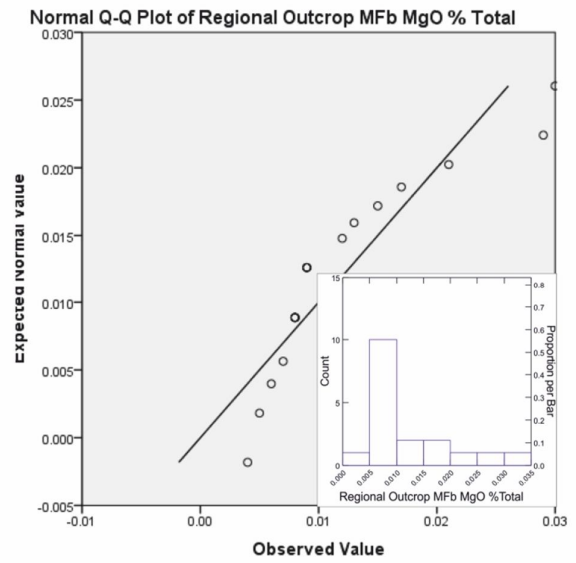
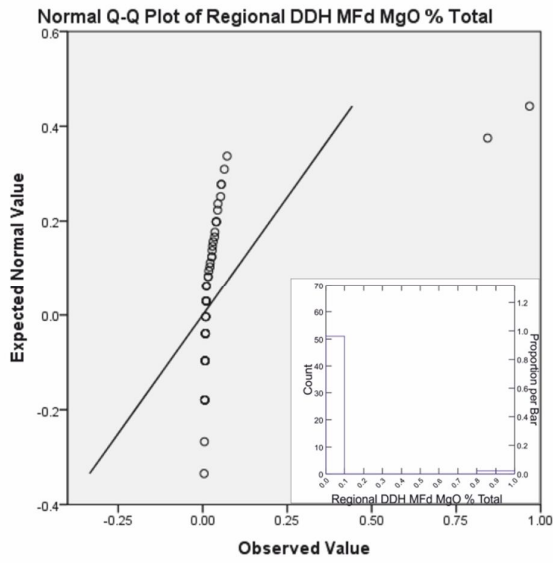


Figure 21: Q-Q and histogram (insets) plots of total digestion MgO values from regional outcrop, regional DDH and sandstones overlying the Phoenix deposit.

Lithium

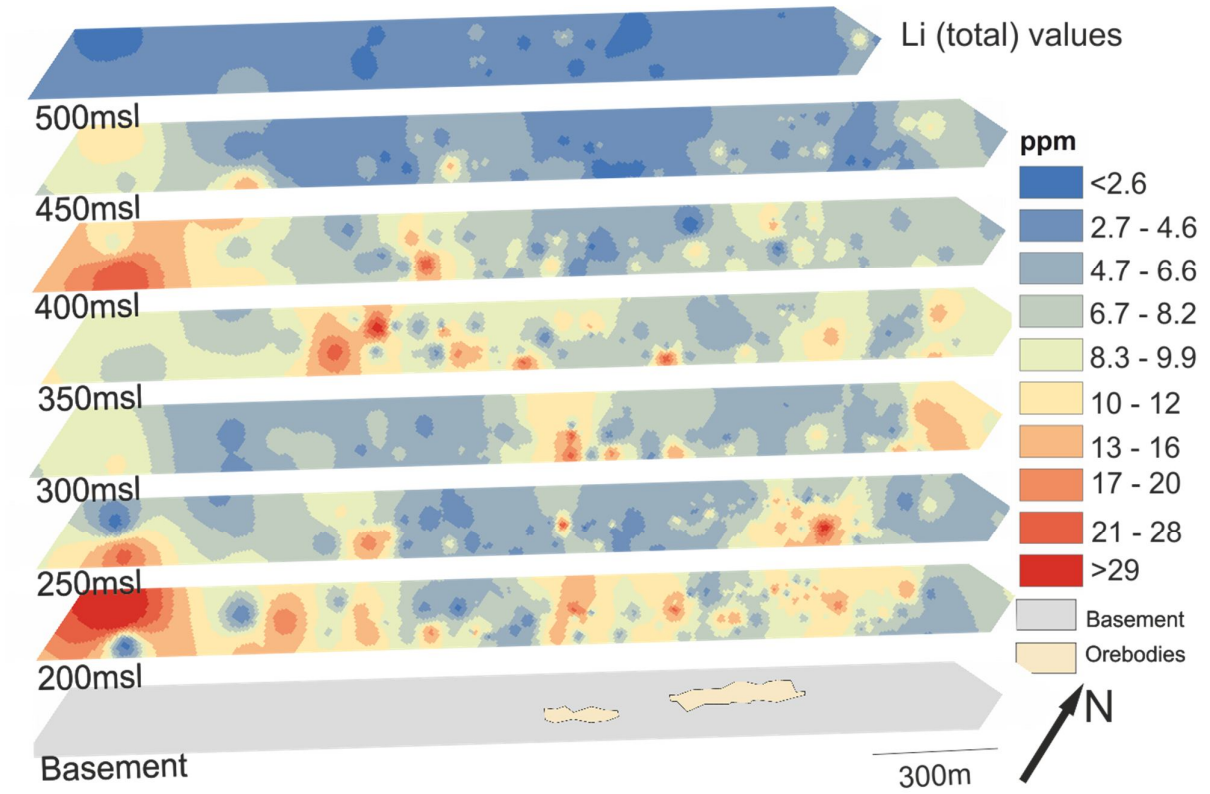
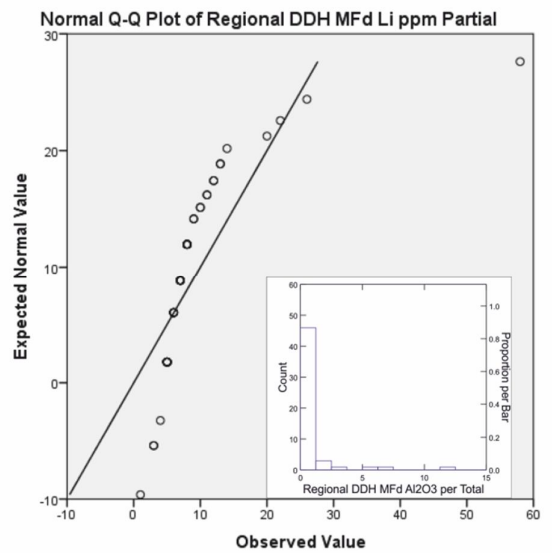
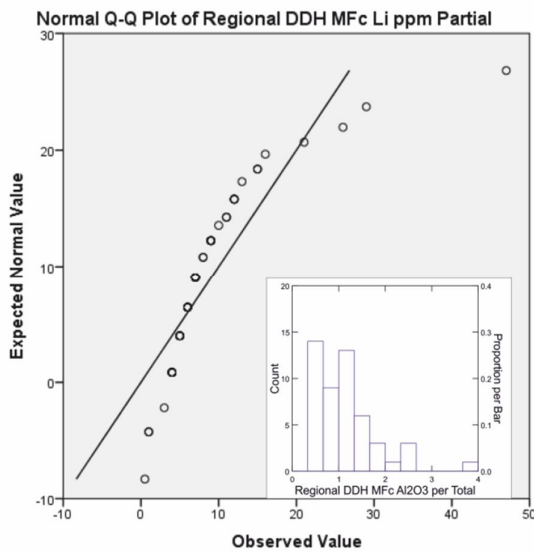
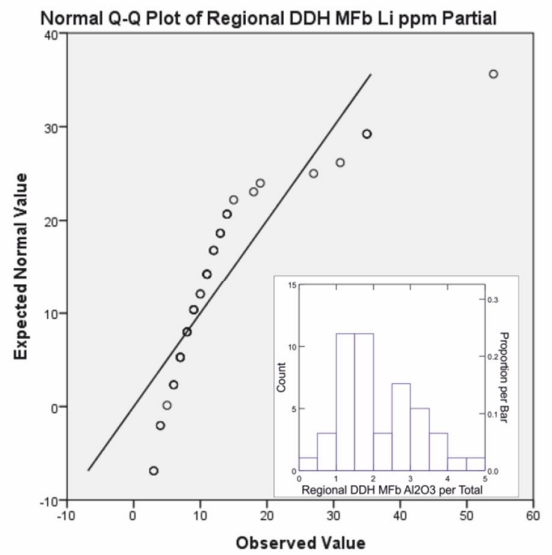
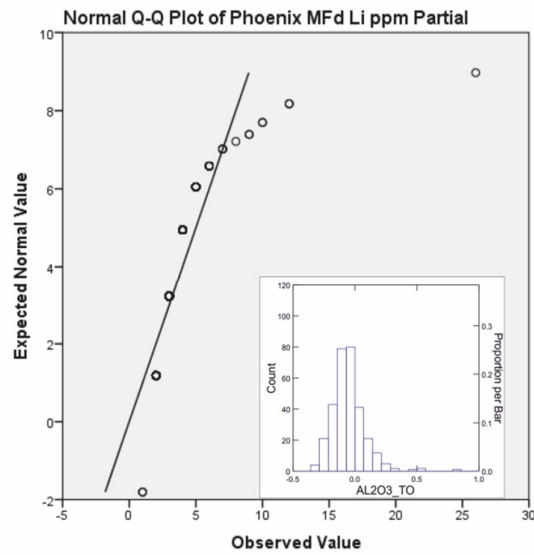
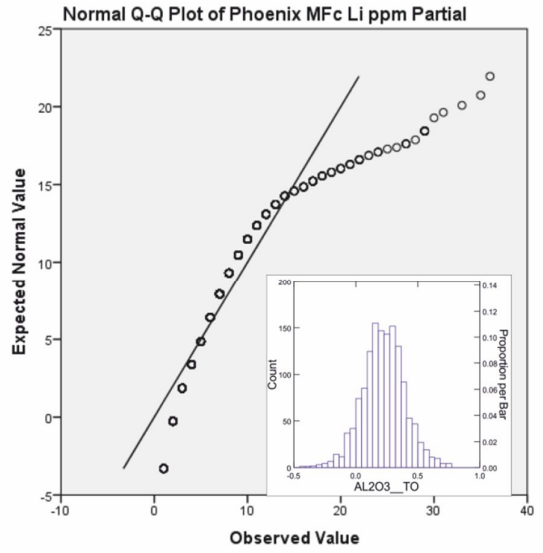
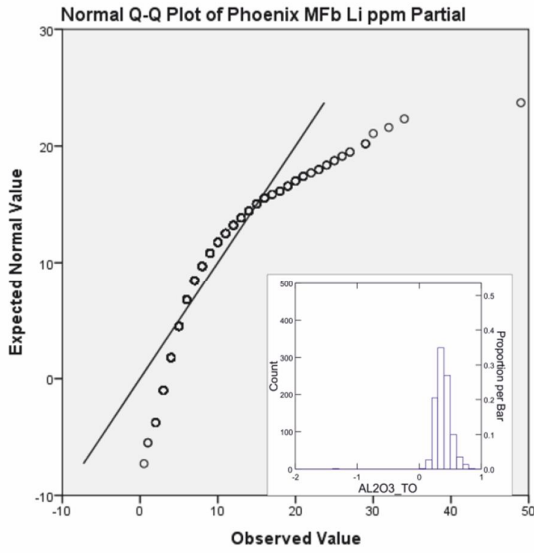


Figure 22: Total lithium values from sandstone overlying the Phoenix deposit. Detection limit of 1 ppm Li.



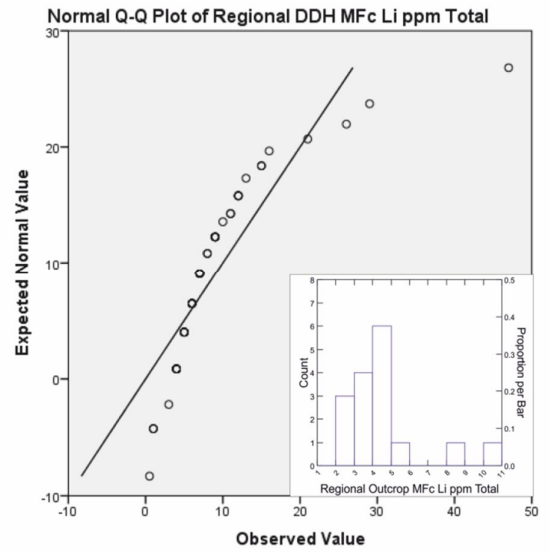
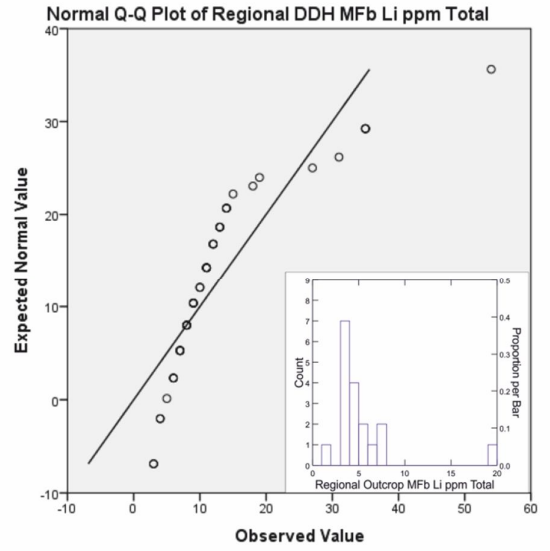
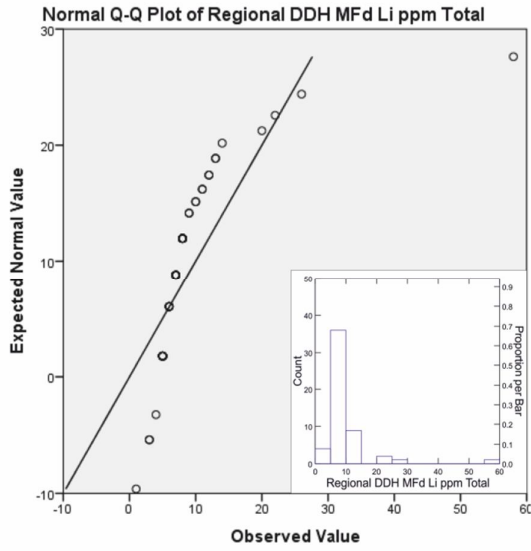


Figure 23: Q-Q and histogram (insets) plots of total digestion lithium values from regional outcrop, regional DDH and sandstones overlying the Phoenix deposit.

Boron

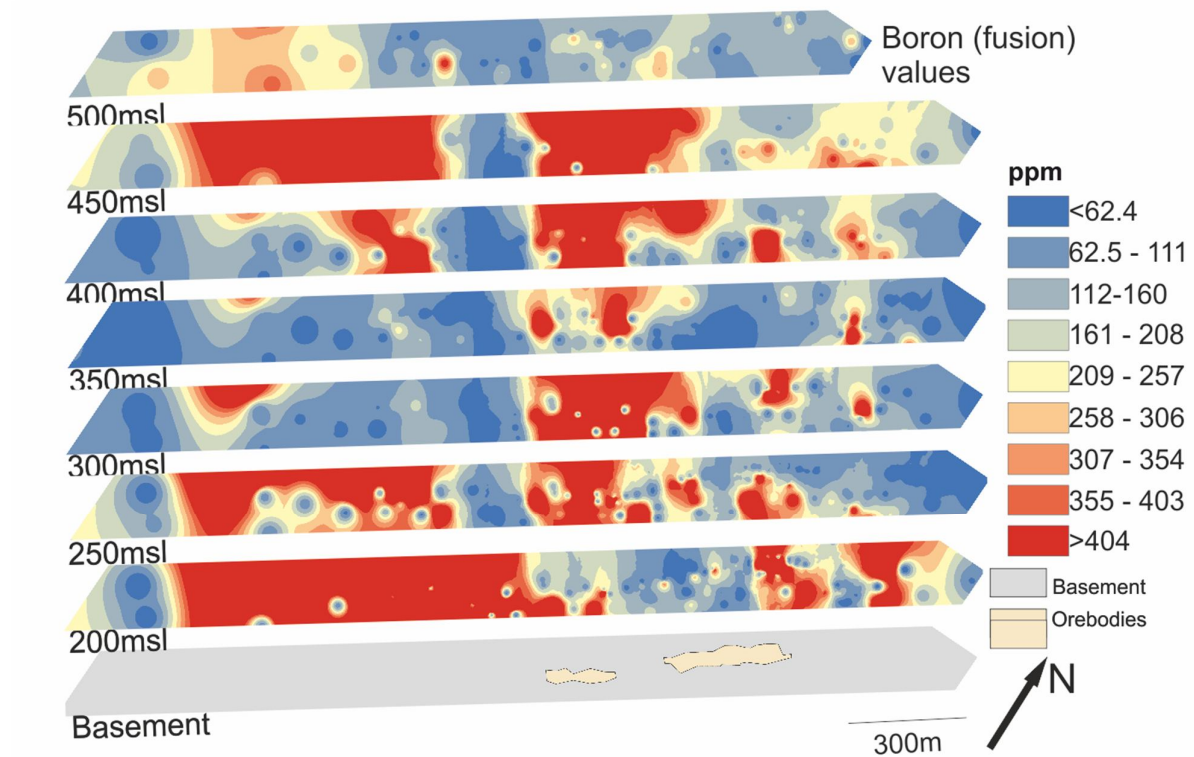


Figure 24: Total fusion values of boron from sandstone overlying the Phoenix deposit. Detection limit of 2 ppm B.

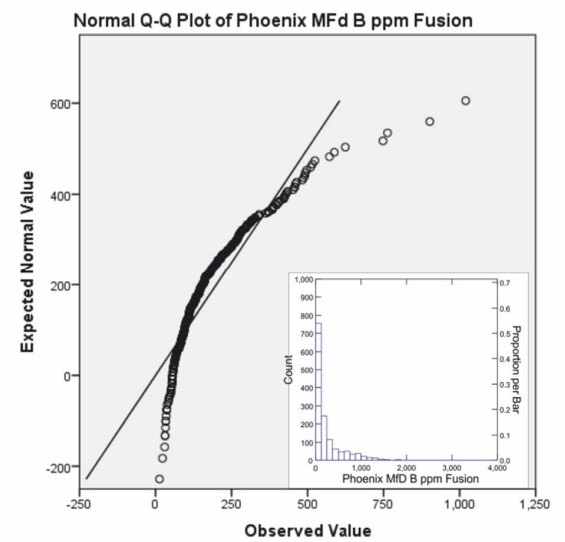
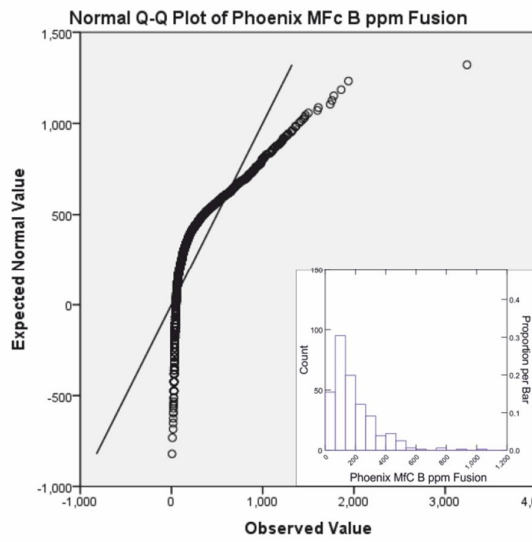
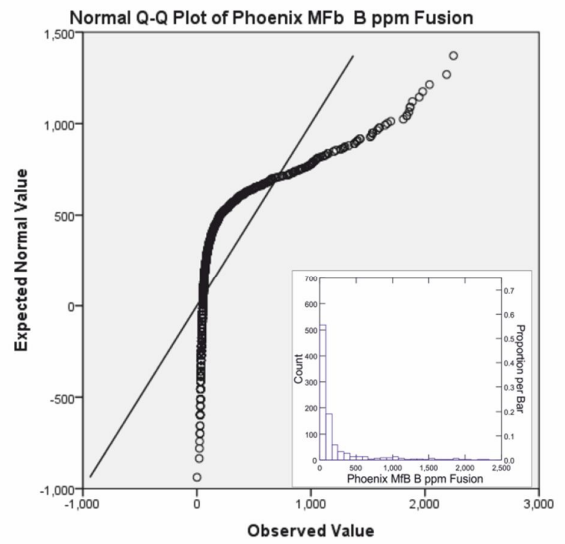
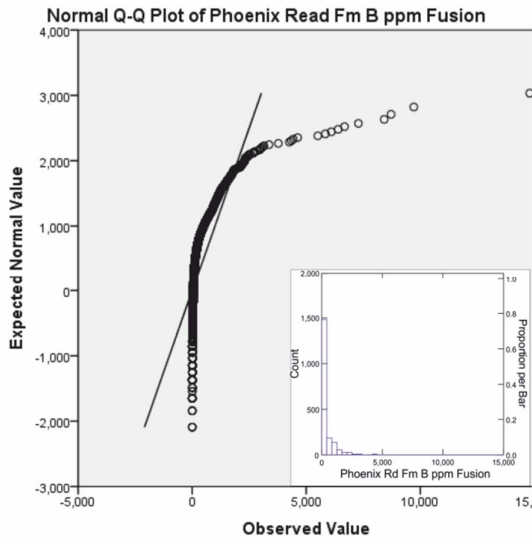


Figure 25: Q-Q and histogram (insets) plots of fusion boron values from sandstones overlying the Phoenix deposit. B data from the regional surveys is absent.

Aluminium

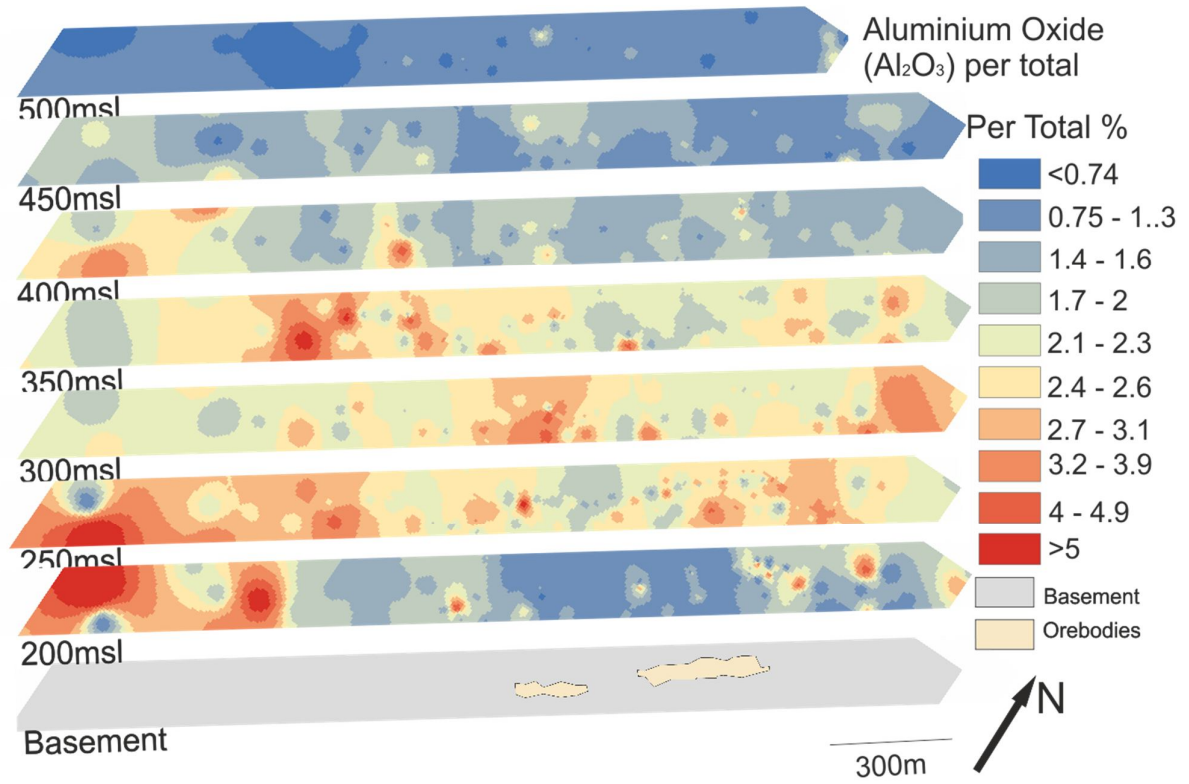
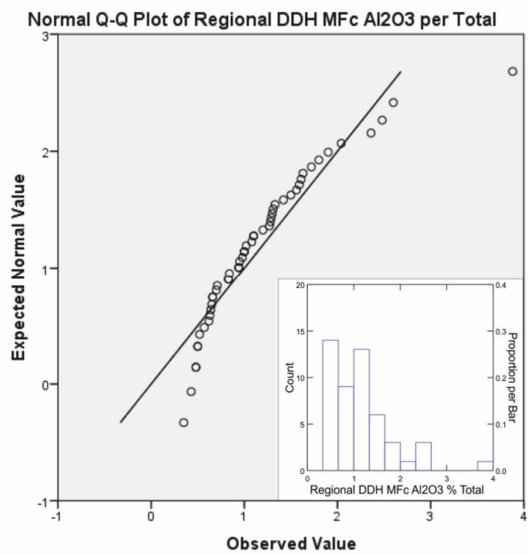
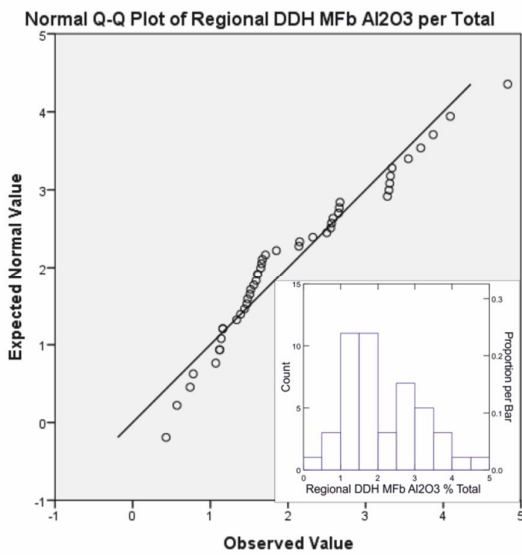
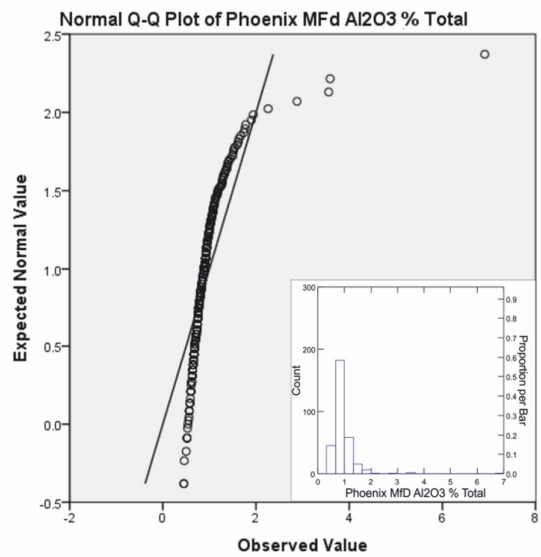
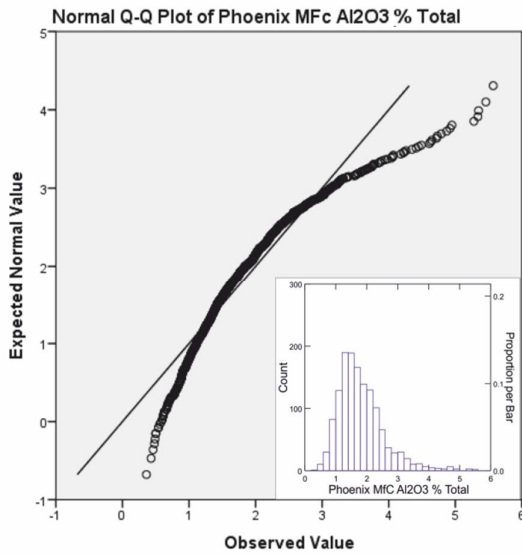
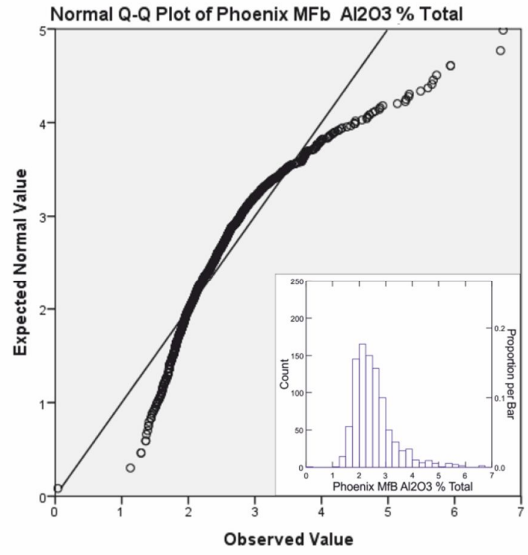
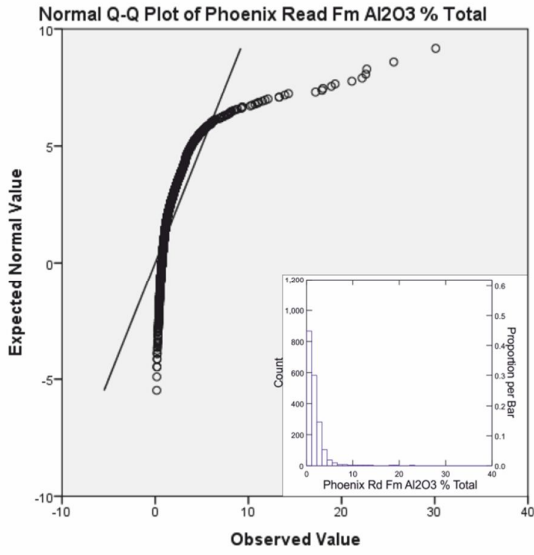


Figure 26: Total digestion aluminium oxide values from sandstone overlying the Phoenix deposit. Detection limit of 0.01% Al_2O_3 .



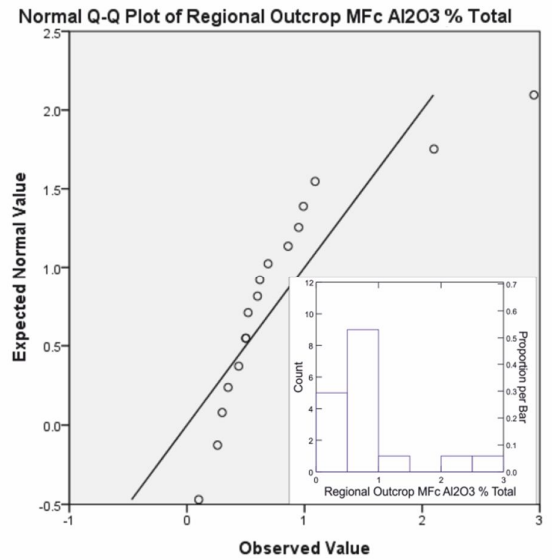
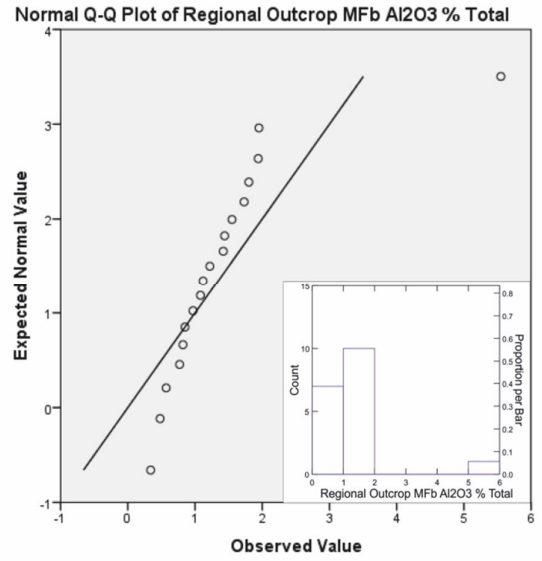
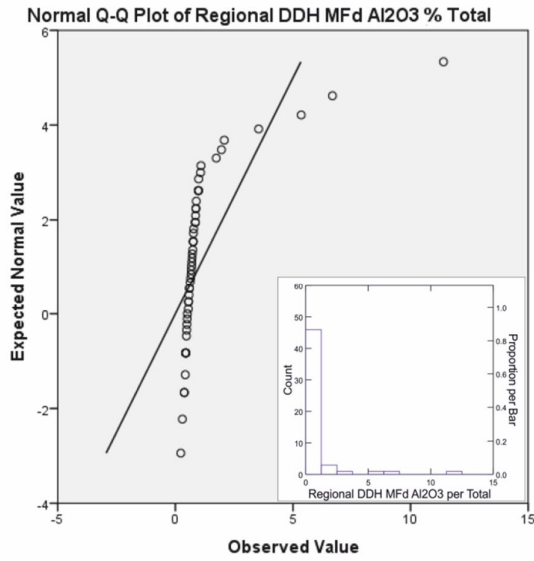


Figure 27: Q-Q and histogram (insets) plots of total digestion aluminium oxide values from regional outcrop, regional DDH and sandstones overlying the Phoenix deposit.

Yttrium

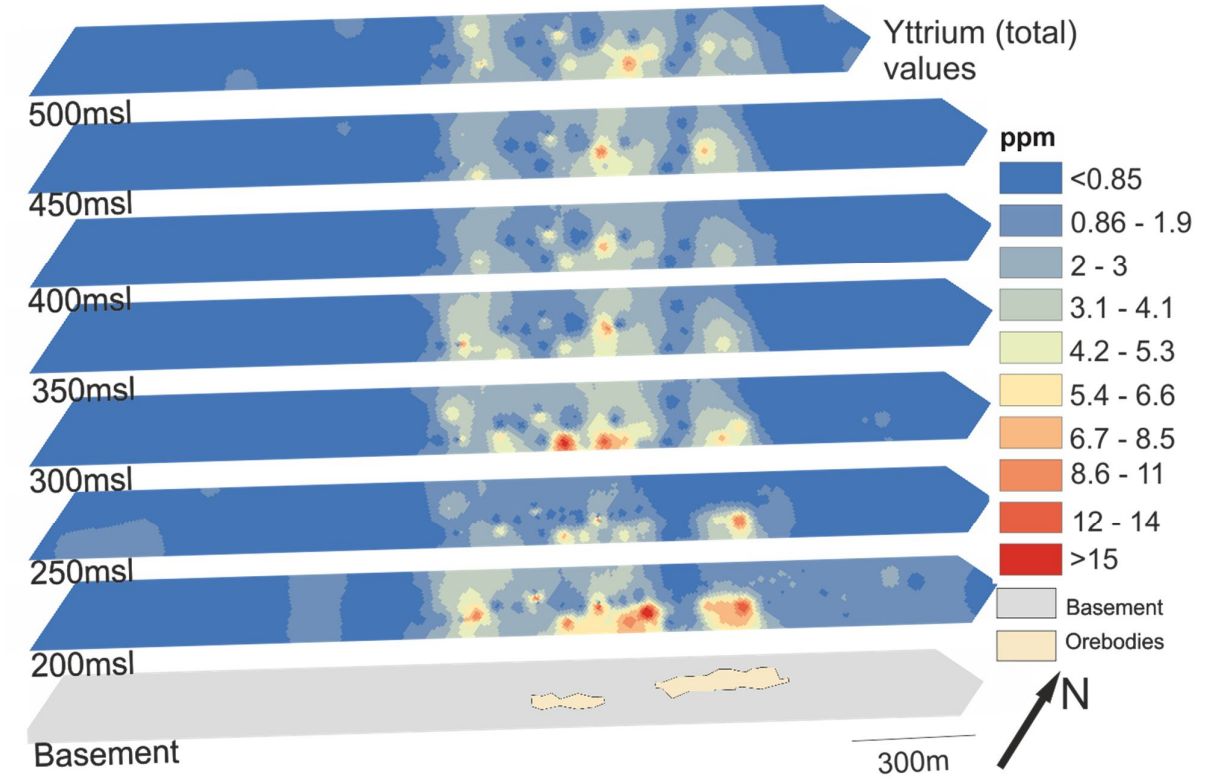
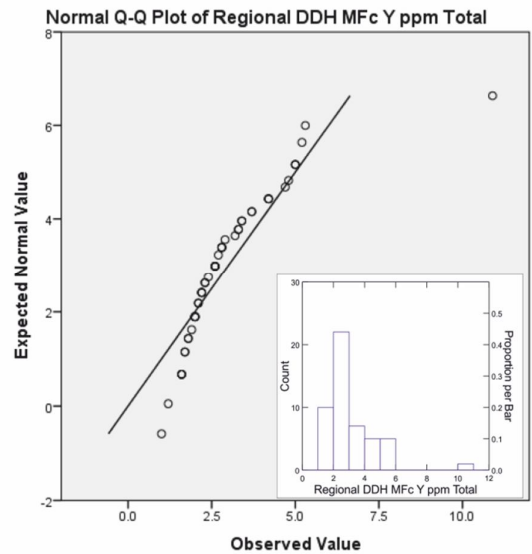
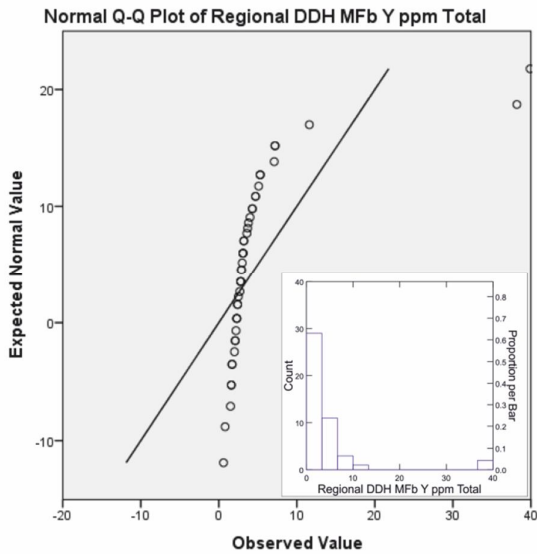
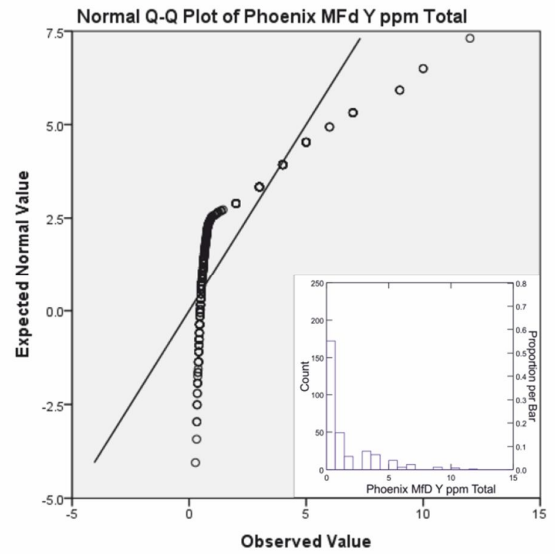
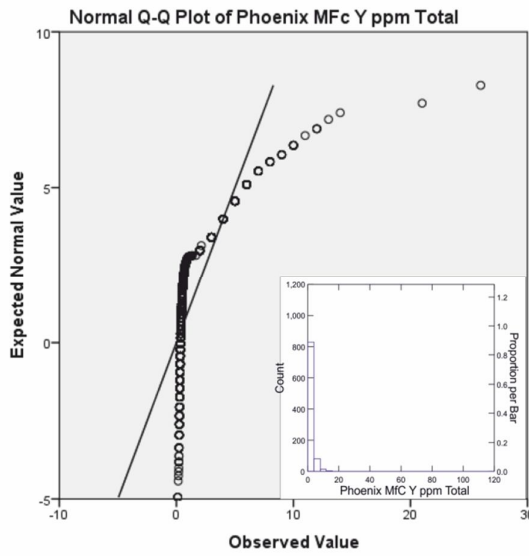
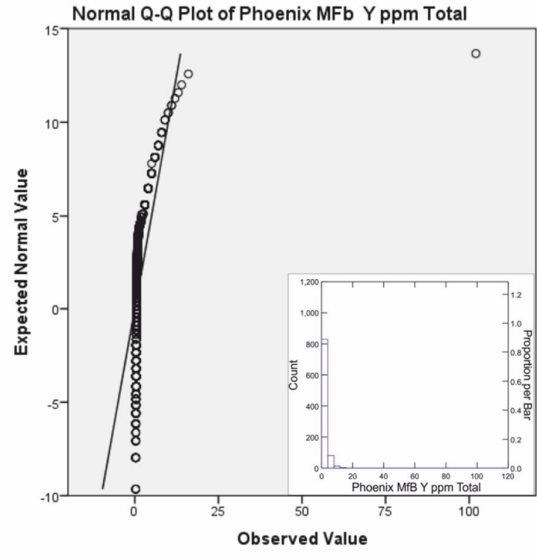
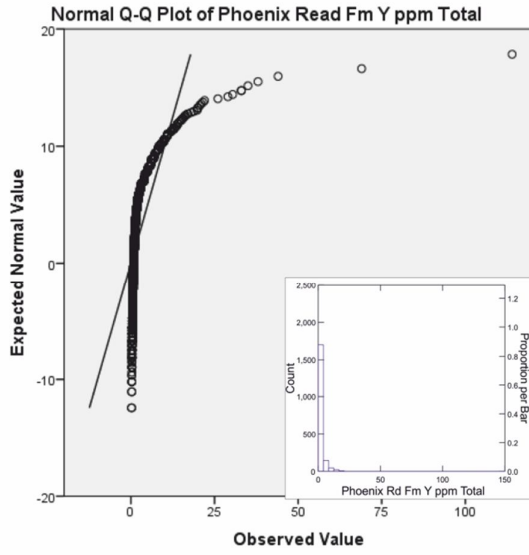


Figure 28: Total digestion yttrium values from sandstone overlying the Phoenix deposit. Detection limit of 0.1 ppm Y.



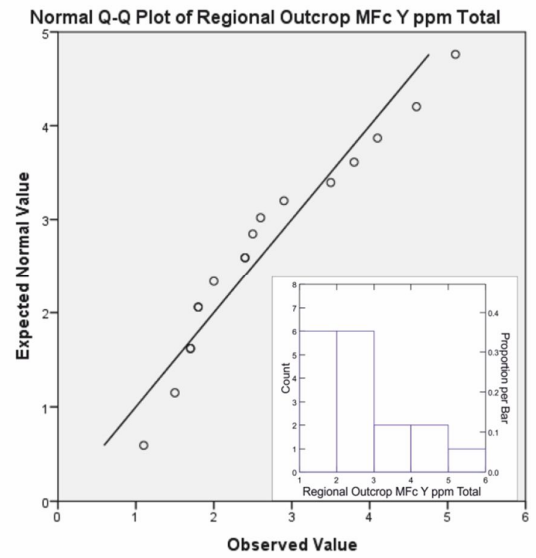
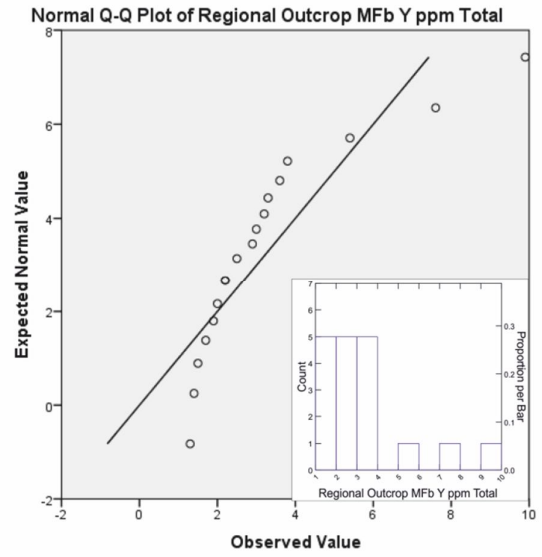
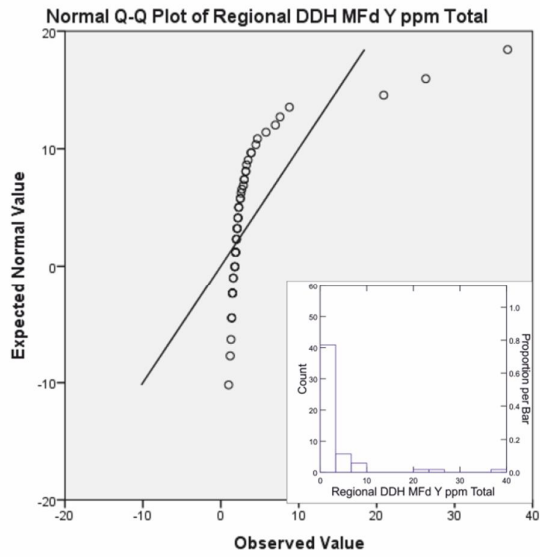


Figure 29: Q-Q and histogram (insets) plots of total digestion yttrium from regional outcrop, regional DDH and sandstones overlying the Phoenix deposit. Statistical analysis includes values at detection limit.

Potassium

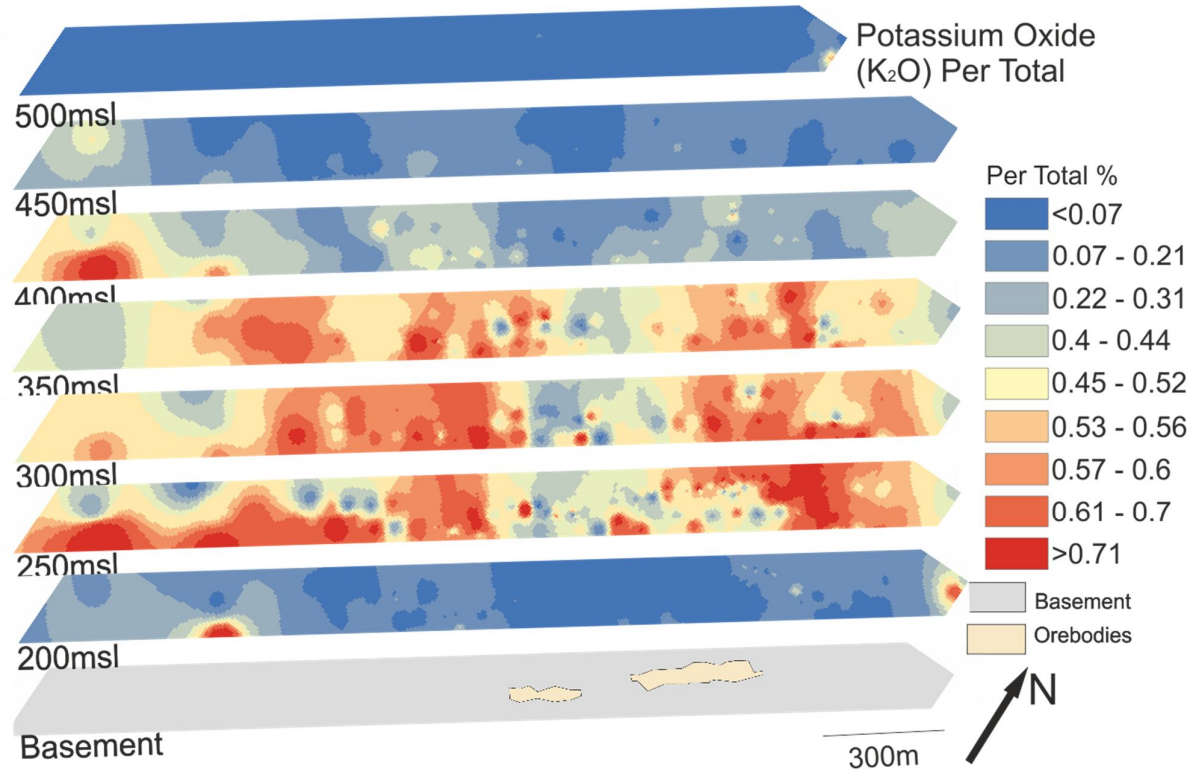
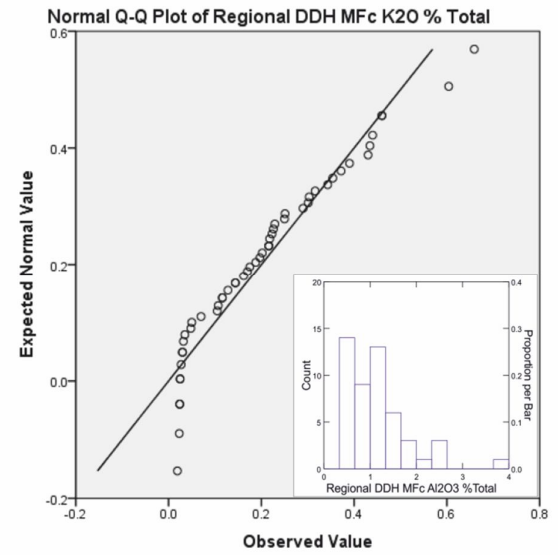
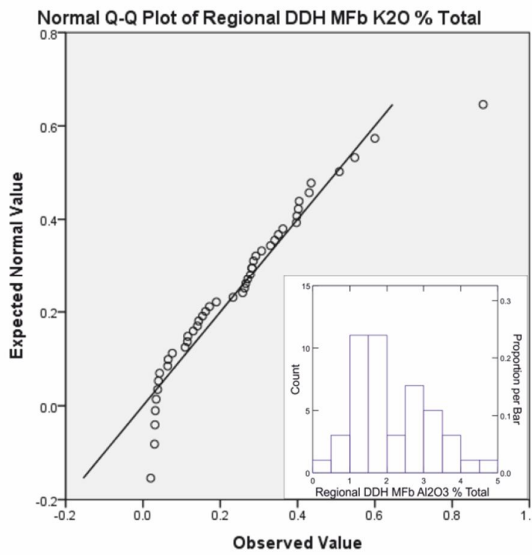
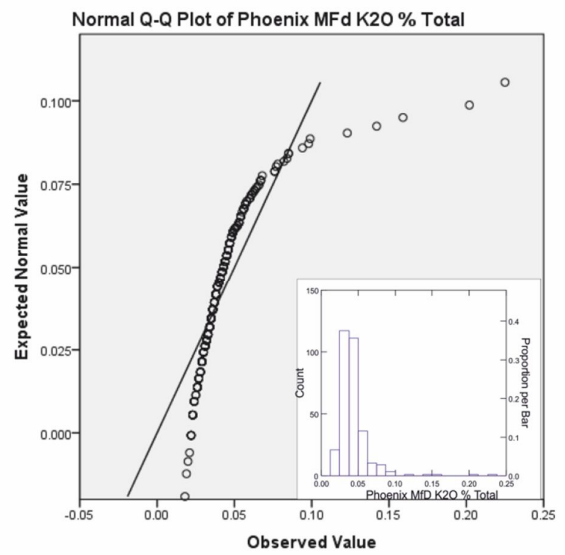
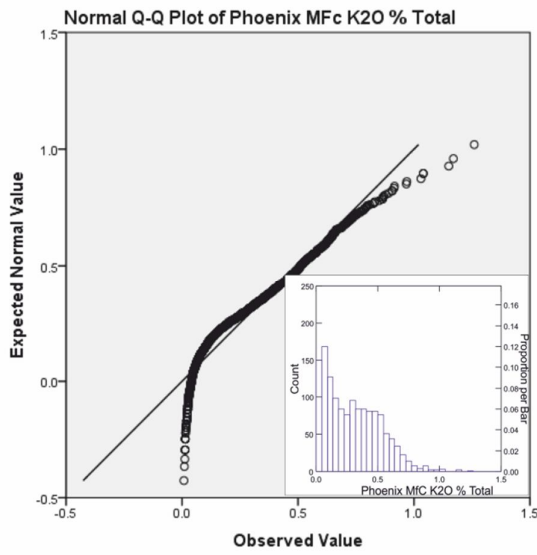
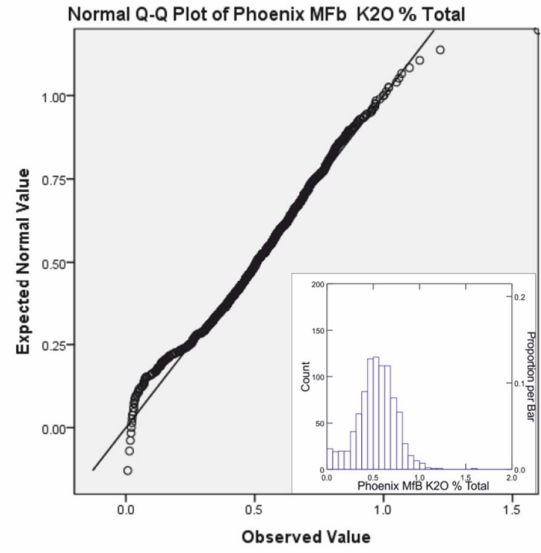
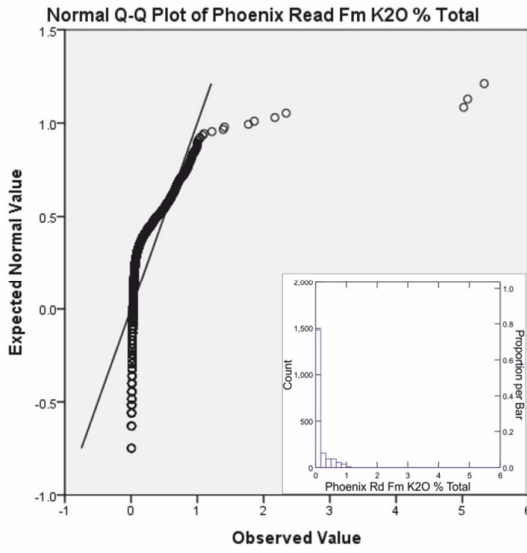


Figure 30: Total digestion potassium oxide values from sandstone overlying the Phoenix deposit.



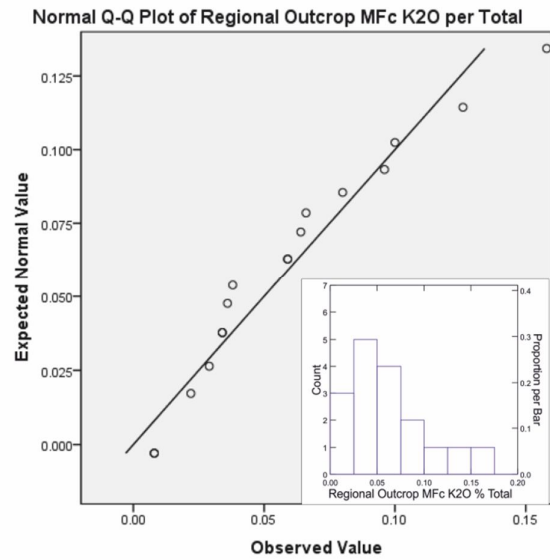
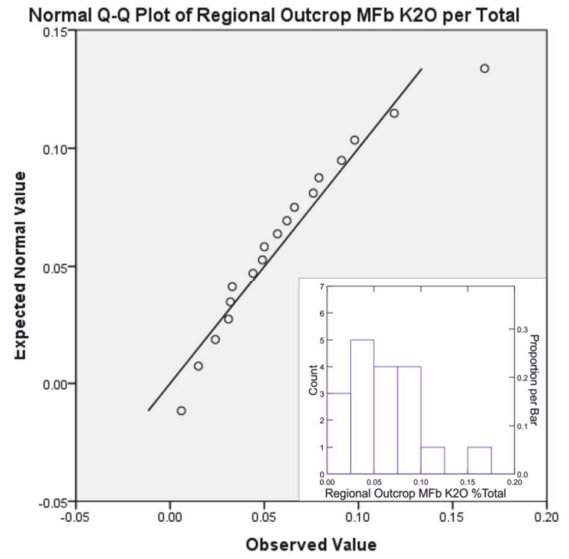
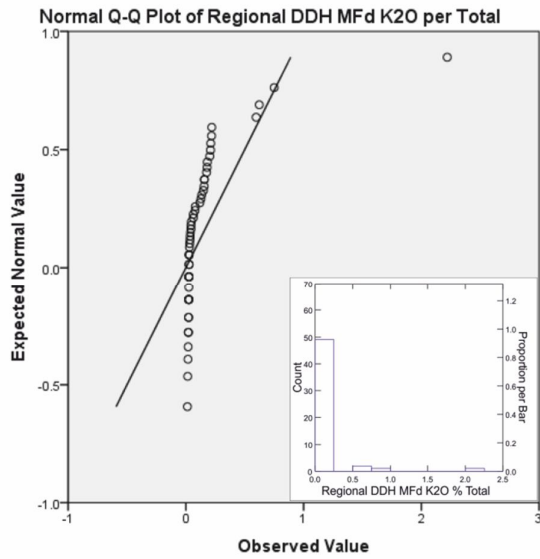


Figure 31: Q-Q and histogram (insets) plots of total digestion potassium oxide values from regional outcrop, regional DDH and sandstones overlying the Phoenix.

Cerium

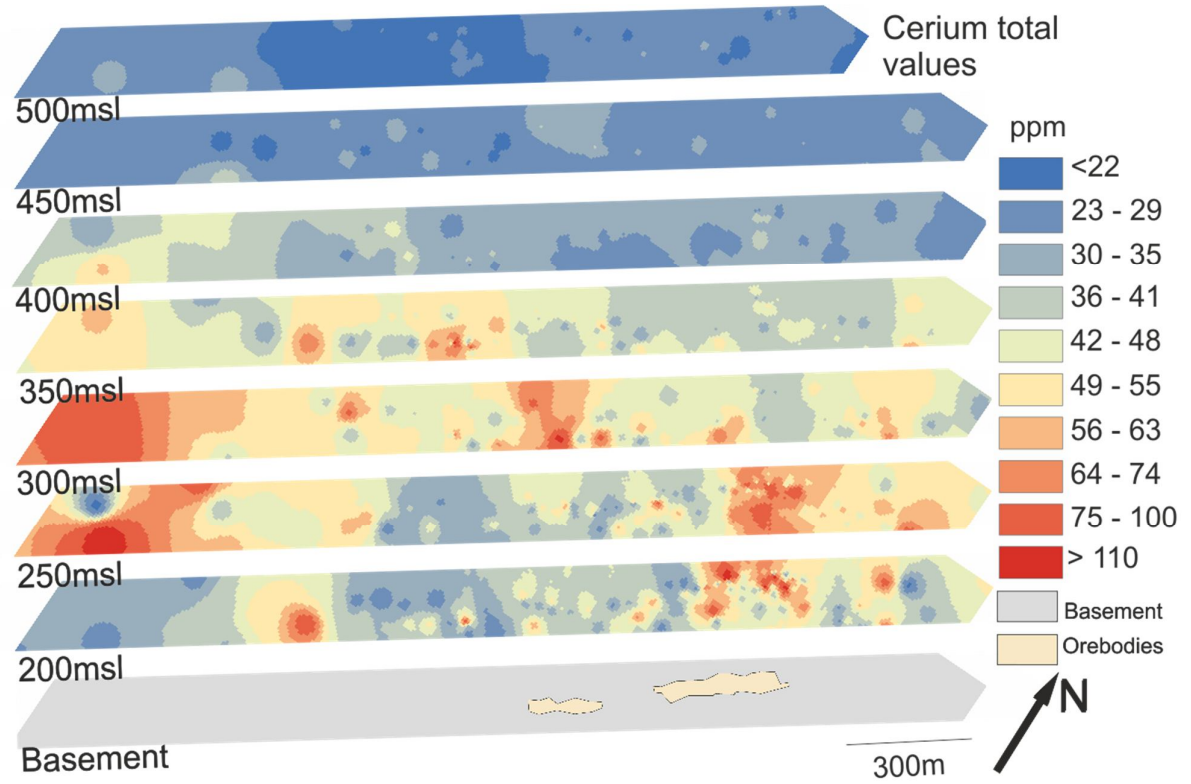
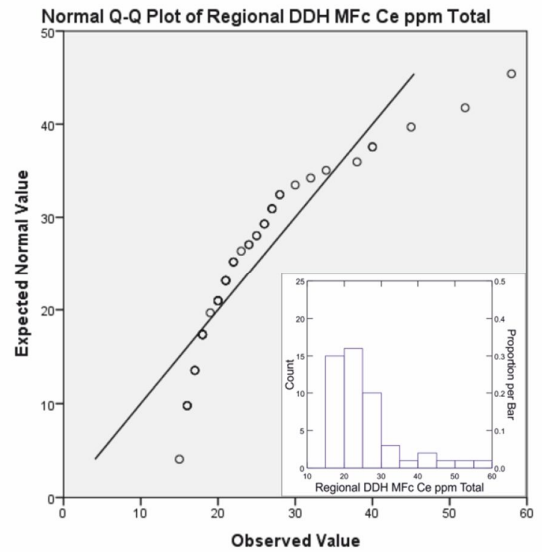
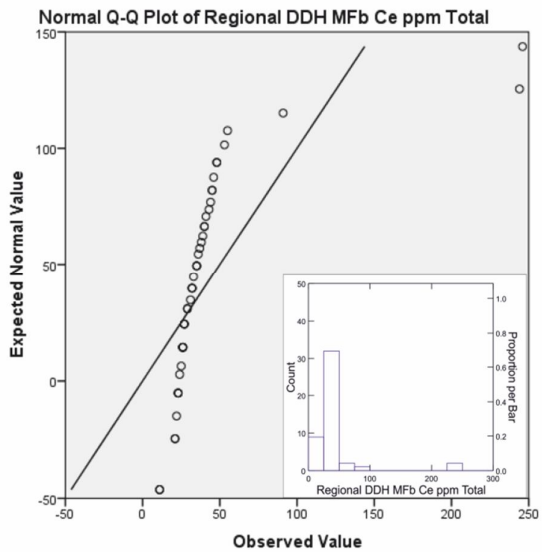
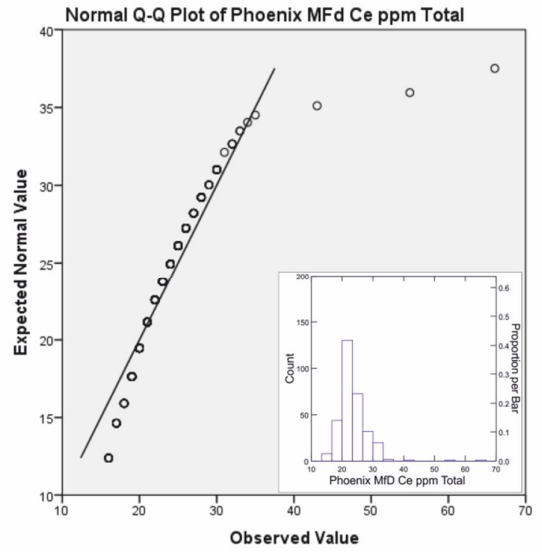
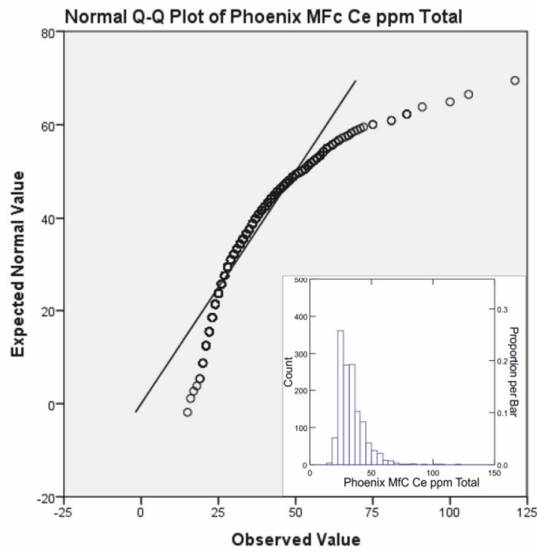
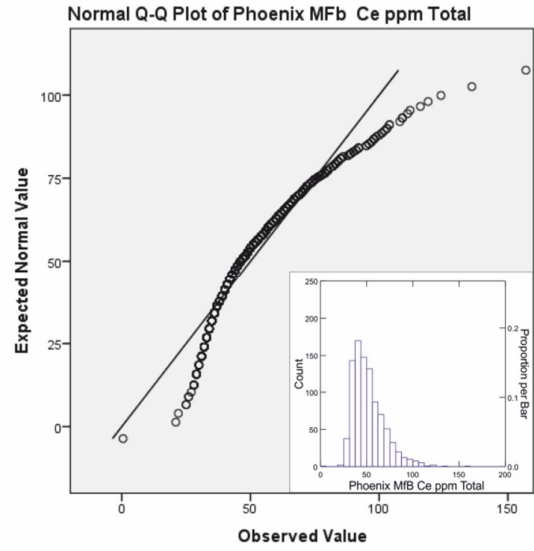
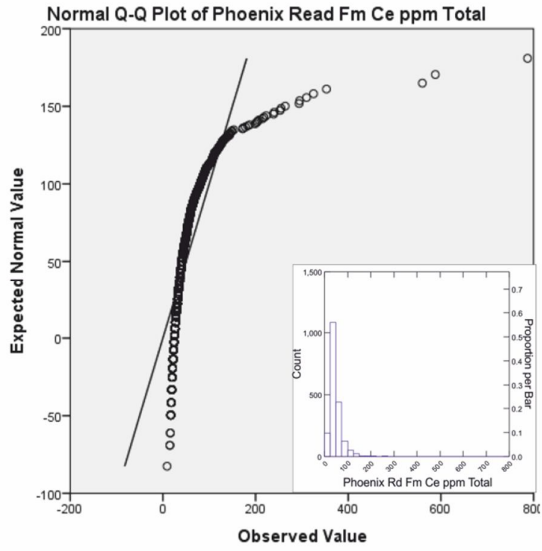


Figure 32: Total digestion cerium values from sandstone overlying the Phoenix deposit. Detection limit of 0.1ppm Ce.



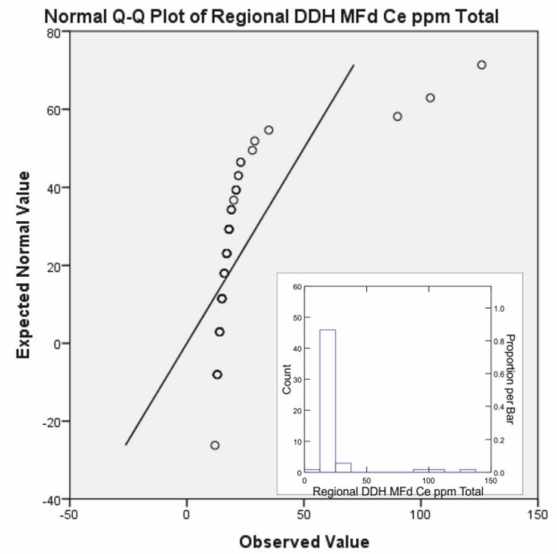
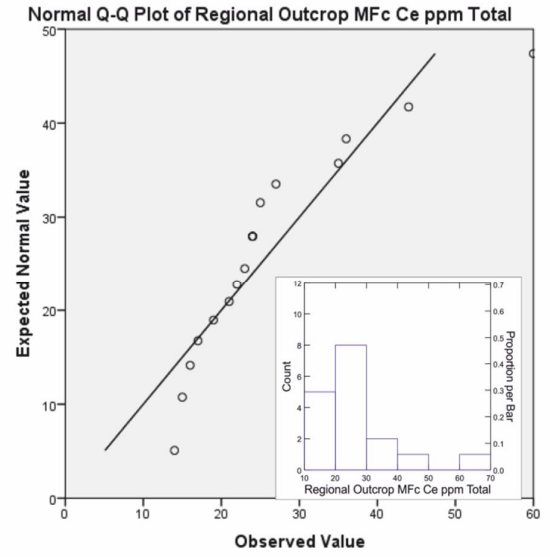
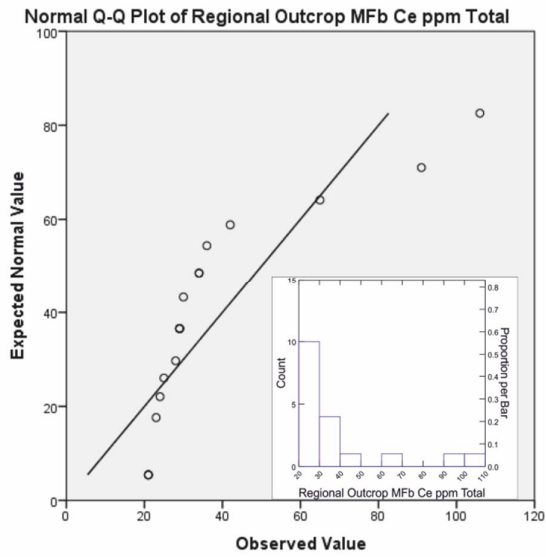


Figure 33: Q-Q and histogram (insets) plots of total digestion cerium values from regional outcrop, regional DDH and sandstones overlying the Phoenix deposit.

Tungsten

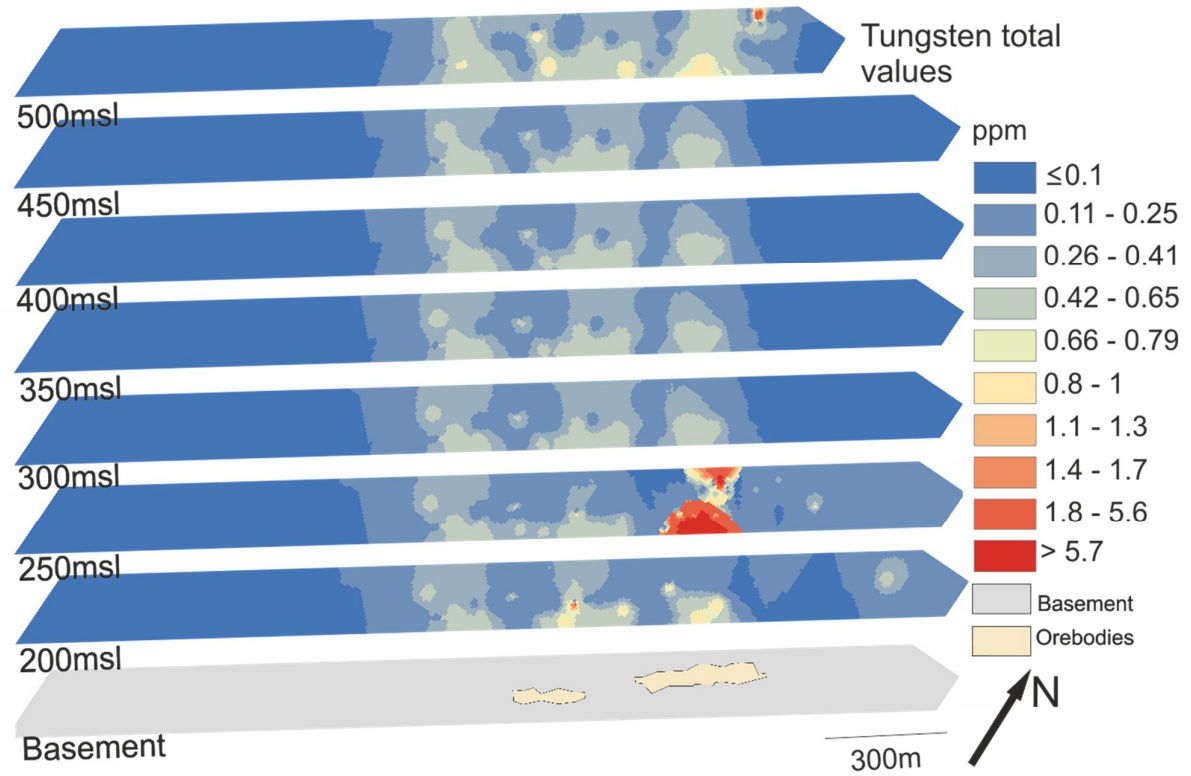
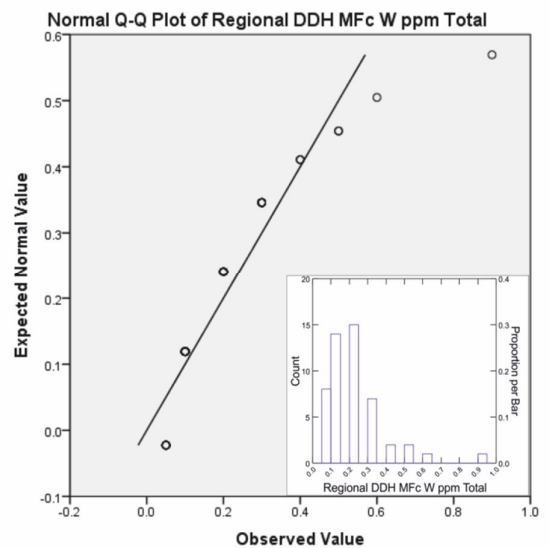
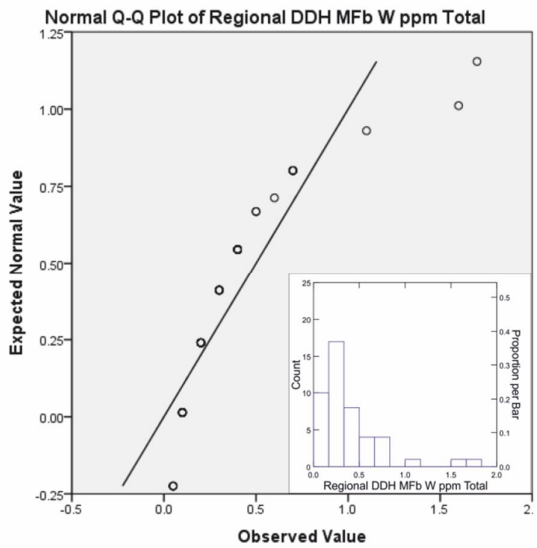
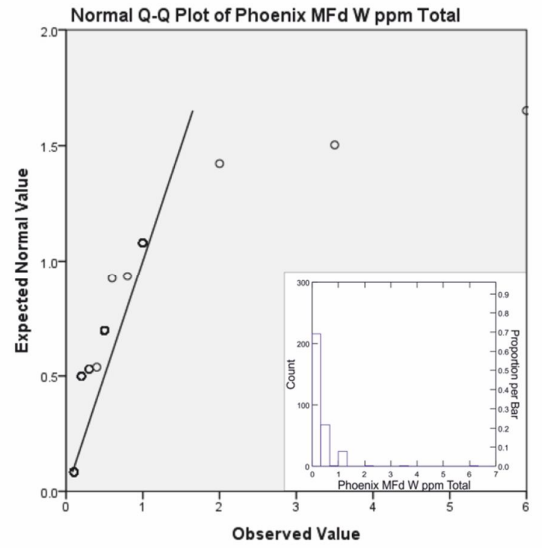
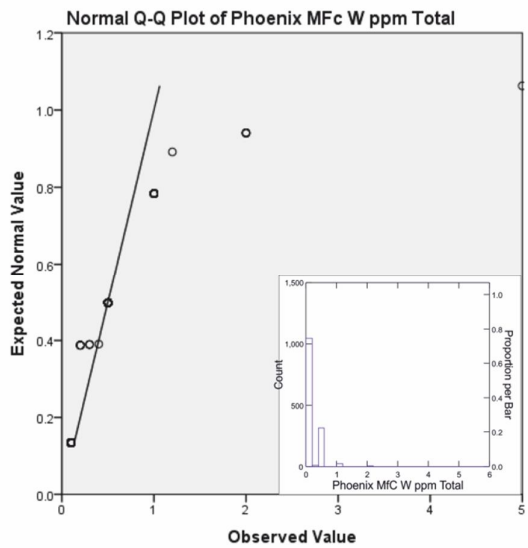
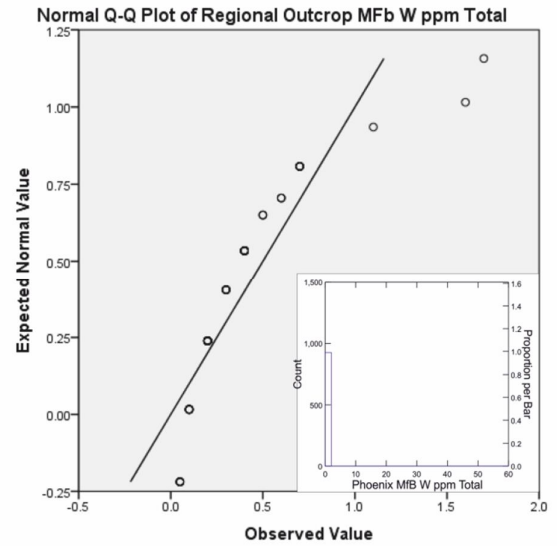
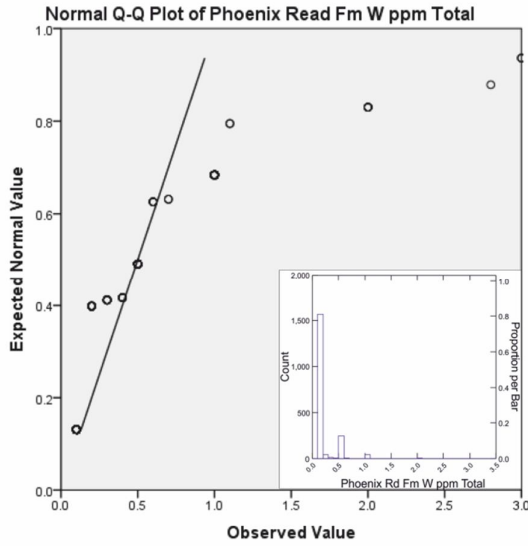


Figure 34: Total digestions tungsten values from sandstone overlying the Phoenix deposit. Detection limit of 0.1ppm W. Median values include values at detection limit. MFb median: 0.1ppm W, σ : 1.82 ppm, MFc median: 0.1ppm W, σ : 0.26 ppm, MFd median: 0.1ppm W, σ : 0.47 ppm.



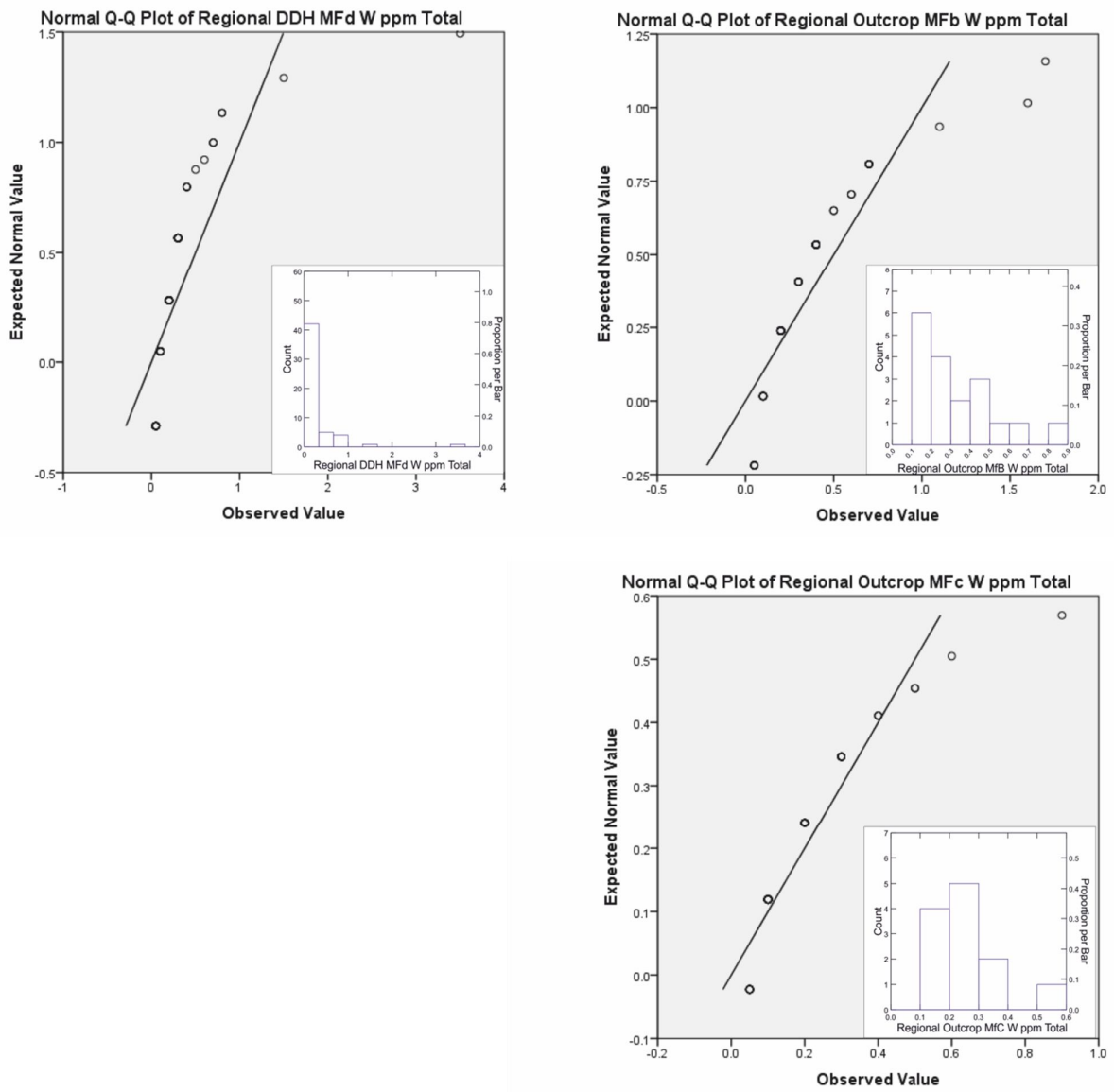


Figure 35: Q-Q and histogram (insets) plots of total digestion tungsten values from regional outcrop, regional DDH and sandstones overlying the Phoenix deposit.

Analysis

Although partial leach uranium values are elevated up to 125m from the deposit, significant areas of elevated values do not extend above 250 msl (Fig. 5). When compared to the MFc regional DDH data (Fig. 6), the Phoenix MFc dataset has a comparable median value, and excluding one 16 ppm U highly elevated value, a smaller range. However, the Phoenix MFc data has a higher population mean (0.34ppm U) and a larger spread in the data than both regional outcrop and DDH data. This is attributed to the single highly elevated value noted above which has skewed the statistics within the MFc.

Partial leach arsenic data yield elevated values in the 250, 300 and 350 msl slices overlying the ore zones, some of which in the 250 msl slice are greatly different, and considerably higher with respect to the regional datasets. While overlying the ore zones, partial leach values in the 200 msl slice are considerably lower than those present at higher msl. Although a cluster of elevated arsenic values is present at the southern extent of the drilling area, it does not contain values that are considerably larger than regional data for any of the Manitou Falls members overlying the Phoenix deposit.

The partial leach cobalt values (Fig. 8) dataset contains numerous elevated values in the sandstones. In particular, elevated values occur: 1) above the northern end of the 'A' ore zone, which has values up to 3 ppm Co at 300msl; and 2) at 400 msl in a multipoint cluster of values (up to 15.2 ppm Co). In comparison to regional data (Fig. 9), the Phoenix cobalt dataset contains elevated values within all the sandstone members, but the highly elevated values overlying ore zone A are concentrated in the MFb member. The Phoenix MFb data has a median of 0.18 ppm and mean of 0.3 ppm Co, while regional outcrop MFb data are significantly lower with a median of 0.02 ppm and a mean of 0.03 ppm Co. The difference between the values of σ for both is also significant, 0.304 and 0.1ppm, respectively.

Partial leach copper concentrations exhibit similar distributions as the partial leach uranium data, with localized, elevated values over the ore zones in the 200 and 250 msl slices (Fig. 10). In relation to regional DDH and outcrop data, partial leach copper values overlying the Phoenix deposit are elevated in all members of the sandstone column, particularly in the MFb member (Fig. 11).

Partial leach molybdenum values (Fig. 12) are weakly elevated in the 200 msl and 250 msl slices overlying the ore zones. Within these slices, there are also numerous single point values above the ore zones that are elevated relative to the regional datasets (Fig. 13 – box whisker plot). At 450msl a single highly elevated point exists, although with no apparent spatial correlation to the ore zones or the major shear structures.

Partial leach nickel values are elevated in the 200 msl slice, with the majority of the slice yielding elevated values with respect to the regional MFb datasets (Fig. 14). These elevated values also extend up to the 300 msl slice directly overlying ore zone A (Fig. 15). The one data point which falls within the MFb contains only 0.48 ppm Ni, while the rest of the MFb over Phoenix contains a mean of 1.78ppm, in contrast to the slice mean of 3.6 ppm. While regional MFb data has a mean of 0.145ppm, regional data for the RD is not available. Overall, nickel concentrations are considerably higher than the regional values over the Phoenix deposit in the MFb and MFc

members, with median and mean values 7.7 times and 9.8 times greater than the regional MFb data, respectively, and a median value 10 times greater than the regional MFc data.

Vanadium concentrations determined by total digestion display a different behaviour than the aforementioned elements. Although there is a small area of elevated values to the north of the ore zones, directly above the ore zones there is no substantial elevation in values (Fig. 16). At 300 msl, values are consistently higher throughout the slice, extending through the sedimentary package into three areas of elevated values at 400 msl.

Partial leach lead concentrations are highly variable in the sandstone units immediately above the ore zones. A 'chimney' of elevated values appears to rise from the ore zones discontinuously to 350 msl, then extend laterally (Fig. 18). While elevated relative to the adjacent slices, the lead concentrations in the chimney are comparable to the regional MFc and MFb datasets. Greatly elevated lead values are present above the 'B' zone at 450 msl, although closer to the surface, at 500 msl, the mean value is lower than the regional mean values for the MFd (Card et al., 2011).

Elevated total digestion magnesium values (Fig. 20) appear to form broad 'chimneys' to the north and south of the ore zones that are considerably higher when compared to the regional datasets. Between 300 and 350 msl, elevated values do occur over the B ore zone and appear to link with elevated data points in the 400 and 450 msl slices.

Total digestion lithium concentrations are slightly elevated above the orebodies (Fig. 22) and include many multipoint areas of elevated values. This distribution is similar to cobalt, with elevated values to the southwest of the ore zones and elevated values throughout the MFb and MFc members. To the north of the 'A' ore zone, there is a cluster of multipoint, elevated values extending up from the basement to the 250 msl slice. In comparison to the regional data, lithium is elevated in the MFb and MFc members over the Phoenix deposit, but lower in the MFd.

Boron fusion data displays clear 'chimneys' composed of elevated values rising from the vicinity of the ore zones and which extend above the 450 msl slice. The most notable area of greatly elevated values are directly above the northern terminus of the 'B' ore zone and the southern terminus of 'A' ore zone, with two smaller minor multipoint areas of elevated values rising from the north of the 'A' ore zone. At 200 msl, boron values are lower (relative to the rest of the slice) directly above the ore zones.

The distribution of total digestion aluminium oxide values (Fig. 25) form features similar to lithium and cobalt concentrations, with a southwesterly trend of elevated values comprised of single point elevated values extending through the MFb, MFc and MFd members. Also, the

aluminium oxide concentrations mirror the behaviour of MgO and B, with a zone of lower values directly overlying the ore zones in the 200 and 400 msl slices. In comparison to regional values, Al_2O_3 is consistently elevated overlying the Phoenix deposit, particularly within the MFc member where it has a much higher median value when compared to regional data (1.68 versus 0.68 wt.% Al_2O_3 , respectively) and mean (1.819 wt.% versus 0.9 wt.% Al_2O_3).

Total digestion yttrium values (Fig. 27) exhibit three, multipoint vertical areas of elevated values that extend from directly above the ore zones through the sandstone in large 'chimneys' to the near surface. It should be noted that the values which form the vertical features in Y are considerably higher than the detection limit, indicating these features are not a relic of the differing detection limits within the two differing analyses. Values throughout the rest of the slices are low (typically below 1ppm Y). Despite these chimneys, the mean Y values above the Phoenix deposit are lower than the regional DDH and outcrop mean values (Fig.28); with the Phoenix Y total from the MFb having a mean of 1.46ppm, and the regional outcrop data and DDH data having means of 3.96ppm and 4.95ppm respectively. In the MFc the low values of the data surrounding Phoenix are more apparent; with the mean from Phoenix (1.38ppm) lower than all values from the regional DDH and outcrop data.

Potassium oxide concentrations, determined by total digestion (Fig. 29), display highly elevated values in the 250, 300 and 350 msl slices. Overall the high values of potassium oxide in the sandstones analysed as part of this study match the observed (via Short Wave Infrared spectrometry; SWIR) distribution of illite in the sandstones and as such, could be treated as a proxy for illite. A vertical column of lower values (relative to the Phoenix dataset) overlies the ore zones, extending from the basement to the 400 msl slice. Overall, when compared to the regional data (Fig. 30) potassium oxide concentrations overlying the Phoenix deposit are elevated, with median values in the MFc double that of regional data and a much greater variance, with σ of 0.218 for MFc Phoenix data, versus σ of 0.039 for the MFc regional data.

Cerium total digestion values (Fig. 31) exhibit elevated values overlying the northern part of the 'A' ore zone and which extend to the 250msl slice. Elevated values sporadically continue up to 400msl to the south of the ore zones in the 300 and 350 msl slices. When compared to regional data (Fig. 32) cerium concentrations are elevated, with population mean and median values all greater than the regional data.

Tungsten total digestion data displays a pattern similar to yttrium, with well-defined vertical columns extending from the lowest slice to the near surface, these columns are at values close to detection limit, and thus their level of spatial and statistical robustness is questionable. In the MFb,

there are many highly elevated values with up to 52 ppm W. While there are insufficient data in the Phoenix dataset for formal statistical comparisons of the Phoenix deposit with the regional datasets, generally the sandstones overlying the Phoenix deposit contain considerably lower tungsten concentrations than the regional data, an observation which is also noted with Y (Fig. 23).

Discussion

The Phoenix deposit is associated with a basement shear zone (the WS Shear) that has dip of 55° to the southeast in the basement and splays into a number of small faults in the overlying sandstones (Arseneau and Revering, 2010). The basement fault may have been a major fluid pathway and the fault splays in the sandstones may have focused fluid movement pre-, syn- and post-ore formation (Arseneau and Revering, 2010; this study). Drilling at the Phoenix deposit was centred on the ore zones, with the majority of inclined DDH angled towards the northeast. Consequently there are few DDH and geochemical data which intersect the WS Shear.

Since there are no major lithological differences between different sandstone members (Yeo et al., 2007), distribution of the elevated values in the geochemistry should not reflect lithological changes between the Manitou Falls members. For certain elements, this lack of stratigraphic control is supported by the presence of elevated values within the geochemistry that extend across member transitions (e.g., partial leach U values in the 300msl slice occur in both the MFb and the MFc members; Table 1). However the distribution of some elements does appear to reflect boundaries between sandstone members. For instance, highly elevated concentrations of aluminium (values containing greater than 4 wt% Al_2O_3), terminate at 350 msl, which is the transition between the MFc and MFb members. In this study, XRD, SWIR and thin section analysis has indicated abundant interstitial clays in samples with elevated Al_2O_3 contents. The sandstones overlying the Phoenix deposit contain considerably higher Al_2O_3 values within the MFb (median 0.12wt% mean: 0.15 wt.% Al_2O_3 ; Fig 26A) and MFc (median: 0.14 wt.% and mean: 0.22 wt.% Al_2O_3 ; Fig. 26B) than the regional datasets.

The sample containing highly elevated lead at 450 msl, over 250m above the ore zones, is also elevated in uranium (partial), zinc (partial), vanadium (partial) and copper (partial), elements which have elevated concentrations within the ore zones (Arseneau and Revering, 2010). The sample of highly elevated 27ppm As (partial) in the MFd sandstone is also elevated in also cobalt (partial), nickel (partial), lead (partial), bismuth (partial), vanadium (partial) and REEs. The present study indicates that bulk rock geochemistry and interpolations of laterally continuous, subsurface datasets can indicate the potential pathways of elements associated with mineralization. This study does have limitations, in that the behaviour of elements and potential structures away from the

drilling area (including the shallow projection of the shear) are unknown, and that elevated values and trends observed in this study may be part of a regional alteration trend which has no relationship to the Phoenix deposit. For example, elevated values of boron may be part of the regional trend of tourmaline alteration and elevated values of K_2O may be derived from a regional illite trend (Earle and Sopuck, 1989). Low values of elements associated with alteration, such as B, MgO, Al and K, directly above the deposits are interpreted to reflect intense silicification in the sandstones.

The mean yttrium concentrations in sandstones overlying the Phoenix deposit are, although forming a definite feature considerably lower than regional DDH and regional outcrop data. MgO, locally associated with the intense chlorite (and to a lesser extent tourmaline) alteration around the Phoenix deposit, yields elevated values in relation to regional data. Al_2O_3 contents are also elevated when compared to regional data, reflecting the widespread presence of clay alteration. Compared to the regional DDH and outcrop data, there are significant elevations in the majority of elements in the MFb and MFc sandstones overlying the Phoenix deposit. However, a number of elements have lower than regional averages in the MFd (i.e., As, Ni, Pb, Li and K). This may record property-scale leaching during formation of the deposit in these elements and that any subsequent enrichment in these elements derived from Phoenix deposit has not reached the MFd unit. Cu, Co, Ce, MgO and Al_2O_3 are enriched across the whole dataset relative to regional DDH and outcrop data.

Implications for Exploration

Geospatial analysis sandstone lithochemical data from sandstones overlying the Phoenix deposit indicates that a number of elements do form geochemically elevated features which not only reflect the alteration mineralogy (Mg and B) but also remobilization of 'pathfinder' elements as reported from unconformity-related uranium deposits (W, LREE, Co, Cu and Pb; Jefferson et al., 2007). However, very high concentrations of certain elements (e.g. Ni and As) do not necessarily directly overlie the ore zones, possibly indicated a structural control not captured in the present study. Furthermore, some elements exhibit well-defined features directly above mineralization, but with values below the regional DDH and outcrop mean values, possibly indicating localized depletion then remobilization. Overall, the preliminary results of this study indicate that certain elements can play a guiding role in the exploration of unconformity-related uranium deposits.

Acknowledgements

This study was made possible through funding from Natural Resources of Canada, Targeted Geoscience Initiative Four (TGI-4) program via a grant to KH and a RAP bursary to JD. Denison Mines Corporation graciously provided logistic support to access the property, access to the geochemical database and is thanked for permission to publish the results.

References

- Annesley, I.R., Madore, C. and Portella, P., 2005. Geology and thermotectonic evolution of the western margin of the Trans-Hudson Orogen: Evidence from the eastern sub-Athabasca basement, Saskatchewan; *Canadian Journal of Earth Sciences*, v. 42, p. 573-597.
- Arseneau, G. and Revering, C., 2010. Technical Report on the Phoenix Deposit (Zones A & B) – Wheeler River Project, Eastern Athabasca Basin, Northern Saskatchewan, Canada; NI 43-101 technical report prepared for Denison Mines Corp., SRK Consulting.
- Bartier, P.M. and Kelley, C.P., 1996. Multivariate interpolation to incorporate thematic surface data using inverse distance weighting (IDW); *Computers and Geosciences*, v.22, p. 795-799
- Bosman, S.A. and Korness, J., 2007. Building Athabasca stratigraphy; revising, redefining, and repositioning; in *Summary of Investigations 2007, Volume 2*, Saskatchewan Geological Survey, Saskatchewan Ministry of Energy and Resources, Misc. RE. 2007-4.2, CD-ROM, Paper A-8, 29p.
- Bosman S.A. and Card, C. D., 2012. Geochemical Analyses of Athabasca Group Drillholes in Saskatchewan (NTS 64L, 74F to 74K, and 74N to 74P) – Supplementary to Data File Reports 24, 29, and 30; Saskatchewan Geological Survey Data File Series DF31: <http://www.er.gov.sk.ca/DF31>
- Card, C.D., Bosman, S.A., Slimmon, W.L., Zmetana, D.J. and Delaney, G.D., 2011. Geochemical Analyses of Athabasca Group Outcrops in Saskatchewan (NTS 64L, 74F to 74K, and 74N to 74P); Saskatchewan Geological Survey Data File Series DF30: <http://www.er.gov.sk.ca/DF30>
- Earle, S. and Sopuck, V.J., 1989. Regional lithogeochemistry of the eastern part of the Athabasca Basin uranium province, Saskatchewan, Canada; in *Uranium Resources and Geology of North America*; IAEA-TECDOC-500, p.264-296.
- Grunsky, E.C., 2010. The interpretation of geochemical survey data; *Geochemistry: Exploration, Environment, Analysis* v. 10, p. 27–74.
- Jefferson, C.W., Thomas, D.J., Gandhi, S.S., Ramaekers, P., Delaney, G., Brisbin, D., Cutts, C., Portella, P. and Olson, R.A., 2007. Unconformity-associated uranium deposits of the Athabasca basin, Saskatchewan and Alberta; in *EXTECH IV: Geology and Uranium EXploration TECHnology of the Proterozoic Athabasca Basin, Saskatchewan and Alberta*, (eds.) C.W. Jefferson and G. Delaney; *Geological Survey of Canada Bulletin* 588, p. 23-67.
- Kane, V., Begovich, C., Butz, T. and Myers, D.E., 1982. Interpretation of regional geochemistry; *Computers and Geoscience* v.8, p. 117-136
- Kerr, W.C., 2010. The Discovery of the Phoenix Deposit: a New High-Grade, Athabasca Basin Unconformity-Type Uranium Deposit, Saskatchewan, Canada; *Society of Economic Geologists, Special Publication* 15, p. 703-728.
- Ramaekers, P., Jefferson, C.W., Yeo, G.M., Collier, B., Long, D.G.F., Drever, G., McHardy, S., Jiricka, D., Cutts, C., Wheatley, K., Catuneanu, O., Bernier, S., Kupsch, B. and Post, R.T., 2007. Revised geological map and stratigraphy of the Athabasca Group, Saskatchewan and Alberta; in *EXTECH IV: Geology and Uranium EXploration TECHnology of the Proterozoic Athabasca Basin, Saskatchewan and Alberta*, (eds.) C.W. Jefferson and G. Delaney; *Geological Survey of Canada Bulletin* 588, p. 155-191.
- Roscoe, W.E. 2012. Technical report on a mineral Resource estimate update for the Phoenix uranium deposits, Wheeler river project, Eastern Athabasca basin, Northern Saskatchewan, Canada; NI 43-101 Report prepared for Denison Mines Corp.

Yeo, G.M., Jefferson, C.W. and Ramaekers, P., 2007. Comparison of lower Athabasca Group stratigraphy among depositional systems, Saskatchewan and Alberta, in EXTECH IV: Geology and Uranium EXploration TECHnology of the Proterozoic Athabasca Basin, Saskatchewan and Alberta, (eds.) C.W. Jefferson and G. Delaney; Geological Survey of Canada Bulletin 588, p.465-488.

Zhang, C., Fay, D., McGrath, D., Grennan, E. and Carton, O.T., 2008. Statistical analyses of geochemical variables in soils of Ireland; *Geoderma* v.146, p. 378–390.